

Sensitivity Analysis of Optimised Large Scale District Heating Heat Pump Concepts

- Master Thesis -

Signe Thomasen

Aalborg University
Thermal Energy and Process Engineering



AALBORG UNIVERSITY

Copyright © Aalborg University 2020

MATLAB R2019b, Overleaf v2, Microsoft Excel, RStudio, Dymola 2020x, GEA RTSelect,
Python 3.7.



AALBORG UNIVERSITY

STUDENT REPORT

Title:

Sensitivity Analysis of Optimised Large Scale District Heating Heat Pump Concepts

Theme:

Master Thesis

Project Period:

Spring 2020

Author:

Signe Thomasen

Supervisor:

Carsten Bojesen
Kim Sørensen
Kasper Vinther

Copies: Submitted digitally

Page Numbers: 118

Date of Completion:

29th of May 2020

Abstract:

The main purpose of the project is to investigate the sensitivity on choice of heat pump concept to variations in boundary conditions. A performance map-based heat pump model will be used to evaluate performance of different heat pump concepts. The heat pump concepts are optimised in terms of concept design and prepared for evaluation of feedback control parameters and on/off strategies, which calls for a nonlinear optimiser such as genetic algorithms. The optimisation considers the operational price of the concept, regarding COP, heating capacity and investment cost and is followed by investigations of the possibility for providing Ancillary services. A sensitivity analysis was carried out to investigate whether, which and how variations in cost function weighting affects the optimisation and consequently the choice of heat pump concept. The results indicate a very robust optimised concept evaluated entirely on normal operation. Additionally, no significant differences in dynamic response was observed.

Preface

The following report is written by Signe Thomasen, energy engineering student from Aalborg University in the period from the 3rd of February 2020 to the 29th of May 2020. This project report makes use findings from a 3rd semester project of thermal energy and process engineering, based on a project oriented internship. The project has been carried out with the guidance of Carsten Bojesen, Associate Professor, Aalborg University, Kim Sørensen, Associate Professor , Aalborg University and Kasper Vinther, engineer, Added Values.

Reading instructions

The report makes use of references according to the Harvard method. The references will occur in the text in the following manner: [Surname/publisher, year (possible page number)], where the end of the report is a comprehensive list of literature.

References are made as hyperlinks in the digital copy. Figures and tables are listed as the chapter number, followed by the figure/table/equation number, as an example Figure 7.2 is the second figure in Chapter 7. Figure and table explanatory text can be found below the figure and above tables. Furthermore, section references are made using the section numbering. The unit system used in the report is the SI system with a dot as decimal separator, with the exception of time which in some cases is stated in hours or minutes. For readability, some temperatures are stated in °C. The term *heat pump concept* in the context of this thesis refers the configuration of heat pumps in terms of number of serial or parallel connections and the capacities of each heat pump.

Aalborg University, 29th of May 2020

Resumé

Formålet med dette studie er at identificere og kvantificere hvilke og i hvilken grad en række parametre har betydning for hvilke valg der gøres i forbindelse med store varmepumper i fjernvarmen. Projektet er udført i samarbejde med Added Values, og er baseret på et aktuelt projekt i Esbjerg, hvor et 460 MW_q kulfyret kraftvarmeværk forventes at lukke i marts 2023. I den forbindelse forventes det, at en del af erstatningen består af et 50 MW_q havvandsvarmepumpekoncept.

Store varmepumper er en relativ ny teknologi i fjernvarmen både på det danske marked men også globalt set. Det betyder blandt andet, at erfaringsgrundlaget er meget lille, når det drejer sig om projektering af varmepumpeprojekter i stor skala. Dertil kommer, at andelen af vedvarende energikilder i det danske energisystem stiger, som et led frem mod at opnå klimamålsætningerne for både 2030 og 2050, der blandt andet indebærer at Danmark skal være 100 % klimaneutrale i år 2050. I takt med den stigende andel af vedvarende og fluktuerende energikilder, stiger behovet for systemydelser på elmarkedet. I dag leveres langt de fleste systemydelser af de konventionelle kraftvarmeværker, men i takt med deres udfasning er alternativer en nødvendighed. I den sammenhæng ses der potentiale i implementeringen af store varmepumper i fjernvarmen, da varmepumperne helt generelt kan forbruge store mængder elektrisk energi og effektivt konvertere det til varme.

Med udgangspunkt i det planlagte projekt i Esbjerg, er formålet med dette studie at udbygge den eksisterende viden i forhold til projektering af store varmepumpeprojekter med fokus på varmepumpe-konceptoptimering og følsomhed overfor prisændringer og ændringer i driftsbetingelser. Konceptoptimering dækker over optimering af varmepumpernes indbyrdes kobling og størrelse.

En dynamisk og lastafhængig *performance map* baseret varmepumpemodell implementeret i det multi-domæne-modelleringsprog, Modelica, danner grundlag for den dynamiske model anvendt for den videre optimering. Den dynamiske model giver mulighed for at koble i alt 9 varmepumper som tre parallelkredse hver med tre varmepumper i serie. Derudover indeholder modellen i Modelica en temperatur- og laststyring og et bud på en kontrolstrategi samt en driftsprofil, som tager udgangspunkt i systemet i Esbjerg. Med udgangspunkt i driftsprofilen, søger optimeringen efter et optimalt varmepumpekoncept, hvor både konfigurationen mellem varmepumperne, det samlede antal varmepumper og størrelserne på de enkelte varmepumper er inkluderet som optimeringsvariable. Til optimeringen, eksporteres modellen ved brug af en *Functional Mockup Unit* (FMU), som tillader, at modellen kan eksekveres i python. Med henblik på videreudvikling af optimeringsomfanget, anvendes en ulineær optimeringsalgoritme, hvor en micro-genetisk algoritme er foreslået.

Optimeringen baseres på varmepumpekonceptets ydeevne i 11 driftskategorier, der repræsenterer eksempler på både fuldlast- og dellast driftsperioder, som et varmepumpkoncept vil opleve henover et år. Varmepumpekoncepterne evalueres ud fra COP, maksimal varmekapacitet og investeringsomkostninger. De to førstnævnte prissættes og vægtes på de forskellige driftskategorier ud fra deres forventede antal driftstimer og leveret varme.

Optimeringsresultaterne indikerer, at når både COP og investeringsomkostninger har indflydelse på konceptvalget, er det i høj grad gevinsten ved høj COP og besparelsen ved få og store enheder, som er udslagsgivende. Selv ved betydelige ændringer i de prismæssige grundlag for COP og for investeringsomkostninger, er et koncept med tre store varmepumper ($\approx 18.2 \text{ MW}_q$) meget robust. Begrænsninger på den maksimalt tilladte kapacitet for en enkelt varmepumpe kan dog ændre på resultatet, som stadig er domineret af en balance mellem maksimering af COP og minimering af investeringsomkostninger. Relativt til et referencekoncept bestående af fire varmepumper fordelt på to parallelkredse hver med to varmepumper i serie, viser optimeringen at der kan opnås besparelser på 1 886 414 kr/år.

En yderligere undersøgelse af den dynamiske respons for det optimerede varmepumpekoncept og referencekonceptet viser, at responsen for de to koncepter - med henblik på kravene for at tilbyde systemydelser - er meget ens. Det indikerer, at det optimerede system med tre store varmepumper i serie, både er robust overfor ændringer og samtidigt egner sig til fleksibel og meget dynamisk drift. Begrænsninger på maksimal kapacitet for de enkelte enheder kan dog medføre, at andre koncepter må tages i betragtning, hvor balancen mellem COP maksimering og investeringsomkostninger bliver mere følsom overfor ændringer i omkostningsbetingelserne. Yderligere medtagelse af blandt andet omkostninger for vedligehold, redundans, systemydelser og kontrolstrategier i forbindelse med optimeringen, kan desuden også påvirke optimeringsresultatet.

Nomenclature

Symbols

α	COP Cost Coefficient	DKK
β	Capacity Cost Coefficient	DKK
Δf	Frequency Deviation	Hz
ΔH	Enthalpy Difference	J kg ⁻¹
ΔT	Temperature Difference	K
δ	Heat Pump Scaling Factor	—
\dot{m}	Mass Flow Rate	kg s ⁻¹
\dot{Q}	Heat Flow Rate	W
\mathcal{N}	Normal Distribution	—
μ	Micro or Mean Value	—
σ	Standard Deviation	—
A	Heat Exchanger Area	m ²
d	Normalised Maximum Distance	—
G	Total Investment Cost	DKK
H	Enthalpy	J kg ⁻¹
k	Tournament Size or Proportional Gain	—
N	Population Size	—
n	Loan Period	year
P	Electric Power	W
r	Interest Rate	%
T	Temperature	°C or K
t	Time	s
U	Overall Heat Transfer Coefficient	W m ⁻² K ⁻¹
u	Hysteresis Limits	%

y Fitness Value

—

Notation

G Equality and Inequality Constrains Matrix

g Equality and Inequality Constrains Vector

u Input Vector with Capacities

v Fixed Input Vector with External Boundary Conditions

x System State Vector

Y Population Fitness Vector

Subscripts

χ Gene/Variable in Individual/Solution

s Solution

air Air Source

c Cooling or Crossover

dh,out District Heating Water, Outlet

dh,return District Heating Water, Return

down Downward Regulation

eva Evaporation Temperature

f Female

h Heating

high Higher Limit

invest Investment

LMTD Logarithmic Mean Temperature Difference

low Lower Limit

m Male

max Maximum

min Minimum

n Nominal

opt	Optimised
ref	Reference
set	Set Point
T1	Test 1
T2	Test 2
up	Upward Regulation

Abbreviations

μ GA	Micro Genetic Algorithm
AC	Alternative Concept
aFRR	Automatic Frequency Restoration Reserve
C	Category
CAPEX	Capital Expenditure
COP	Coefficient of Performance
CPU	Central Processing Unit
CS	Co-simulation
DAE	Differential Algebraic Equation
DE	Depreciation Expense
DK1	Western Denmark
DK2	Eastern Denmark
DKK	Danish Krone
DTU	Technical University of Denmark
E1	Energist 1
EB	Electric Boiler
EN	Energinet
EOS	Economy of Scale
FCR	Frequency Containment Reserve
FCR-D	Frequency Containment Reserve for Disturbances

FCR-N	Frequency Containment Reserve for Normal Operation
FMI	Functional Mock-up Interface
FMU	Functional Mock-up Unit
GB	Gas Boilers
HFC	Hydro-Fluorocarbons
HP	Heat Pump
HVAC	Heating, Ventilation and Air Conditioning
ME	Model-exchange
mFRR	Manual Frequency Restoration Reserve
PI	Proportional Integral
SI-units	Système International d'Unités
VSD	Variable Speed Drive
WCB	Wood Chip Boiler

Contents

Preface	v
Nomenclature	ix
1 Introduction	1
1.1 Heat Pumps in the Danish District Heating System	2
1.2 Esbjerg Case study	4
1.3 Heat Pump Integration	6
2 Thesis Statement	13
3 Modelling	15
3.1 Heat pump performance map	15
3.2 Heat pump system	17
4 Simulation Tests	27
4.1 Nominal Conditions	27
4.2 System Test	28
5 Optimisation	31
5.1 The Optimisation Problem	31
5.2 Optimisation Algorithm - μ GA	39
5.3 Dynamic Response and Ancillary Services: System Setup	44
6 Optimisation Results	47
6.1 Cost Allocation	49
6.2 Cost Comparison	52
6.3 Ancillary Services and Dynamic Response	53
7 Sensitivity Analysis	57
7.1 COP - Sensitivity to Electricity Costs	57
7.2 Investment Cost	60
7.3 Maximum Capacity Reduction	64
7.4 Comparison	66
8 Discussion	69
9 Conclusion	77
Bibliography	79

Appendix	84
A Performance Map Test	85
B Ancillary Services	87
B.1 Introduction to ancillary services	87
Enclosure	91
A Dymola: System setup	93
B μGA Python code	97

1 Introduction

As a part of the green transition of the energy systems, large scale heat pumps are expected to play a significant role to provide climate friendly heat. EU regulation requires that Denmark by 2030 reduce emissions in the so called non-quota sectors, which among other things include agriculture, transport and some residential heating, by 39 % compared to 2005 levels. Political targets are even more ambitious, and aims to reach a 70 % reduction to 1990 levels in 2030. Furthermore, a 100 % renewable energy target is set to be fulfilled by 2050. [Klima-, energi- og forsyningsministeriet, 2019]

As the discussion of power-to-x becomes gradually more and more interesting due to the increasing amount of renewable energy dominating the power grid, the heating sector has the potential to become an important player. The heating sector can absorb a large amount of electricity, and does additionally have the potential to store the energy [Bach et al., 2016].

According to a study from [Møller et al., 2018], around 64 % of the households in Denmark are supplied by heat from the district heating network. Despite district heating itself being a good step in reaching the climate targets, the heating sector still faces some challenges, as 2018 numbers show that 40 % of this heat is produced from fossil fuels. Figure 1.1 shows the district heating production from different district heating production units.

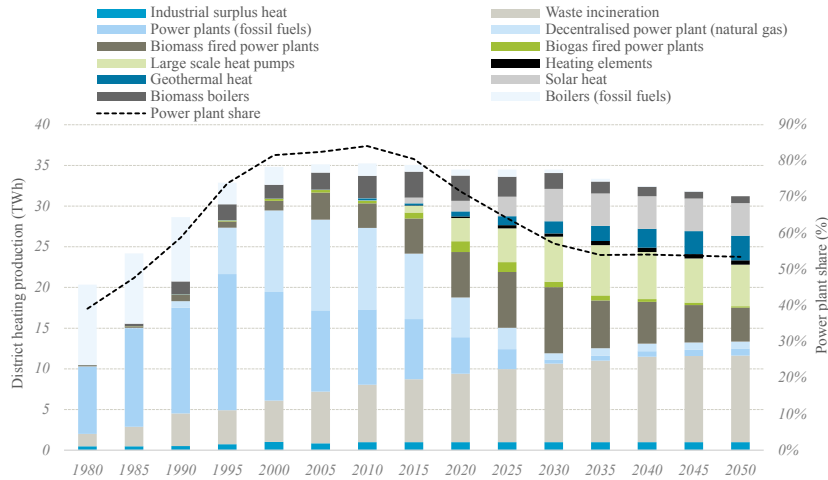


Figure 1.1: District heating production from different units from 1980 to expected heat production distribution in 2050 [Møller Thomsen et al., 2018]

What is notable in Figure 1.1 is how the share of more renewable and environmental friendly district heating production units is expected to continue increasing. However, some of the challenges, which was also outlined in a study from [Popovski et al., 2019]

for a German district heating system, have been the costs related to the integration of new and environmental friendly solutions as for instance large scale heat pumps. In Denmark, some political steps haven been taken to assist reaching the climate targets. This includes relaxing the rules regarding heating production as well as taxes for electricity for heat production. This, in combination with a complete phase-out of coal and withdrawn subvention for gas-supplied units supports the electrification of the heating sector. Some of the rule relaxations and tax reductions relevant for the advancement of electrification are listed below:

- **Electric energy taxes**

The electric energy taxes reduces from 405 DKK/MWh_e to 155 DKK/MWh_e over the years 2018 to 2021 [Boye Petersen, 2018].

- **Requirements for power plant heat.**

Traditionally, the production of both power and heat have been a requirement for power plant heat. These requirements are now open for exemption. [Siemens A/S et al., 2018].

- **Taxes on surplus heat**

Previous taxes of 51 DKK/GJ is replaced by fixed tax of 25 DKK/GJ, (possibility of reduction to 10 DKK/GJ) [PricewaterhouseCoopers, 2019].

All of the above mentioned relaxations increase the incentive for large scale heat pumps, as it become desirable to utilise wind power and photovoltaics for heat production. Additionally, large scale heat pumps take advantage of local, usually unutilised heat from renewable energy sources as sea water, sewage water or air.

1.1 Heat Pumps in the Danish District Heating System

A number of recent studies investigate the potential of large scale heat pumps in district heating systems. The socioeconomic study in [Lund et al., 2016] finds that, the potential for heat pumps can ideally mount up to a socioeconomic benefit of 750 million DKK pr year despite being sensitive to electricity and fuel prices. The study also concluded that variations in performance and investment costs did not appear as a risk to the feasibility of large scale heat pumps. A script produced for *Danish Energy Agency* and *Grøn Energi*, [Kortegaard Støchkel et al., 2017], describes how large scale heat pumps have some unique features:

- Allows for the usage of energy from low temperature heat sources as sea water, air or waste water.
- Combines the usage of surplus heat and the industrial need for cooling with heat production.
- Increases the efficiency of existing units (boilers, power plants etc.) by using the surplus heat in the flue-gas.

All of these features are either related to the usage of renewable energy sources or to the usage of energy which otherwise was wasted. [Kortegaard Støchkel et al., 2017]

In the technology catalogue presented from Danish Energy Agency and Energinet [2016], it is described how learning curves express the idea, that each time a unit from a particular technology is produced, some learning is accumulated. As a result, the next unit becomes cheaper. Additionally, the innovation of the particular technology has two aspects: the market-pull model and the market-push model. The first mentioned includes the technologies evolving and thereby pushing themselves into the market, whereas market pull where the market itself leads to development and innovation of the technology. Last mentioned is to a great extent dependent on climate and energy policies, which currently attracts an increasing amount of attention. Since heat pumps as described are a promising tool for increasing the efficiency of existing energy systems, these are expected to see a significant market-pull. Based on this, the incentive to acquire more information and experience regarding large scale heat pumps and the application of them increases. While the existing experience is very limited, modelling results and new knowledge on sensitivity on heat pumps systems become interesting for future design and development of such systems. Additionally, large investments in heat pump systems are associated with a number of uncertainties, since investment costs and performance is evaluated against fuel and electricity prices. With high electricity prices, it would be profitable with a more expensive but better system in terms of performance, while low electricity costs might imply that low investment costs are more important than performance. Furthermore, the costs of fuel influences the competitiveness of the heat pumps. [Danish Energy Agency and Energinet, 2016]

One reason for large scale heat pumps being particular interesting in the debate of the modern energy systems in Denmark is, aside from the recent relaxation of regulations and its potential for using renewable energy sources, its possibilities for providing ancillary services. The report from Energinet, [Moll Rasmussen et al., 2019] which outlines the assumptions and conditions for analysis and reports published by Energinet, describes how an increasing electricity demand in the coming year is associated with a number of uncertainties mainly due to the limited experiences with projecting new technologies as large scale heat pumps. A number of existing coal-fired units faces a phase-out and many of these are most likely set to be replaced by (among other things) large scale heat pumps. The expected capacity increase for large scale heat pumps is expected to be in the order of 350 MW_e in 2040. This is followed by a capacity increase for both wind- and solar power. The underlying challenge is that the development and the forecasts depends strongly on the development of the new technologies in terms of efficiency improvement and fuel costs [Moll Rasmussen et al., 2019].

Figure 1.2 illustrates how the electricity consumption for large scale heat pumps is expected until 2040.

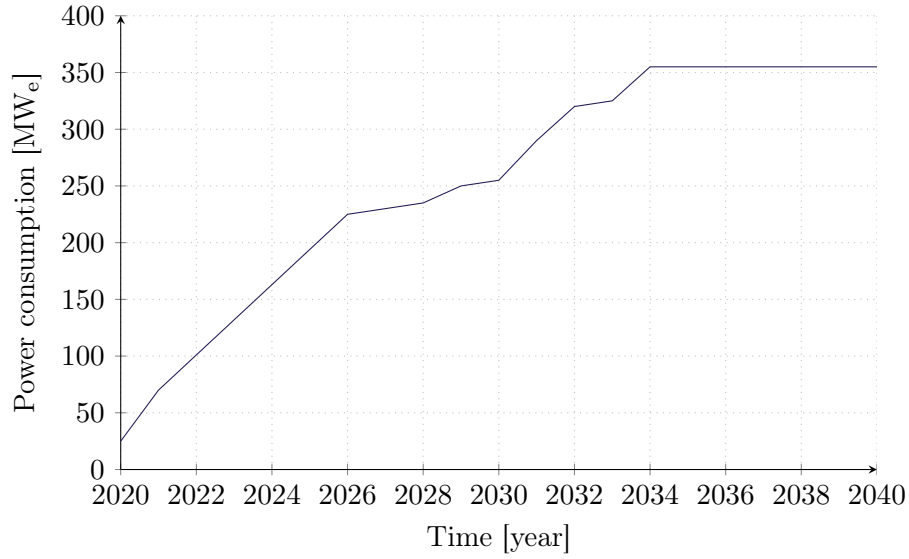


Figure 1.2: Expected electricity demand for both centralised and decentralised heat pump units in the Danish district heating. [Moll Rasmussen et al., 2019]

A distinct increasing tendency is seen in Figure 1.2. Furthermore, the tendency indicates that a significant increase is expected in a short-term perspective. One decisive reason for this tendency is however based on the expected lifetime of the existing units (e.g. a number of existing power plants is expected to be replaced). In continuation hereof it was found that the operators almost without exception want long-term conversions of their existing centralised power units to a more decentralised heat production based on a mix of smaller units. An example of a system, which is already in the process of planning such a phase out of a centralised coal fired plant is located in Esbjerg, Denmark. This plant will further form the basis for the example system used in this thesis.

1.2 Esbjerg Case study

This project is conducted in cooperation with Added Values and revolves around a subject related to an ongoing project in Esbjerg.

In March 2023 a 460 MW_q coal fired power plant is set to close along with a number of other small oil-fired reserve plants. The system and the planned phasing out of the oil- and coal fired plants in and around Esbjerg is seen in Figure 1.3.

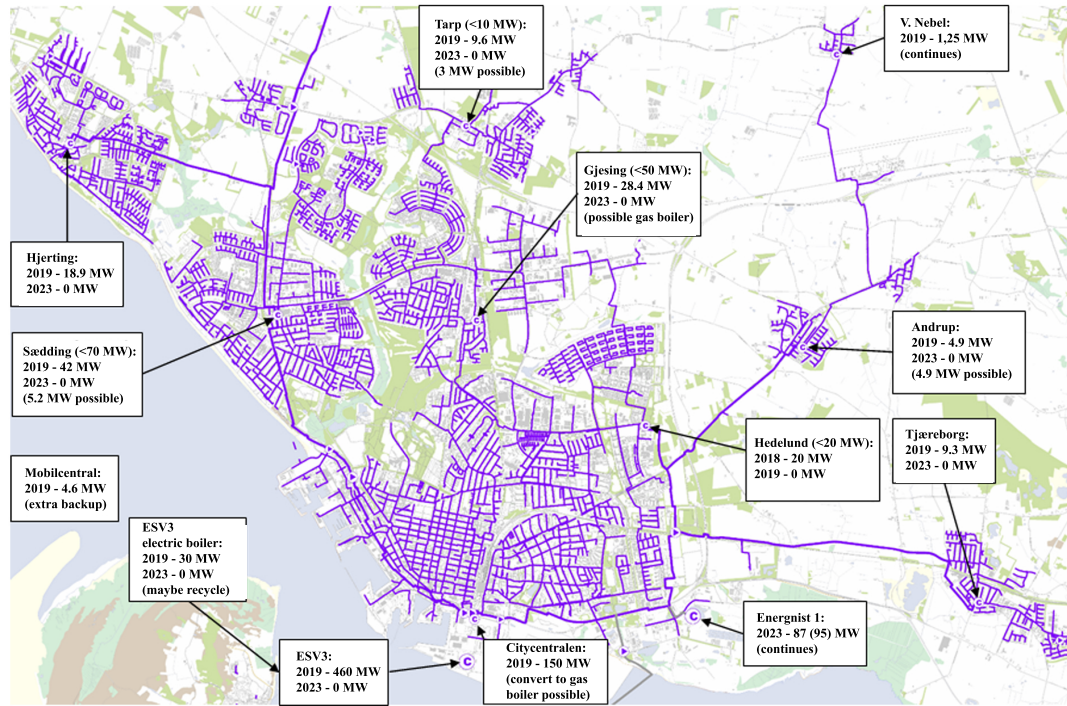


Figure 1.3: Map of the planned phasing out of oil- and coal fired plants in and around Esbjerg.

An apparent consequence of this, is that new units must be introduced to replace the coal- and oil fired capacity. As a part of the solution, a considerable amount of large scale heat pumps is expected to be relevant. The integration of heat pumps in such a system can be accomplished in many ways, where an example of how such a system could be designed can be seen in Figure 1.4.

Among both wood chip boilers, electric boilers, gas boilers and a waste incineration, a 50 MW_q sea water heat pump unit is expected to be implemented. These sea water heat pumps in a system as presented in Figure 1.4 will form the underlying basis for the requirements and operating conditions presented in this study.

One contributing reason for Figure 1.4 being a reasonably suggestion to a system design is its potential for ancillary services. Aside from the heat pumps, a relatively large wood chip boiler is introduced to boost and maintain the temperature of the district heating water. The heat pump does, aside from its advantages in using renewable energy for district heating production, in combination with the electric boiler form a reasonable potential for providing ancillary services. This due to an expectation of that the heat pumps can be within a short amount of time can reduced in load while the electric boilers (which by default is switched off), consumes power almost immediately. However, especially due to the very limited amount of experience, a number of questions regarding the implementation can be raised. First of all, the heat pump unit in Figure 1.4 would have to be a designed as a concept consisting

of a number of heat pumps, which can be combined in series or in parallel or in a combination of the two. Secondly, the interest in ancillary services is associated with further requirements for the performance and must consequently be included in the design considerations.

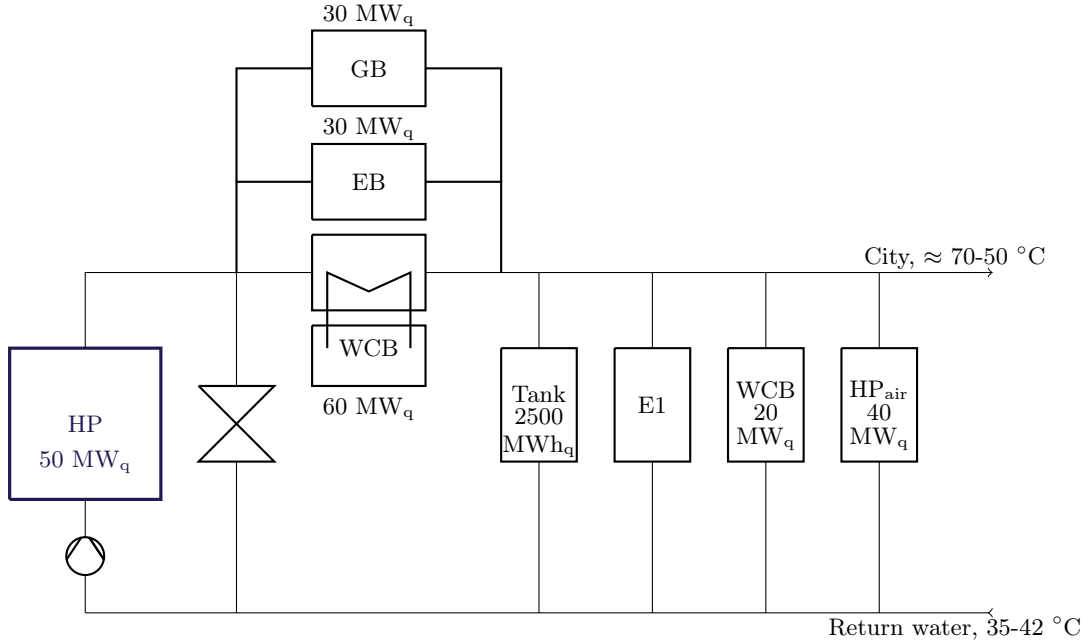


Figure 1.4: Expected system design for Esbjerg used for the case study. HP is the heat pump concept, WCB represents wood chip boilers, EB is an electric boiler, tank is a heat storage tank, GB gas boilers, E1 represents the waste incineration, *Energist 1* and HP_{air} is air source heat pumps.

1.3 Heat Pump Integration

The following sections seeks to investigate and describe some of the existing experience and knowledge for the integration of large scale heat pumps in preparation for integration in a Danish energy system.

1.3.1 Concept Design

When deciding for a concept design for an integrated heat pump system, there is various combinations and design options to consider. In the end, the main objective seen from the perspective of the operator of the heating plant, is to deliver heat to the consumers at the lowest possible price. However, the price of a heat pump concept, and in the end the heating price, does also depend on a number of parameters, which includes the size (capacity) of the system and the heat source. [Henrik et al., 2018]

In October 2019 [Rambøll et al., 2019] published a report with the purpose of gathering information of large scale heat pumps already in operation in the Danish district heating. Despite sharing experience from 24 existing heat pump units, the report included only a single 5 MW_q sea water heat pump. Flue gas and air source heat pumps seems to dominate the danish market, and additionally, the maximum observed unit, was listed with a capacity of 10 MW_q.

The price and performance of the heat pump systems depend on many parameters as design and heat sources. Some heat sources have limited availability, while other, as sea water is practically unlimited - but these are in some cases associated with other challenges or disadvantages. The sea water heat pumps expected for the project in Esbjerg, has the advantage that sea water is an unlimited heat source. On the other hand, the temperature of the sea water usually reduces significantly during the winter, where the heat demand peaks. The low heat source temperature does in worst case imply that the heat pump can not operate. Generally large temperature differences or temperature lifts between the heat sink and heat source causes the COP to reduce. This is additionally one motive for serial coupling of heat pumps, as the reduced ΔT for the heat pumps causes the Coefficient of performance (COP) to increase. The COP represents the ratio between the useful heat and the power supplied to the heat pump, $\text{COP} = \frac{\dot{Q}_h}{P}$. However, any general solution or disruptive experiences on capacity and design have been demonstrated yet. [Elmegaard et al., 2015b]

In terms of concept design, the effect of serial coupling of heat pumps was investigated in [Baik et al., 2013]. The study found that the more heat pumps in series, the higher overall COP. Generally heat pumps in series allows for good performance even when large temperature lifts are necessary. On the other hand, the requirement for controls increases and it is a typical requirement to have the same mass flow rate through each unit which additionally will have to be equally sized. On the other hand, a more easy-to-control system can be achieved by a parallel arrangement, which however reduces the performance at high temperature difference. [Rudio and Controls, 2010]

Aside from indications, expectations and small scale experience as listed in the previous sections, this knowledge can not alone decide how to design a large scale heat pump concept for an energy system. As was outlined in several papers and reports as [Elmegaard et al., 2015b] and [Rambøll, 2019], one of the major challenges is the lack of experience.

Existing Large Scale heat pump units

As was additionally found in [Rambøll et al., 2019], most existing units in the Danish energy system are units with significantly lower heating capacity than what is planned in Esbjerg. Additionally most existing units operate with other types of

heat sources, than the planned sea water in Esbjerg. However, by broadening the search area slightly examples of large scale heat pump units in operation for the district heating network can be found.

In Drammen, Norway, a 15 MW_q base load heat pump system was designed and implemented in 2010. The system consists of three identical two-stage ammonia screw compressor heat pumps. One of the special and interesting things about the system in Drammen, is the use of Ammonia as refrigerant. In Denmark, rules regarding HFC-refrigerants (hydro-fluorocarbons) are only allowed with a maximum of 10 kg per unit. This mean, that for larger units, as the one in Drammen and the planned unit in Esbjerg, natural refrigerants are preferable. The unit in Drammen, delivers district heating water at 90 °C during peak load periods. In the summer, the demand is <2 MW_q and the temperature of the district heating water is reduced to 65 °C. The temperature of the return water is 60-65 °C all year, similar to the sea water, which is extracted at a depth of around 40 m ensure constant temperatures of 8-9 °C all year. One of the greatest challenges in projecting large scale systems is to get the design right. To maximise the efficiency of the system in Drammen, the district heating water is heated by the three heat pumps arranged in series for the main flow. This mean, that all three heat pumps in the series increase the temperature in three equal sized steps. This furthermore ensures, that the system is capable of delivering 90 °C in case of failure of a unit. [Hoffmann and Forbes Pearson, 2011]

In Stockholm, the worlds biggest sea water heat pump facility has been in operation since 1986. It consists of 6×30 MW_q units. The system was originally using R22, but was retrofitted to R134a in 2003. The heat pumps deliver district heating at around 80 °C, with a return temperature around 57 °C and a constant temperature of the seawater at 3 °C. The seawater is extracted at 15 m depth. [Friotheim AG, 2017].

Despite seeking inspiration and experience in some neighbouring countries to Denmark, any straightforward solutions does not seem to be present. The immediate conclusion is that large scale heat pumps systems exists and can be operated successfully. Furthermore, the existing units does not give any general solutions especially when considering the possibilities and best designs for providing ancillary services.

1.3.2 Ancillary Services

Historically, most of the ancillary services have been provided by the conventional power generation units, but since these are gradually being replaced by renewable energy units, other solutions become necessary. Additionally, the conventional units are in most cases replaced by renewable energy as wind and solar power, which in nature is rather intermittent. This cause the planning, operation and design to be challenging, and increases the necessity of ancillary services, to ensure stable and reliable operation of the electricity grid. [Elmegaard et al., 2015a]

Ancillary- or grid balancing services are necessary to preserve the stability and balance in the power grid. In short, ancillary services covers all electricity production- and consumption. In Denmark, Energinet is the operator of these ancillary services, and have the responsibility of buying the reserves. Despite the portfolio of ancillary services being extensive and the use of them very complex, the purpose is simple: to maintain the balance in the electricity market and the general stability in the electricity grid.[Energinet.dk, 2018]

The grid balance depends on the balance between the production and the power consumption. Changes in the consumption or disturbances in the production affect the balance in the system and cause frequency variations. Energinet similarly buys the ancillary services from either the power producers or consumers. Different deployments and different requirements applies to different types of services. [Energinet.dk et al., 2019]

The different types of ancillary services can in general be divided into the three categories illustrated in Figure 1.5.

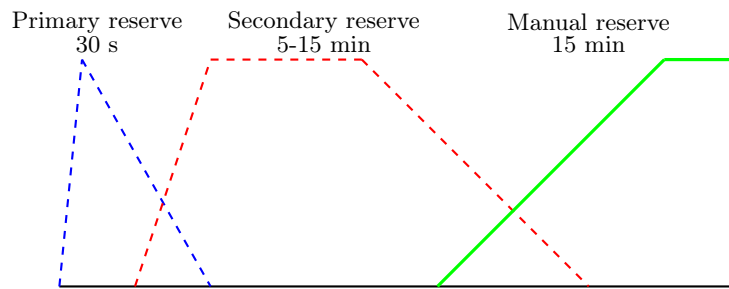


Figure 1.5: Time of delivery for the three ancillary services in question. [Kortegaard Støchkel et al., 2017]

A review of the different types and the general purpose of ancillary service can be found in Appendix B. For the extent of this thesis, the main focus is on the primary and secondary reserves; the Frequency Containment Reserve, FCR and the Automatic Frequency Restoration Reserve, aFRR. Table 1.1 gives a summary some of the technical requirements for FCR and aFRR in the western Denmark, DK1, and Table 1.2 list the 2019 average payments for aFRR and FCR.

Table 1.1: Overview of technical requirements and market rules and regulations for FCR and aFRR [Smed and Rambøll, 2019]

Technical requirement	FCR	aFRR
Direction	Up/down Asymmetric	Up/down symmetric
Total volume requirement	± 21 MW	± 90 MW
Ramping time	≤ 30 s	≤ 15 min
Part availability	50 % within 15 s	NA
End	≥ 15 min (until aFRR)	Maintain continuously
Minimum volume of bid	0.3 MW	1 MW
Maximum volume of bid	NA	50 MW
Availability Payment	Yes - pay-as-cleared	Yes - pay-as-bid

The profitable payments listed in Table 1.2 are along with the increasing necessity one of the motives to the increased focus on ancillary services.

Table 1.2: Average payments for ancillary services based on 2019 numbers. [Energinet, 2019]

Reserve	Availability payment [DKK/MW _e /h]	Activation payment [DKK/MW _e /h]
FCR _{up}	276	none
FCR _{down}	26	none
aFRR _{up/down}	648 ¹	elspot ± 100 DKK

1.3.3 Experience and Potential in Grid Balancing Services

In connection with EnergyLab Nordhavn and in cooperation with DTU (Technical University of Denmark), HORFOR A/S has conducted a test on a system of a heat pump and an electric boiler in preparation for delivering ancillary services. The test was conducted on a 0.25 MW_e two stage ammonia heat pump from Johnson Controls. It was found, that during a test run of the heat pump with both full-load and part-load operation, most of the regulation times were compatible with the requirements for DK2 aFRR and mFRR (Manual reserve, Manual Frequency Restoration Reserves), but do not meet the requirements for FCR-N and FCR-D which mean that full capacity must be delivered within 150 s and 30 s (with the first 50 % delivered within 5 s) respectively. With the exception of a complete shut down, all load regulation times was found to be ≥ 2 minutes for both upward and downward regulation.

¹aFRR is a relatively new market open for ancillary services, and prices will presumably reduce when more units is in play for the reserve. An estimate of the future levels is ≈ 150 DKK/MW_e

However, a change of control strategy was found to improve the response time, so that for FCR-N the expected response time for a part of the capacity reduces to ≤ 150 s, which fulfils the requirements. For the FCR-D, it was found that the heat pump can actually shut down almost momentarily, meaning that the services can be provided within ≈ 30 s. However, the requirement about the 50 % within the first 5 s, can not be met. Furthermore, a requirement for FCR-D is that the reserve must be reestablished in less than 15 minutes after completed regulation. This was found to be a challenge, since the heat pump was stationary for ≈ 20 minutes before the start-up of the system, which was found to take another 6 minutes, could begin. The test results indicated, that heat pumps certainly could offer themselves in ancillary services markets, but for DK2, some adjustments to the regulations and requirements are needed, if heat pumps should be relevant for all types of reserves. It is additionally suggested, that heat pumps should be preferred for up-regulation solely.[Rambøll, 2019]

While a more practical test to investigate the possibility for ancillary services was presented in [Rambøll, 2019], other studies investigate the flexibility and possibility of integrating large scale heat pumps as a player in energy systems by different modelling approaches. In [Meesenburg et al., 2018], a thermoeconomic (exergoeconomic) analysis of a heat pump system used for ancillary services was carried out. It is stated, that despite knowing that large scale heat pumps are promising for the integration of large amounts of renewable energy into energy systems, the ability and limitations in terms of flexibility and performance for ancillary services needs further investigation. The study presented in [Meesenburg et al., 2018] focus on the integration between the heating and the power system, which basically provides two products: heat supplied to the district heating grid and ancillary services to the electricity grid. Last mentioned was found to have several consequences to the operation of the heat pump. One of the important points found in the study is that during the design process of the system, it is important to consider the possibility of flexible operation. The paper uses a constant part load efficiency and performance map based heat pump model implemented in the Modelica language to describe the heat output of the heat pump. It was found that by large overdimensioning the system, the flexibility increased, but additionally also increased the heat losses and need for support from electric heaters.

In [Terros et al., 2020] the potential for large scale heat pumps in the Austrian energy system was investigated with regard to electricity market options. Austria faces some of the same challenges as in Denmark, with a very limited experiences in designing and planning large heat pump systems especially with regard to possible ancillary services. However, the study concluded that heat pumps have the potential to be active players in the Austrian reserve market. Opposite to what was suggested in [Rambøll, 2019], the paper propose that a reasonable bidding strategy could be to operate at the decided minimum load of 50 %, and offer the remaining 50 % for balancing services in the aFRR market. One consequence of this was however, that the

feasibility of the heat pump system depends a lot on the amount of bidding rounds won.

To summarise, large scale heat pumps will undoubtedly play an important role in future energy systems. Large scale heat pumps provides great opportunities for increasing the implementation of renewable energies, as the heating sector can absorb large amounts of electricity. The challenge is currently related to the various uncertainties associated when planning large scale heat pump systems. It is naturally important to ensure, that the system is designed properly in terms of efficiency. However, many parameters affects both the operation and in the end the cost of a system. Based on a planned project in Esbjerg, the design of a 50 MW_q heat pump concept should be investigated. This includes base load operation as well as possibilities for ancillary services, since the necessity for these increase, concurrently with the increase in the share of renewable energy.

2 | Thesis Statement

In Chapter 1, the potential for integrating large scale heat pumps in future Danish energy systems was examined along with its challenges and market premise. The existing experience in projecting large scale heat pump concepts¹ for Danish energy systems is limited, causing predictions of cost and performance to be associated with numerous uncertainties. This project seeks to enhance the knowledge in large scale heat pumps based on a projected case in Esbjerg, Denmark. The main field of concern in this thesis revolves around quantification of effects from operating conditions and variations in these to the choice of heat pump concept.

Given a specified operational profile, how should the heat pump concept be designed and which parameters and to what extent does variations in cost predictions affect the choice of heat pump concept? Furthermore, how does different concepts affect the performance during dynamic operation with the purpose of providing ancillary services?

For the system in Esbjerg, much attention is put in the opportunity and possibility for providing ancillary services. This has several reasons, but most importantly, it plays an important and useful role in our future energy system and secondly it has some beneficial economical advantages.

This study will focus on the development and investigation of the following aspects:

- By the use of a suitable dynamic modelling language, the development of a dynamic simulation model of a heat pump system with the purpose of evaluating the system performance and dynamic response.
- With an appropriate nonlinear optimiser find the optimised heat pump concept in terms of costs for operation and investment.
- Investigate the robustness of the optimised concept. This includes identification of the which parameters and to what extent changes in these affects the optimum concept.
- Based on the findings of optimum designs, investigate and evaluate whether and how much different concepts performs if subject to FCR and aFRR ancillary services.

¹In this context, a heat pump concept is defined as: the configuration of heat pumps in terms of number of serial or parallel connections and the capacities of each of the heat pumps.

3 | Modelling

This chapter describes the underlying base of the heat pump model used for the optimisation. The heat pump unit itself and the system around including pipes and controls are developed in the Modelica Language and later exported as an FMU for optimisation in Python.

3.1 Heat pump performance map

The heat pump used for the concept modelling is based on the performance map developed in [Thomasen, 2020]. Equation-fit models or parameter estimation models can be considered as some kind of black-box modelling, which, based on one or a few equations is capable of describing the performance. This can fundamentally be done on both small-component scale or on a full-system scale. For the extent of this study, the potential and advantages of a performance map model will be the leading argument for the choice of modelling approach and the discussion of whether a performance map model or a full physical/refrigerant cycle based model is necessary is delimited to a discussion of limitations.

On component level, the equation fit approach is commonly used in energy calculating and simulation software [Jin and D. Spilter, 2002]. The equation fit approach used for the heat pump model in this thesis, is based on manufacturer data conducted from GEA RTSelect, which is a software designed for selection and configuration of GEA products [GEA Group, 2019]. A more comprehensive description of the development of the performance map can be found in [Thomasen, 2020]. One of the special features incorporated in the performance map for the heat pump is the load dependency. In many existing studies as [Dott et al., 2013] and [Tran et al., 2016], applies and validates the performance map approach, but does not take into account the performance degradation when operating in part load. Similar for studies with focus on different aspects of the annual operation of heat pumps, as was found in i.a. [Grønnegaard Nielsen et al., 2016], the COP was assumed constant during operation. However, as was also accounted for in [Bach et al., 2016], the COP changes with temperatures but also load variations. An example of this degradation is seen in Figure 3.1. In [Thomasen, 2020] a full year simulation using a load dependent performance map additionally indicated, that the load dependency affects the final costs compared to simulations made under the assumption that the COP remains constant when the load is kept above 40 % at all times. For this reason, the load dependent performance map developed in [Thomasen, 2020] will be used to represent the heat pump performance.

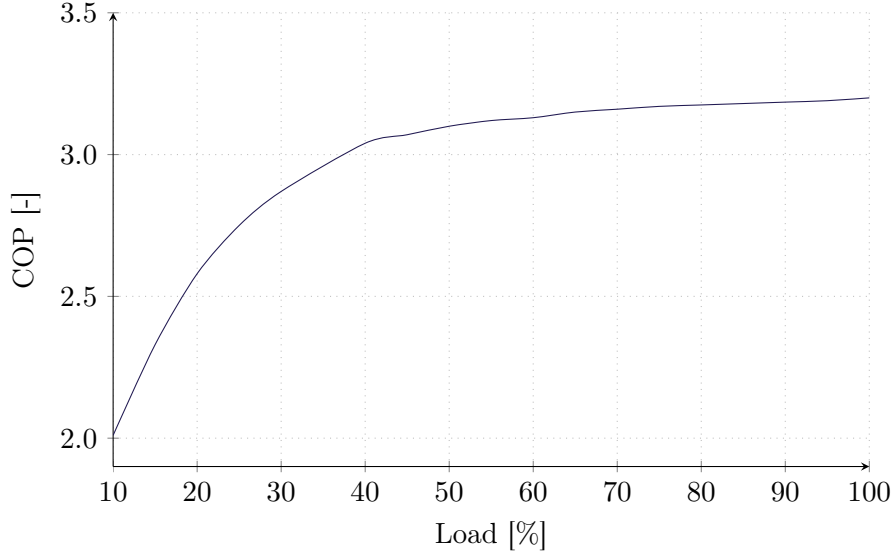


Figure 3.1: COP as a function of load at fixed evaporator temperature and condenser outlet temperatures of $-5\text{ }^{\circ}\text{C}$ and $79\text{ }^{\circ}\text{C}$ respectively. Data from GEA RTSelect [GEA Group, 2019].

The performance map consists of two equations: one describing the heat output and one describing the COP. Both as a function of the evaporation temperature, T_{eva} measured in Kelvin [K], the temperature of the district heating water, $T_{\text{dh,out}}$ [K], and the *Load* in percentages [%]. The two equations can be found in Equation 3.1 and Equation 3.2.

$$\begin{aligned} \dot{Q}_h = & -2410000 - 1063000 \text{ Load} + 70.96 \text{ Load}^2 - 1667 T_{\text{eva}} + 10030 T_{\text{dh,out}} \\ & + 4001 \text{ Load} T_{\text{eva}} + 306.7 \text{ Load} T_{\text{dh,out}} \end{aligned} \quad (3.1)$$

With \dot{Q}_h representing the heat flow to the district heating water in watts [W].

$$\begin{aligned} \text{COP} = & -12.52 - 3.08 \exp(-0.07 \text{ Load}) + 0.71 T_{\text{eva}} + 0.00097 T_{\text{eva}}^2 \\ & + 0.03 (-12.52 - 3.08 \exp(-0.07 \text{ Load})) T_{\text{eva}} - 0.47 T_{\text{dh,out}} \\ & + 0.001 T_{\text{dh,out}}^2 - 0.03 (-12.52 - 3.076 \exp(-0.07 \text{ Load})) T_{\text{dh,out}} \\ & - 0.002 T_{\text{eva}} T_{\text{dh,out}} \end{aligned} \quad (3.2)$$

Equation 3.1 and Equation 3.2 form the base of the heat pumps unit used for modelling the system of heat pump units, and predicts \dot{Q}_h and COP with maximum deviations from the manufacturer data from GEA of around 6 % and 7 % respectively. The highest deviations are generally associated with very low loads. A further validation of the performance map can be found in [Thomasen, 2020].

When using the equation-fit approach for heat pump modelling, it is important to be aware of the limitations that occur due to the extent of the data which the equations are based on. In this case, the temperature ranges are as listed in Table 3.1 for all loads.

Table 3.1: Temperature intervals used for the development of the performance map of \dot{Q}_h and COP.

*For outlet temperatures of above 69 °C, the GEA RTSelect failed to produce useful results below 10 °C evaporator temperature.

	$T_{\text{dh,out}}$ [°C]	T_{eva} [°C]
T_{min}	44	-5
T_{max}	79	10*

Outside the temperature range, gradients may change and unfeasible or nonphysical results might occur. Additionally, the evaporation temperature and the temperature of the sea water T_{sea} , will be implemented with a constant $\Delta T = 7$ K due to a potential brine. A further investigation of the validity and the behaviour of the map at conditions beyond its limits is found in Appendix A.

3.2 Heat pump system

The heat pump performance map presented in Section 3.1 was implemented in the object-oriented, multi-domain modelling language, Modelica. This section gives a brief description of the Modelica modelling language and a description of how the heat pump system is build and implemented in the Modelica simulation engine Dymola.

3.2.1 The Modelica Language

In short, Modelica allows to describe mathematical behaviour with a high-level declarative language. It is typically very suitable for many engineering systems. The modeller describes the behaviour of different types of engineering components across engineering domains. The reason for using Modelica is its technical capability. Behind the relatively easy-to-use interface, Modelica uses complex algorithms and the Modelica compiler allows to focus on the high-level mathematical descriptions of components and component behaviour. In return, Modelica also provides high performance simulation capability without having to relate to the DAE's (Differential Algebraic Equation), symbolic manipulation, solvers or even the post processing part. Modelica supports both causal modelling (typically relevant for control systems) and acausal modelling within the same model. Another advantage of Modelica, it that it is designed as an open language, meaning that all specifications are freely available. [M. Tiller, 2014]

In [Richert et al., 2004] a comparison of Modelica and Matlab was conducted by the means of a diesel engine model, which was well known and tested in the causal modelling approach MATLAB/Simulink and build from scratch in the acausal Modelica/Dymola. The two modelling approaches were compared in terms of model build up, simulation, visualisation of results and further post-processing. One main conclusion was, that it is not a questing of deciding for the one and only correct modelling approach and in fact, combinations of abilities and features probably leads to the best results. The Modelica simulation engine Dymola, which will also be used in this thesis, was developed for graphical, fast and numerically stable modelling, and is good at it. However, in other aspects, Matlab was found invincible, supporting the statement, that no single approach is reigning supreme. Dymola however, offers a number of features allowing the modeller to combine products for simulation. This also appeared to be a convenient feature for the purpose of this thesis, where the export to FMU option was utilised.

The Buildings library

One usefull feature of Modelica is the combination of its *package* system and the fact that Modelica is an open-source programming language. A package in Modelica can be considered as a dictionary holding a collection of Modelica entities. The entities can from the package be reused or referenced, rather than having to repeat them. The packages organise types, models, functions etc. A "base" package called the *Modelica Standard Library* maintained by the Modelica Association is a package/library that includes definitions that is generally useful for engineering purposes (physical/machine constants, SI-units, models for among other things control, electrical systems, mechanical systems, fluids and thermal systems). [M. Tiller, 2014]

While the Modelica Standard library consists of a wide range of basic definitions across domains, a wide number of additional open source Modelica libraries exists. One of these is the *Buildings* library, which provides models for HVAC systems, controls, heat transfer, airflow and ventilation etc. The library is originally designed for simulation models of buildings, control systems and district heat, which in most cases extent packages from the *Modelica Standard Library*. It implies that the models in the *Buildings* library are compatible with the *Modelica Standard Library* and furthermore, *Buildings* is a well tested library being numerically very stable. The buildings library does for instance provide a simplified medium-model for water, that assumes constant density, which is applied for simplification and with regard to computation time. [Wetter et al., 2014]

3.2.2 Overall heat pump system

The system used for the concept optimisation and sensitivity analysis, generally consists of a number of heat pump units, the coupling between them and some control, to ensure the desired output. The purpose of the following optimisation is to decide

the optimum number and capacities of heat pump units and the connections between. For this reason the simulation model must be designed to allow for different configurations and capacities while still delivering the desired output in terms of district heating water temperature and heat output or power consumption.

A simplified sketch of the full system is seen in Figure 3.2.

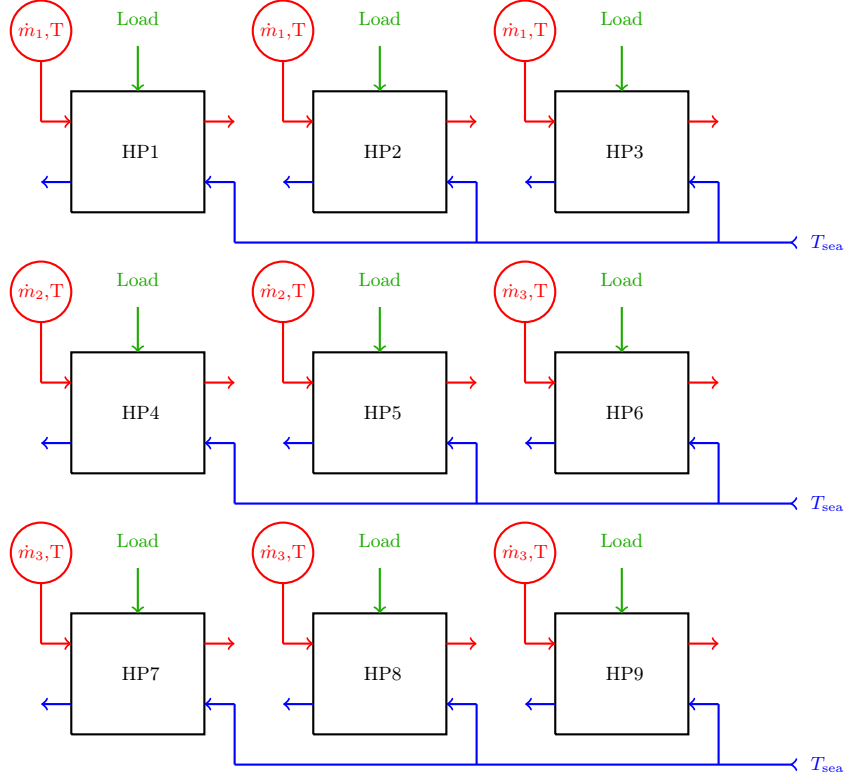


Figure 3.2: Simplified sketch of system used for simulation and optimisation.

The overall system in Figure 3.2 basically consists of nine individual heat pumps denoted HP1-HP9, each with a separate mass flow source which is however identical for each parallel string (e.g. HP1, HP2 and HP3). The inputs to the system are based on conditions expected for the case in Esbjerg. The graphical representation of the simulation setup in Dymola can be found in Enclosure A.

The following sections describe the development of the system in Figure 3.2, starting from the heat pump unit itself.

Heat pump unit

The heat pump unit designed in Dymola is illustrated in Figure 3.3.

The icon view seen in Figure 3.3a is the graphical representation of the heat pump component, as it will appear in the full system, with two sets of fluid ports, one

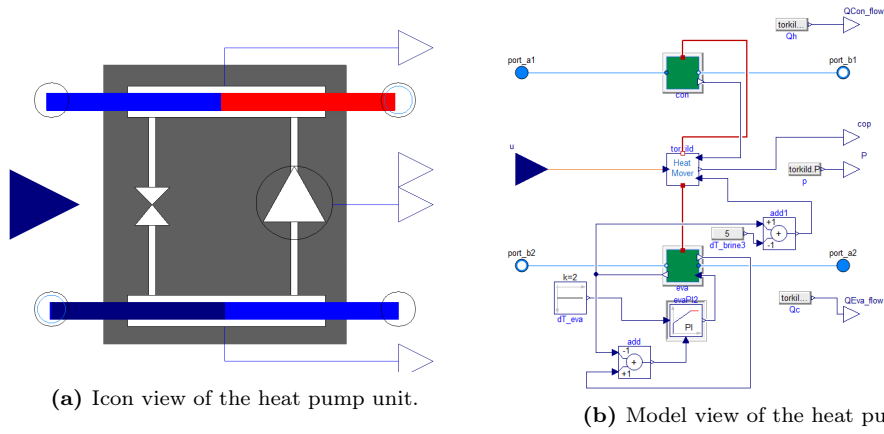


Figure 3.3: Modelica representation of the heat pump unit. Figure A illustrates the icon representing the heat pump component. Figure B, illustrates the connections inside the heat pump component.

input port and four output ports, which as can be seen in Figure 3.3b represents the inlet and outlet of the district heating water (denoted $port_a1$ and $port_b1$), the heat source ($port_b2$ and $port_a1$), the load input and the heat output, COP, power consumption and cooling rate. The heat pump unit consists basically of two pipes and a *heat mover*. The two pipes are seen from the green boxes in Figure 3.3b and represents the condenser and the evaporator respectively. It has been assumed, that a constant temperature difference, ΔT_{eva} across the evaporator is a reasonable target. This is ensured by the PI-controller, which adjusts the mass flow rate through the evaporator.

The output ports, which are represented by the white, triangular shaped ports, allow to measure the heating rate, the COP, the power consumption and the cooling rate which is all calculated inside the *heat mover* unit. The principle of the *heat mover* unit is seen in Figure 3.4.

Figure 3.4a is the icon view of the heat mover model, which was seen inside the heat pump unit in Figure 3.3b. The heat mover has three input ports, two heat ports (one in the bottom and one at the top) and one output port. The three input ports represent the variables ($T_{dh,out}$, T_{eva} and Load), which the performance map in Equation 3.1 and Equation 3.2 was based on. The heat output and the COP are then calculated from Equation 3.1 and Equation 3.2, and from this the cooling rate and the power consumption are calculated using Equation 3.3 and Equation 3.4.

$$\dot{Q}_c = P (COP - 1) \quad (3.3)$$

$$P = \dot{Q}_h - \dot{Q}_c \quad (3.4)$$

The heat flow rate \dot{Q}_h is injected to the district heating water and \dot{Q}_c is the heat flow

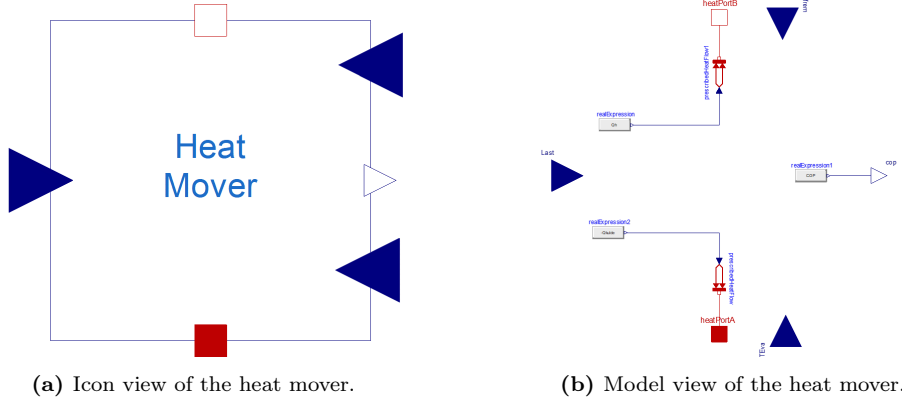


Figure 3.4: Modelica representation of the unit to transfer heat between the condenser and the evaporator.

rate extracted from the heat source, which in this case is sea water. This is done using the *prescribed heat flow boundary* components from the Modelica standard library. They allow the specified heat flow rates \dot{Q}_h and \dot{Q}_c to be injected to a thermal system at a given heat port. The heat ports are found in the Modelica Standard library, and are seen at the top and bottom of Figure 3.4. The heat ports allow for the heat transfer into the pipes found in the condenser and the evaporator component seen in Figure 3.5.

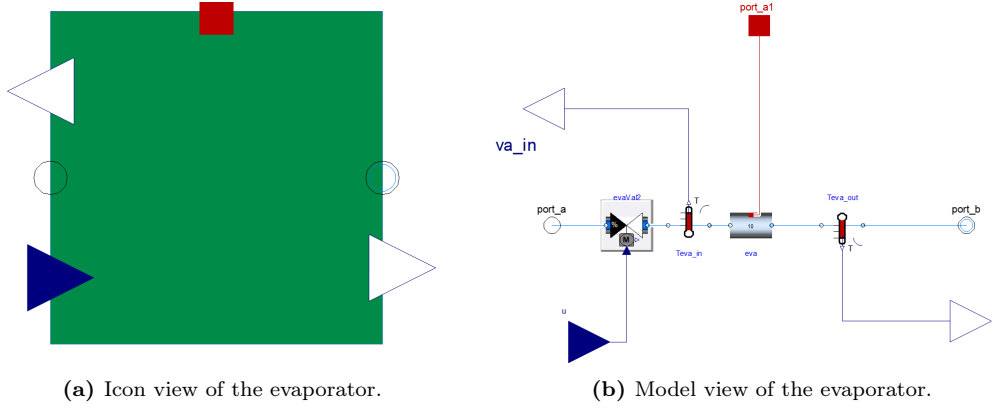


Figure 3.5: Modelica representation of the simplified evaporator.

The construction for the condenser and for the evaporator is almost identical, which is why only the evaporator is illustrated. The condenser and the evaporator components originate from the same base model, and makes use of the *replaceable* keyword allowing the modeller to change or redeclare components in a model. For the evaporator, the replaceable component is the valve that controls the mass flow rate to ensure $\Delta T_{eva} = 2$ K. In the condenser, this valve is not necessary, and consequently replaced by a pipe with no pressure loss. The pipe named *eva* in Figure 3.5b repre-

sent the heat exchanger (i.a. the actual evaporator and the condenser). The pipe is found in the buildings library as (Buildings.Fluid.FixedResistances.Pipe). The pipe allows for external heat exchange which is utilised too extract or add the heat flow rate from the heat pump. The dynamics related to the evaporator and the condenser is included by assigning a reasonable volume to the pipe (i.a. an estimation on the size of the heat exchangers. The volume of the pipes is calculated using Equation 3.5 and Equation 3.6.

$$\dot{Q}_h = U A T_{\text{LMTD}} \quad (3.5)$$

$$T_{\text{LMTD}} = \frac{\Delta T_1 - \Delta T_2}{\ln\left(\frac{\Delta T_1}{\Delta T_2}\right)} \quad (3.6)$$

As an example for the condenser assuming $U = 3.0 \text{ kW/m}^2\text{K}$, $\dot{Q}_h = 10 \text{ MW}_q$, and a temperature increase from $40 \text{ }^\circ\text{C}$ to $60 \text{ }^\circ\text{C}$ with $62 \text{ }^\circ\text{C}$ for the condensing side, the volume of the water is set to 2 m^3 . The heat exchangers are additionally assumed to be plate heat exchangers with a typical plate distance of 0.0005 m .

The essential principles of the heat pump model are, that it is simply considered as a *heat mover* that moves heat between two pipes representing the evaporator and the condenser. The heating rate and the COP of the heat pump is determined by the incorporate performance map, which takes T_{eva} , $T_{\text{dh,out}}$ and the load as input.

Recalling the full system for simulation in Figure 3.2; each of the HP-boxes represents a heat pump unit as described in the previous section. As seen, each heat pump unit is connected individually to a mass flow source, which produces a prescribed mass flow with a prescribed temperature (Buildings.Fluid.Sources.MassFlowSource_T). The mass flow rate delivered by the mass flow source is managed by a temperature controller that ensures, that the outlet temperature of the district heating water leaving the last activated heat pump in each parallel string has the desired temperature.

3.2.3 Control

One of the main challenges in the development of a system capable of operating under various configurations are the control. Two controllers are implemented:

- A mass flow rate controller to ensure a specified temperature of the district heating water.
- A load control that ensures, that the desired heating rate is delivered.

Mass flow rate control

Despite each heat pump having individual mass flow sources, each parallel string should be considered as connected in series on the district heating water side, and

connected in parallel on the sea water side. The reason for the model-decoupling is to ensure that only the dynamics of the activated heat pumps is included. This means, that the mass flow source \dot{m}_1 supplies HP1, with a mass flow rate defined by the temperature controller, and with a temperature defined by the expected operation in Esbjerg. For the next heat pump in the string, HP2, the mass flow rate is similarly \dot{m}_1 . The temperature entering HP2 should however be different from the temperature entering HP1 (assuming HP1 is deployed). The temperature entering HP2 should equal the temperature leaving HP1. The immediate solution was to simply measure and apply the HP1-leaving temperature. However, in cases, where the heat pump *ahead* is not activated, this will lead to errors. Instead, the temperature entering each heat pump is calculated as the district heating return temperature (which corresponds to the input to the first heat pump in each string) plus the temperature difference measured for each of the heat pumps in front, as e.g. $T_{\text{dh,HP2,in}} = T_{\text{dh,return}} + \Delta T_{\text{dh,HP1}}$, with $\Delta T_{\text{dh,HP1}}$ corresponding to the total temperature difference between the return temperature and the temperature increase achieved from HP1.

The input to the temperature control is the district heating outlet temperature. However, depending on the concept, the temperature measurement for this temperature is located either after the first, second or third heat pump in each string if any heat pumps are activated. This is addressed by using control the highest measured temperature in each parallel string.

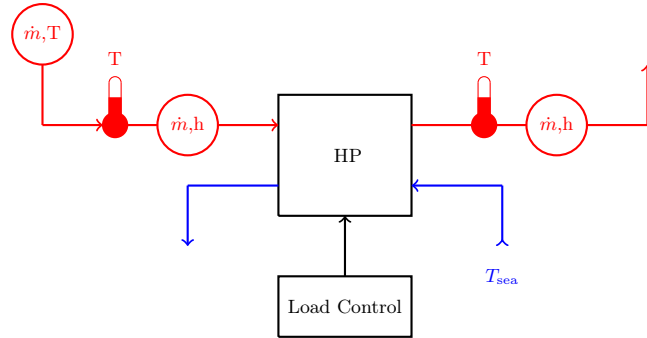


Figure 3.6: Excerpt of the heat pump simulation model that shows a single heat pump and its control measurements.

Load control

In [Rambøll, 2019] it was suggested, that controlling the power consumption instead of the heating output allows for much faster regulation. The reason for this is that the dynamics related to the thermal system is most likely dominating compared to the dynamics in the compressor [Farouk Fardoun et al., 2011]. The power control suggestion will also be considered for the dynamic evaluation in this project. However, it is additionally desirable to be able to use the heat output as a setpoint for simulation. For this reason the load control will be allowed to switch between a heat output setpoint and a power consumption setpoint. Figure 3.6 sketch the control

principles of a single heat pump unit.

For the heat output control, the input to the controller (i.a. the heating rate) is found using an *ideal enthalpy flow rate sensor* from the Buildings library (Buildings.Fluid.Sensors.EnthalpyFlowRate). The enthalpy flow rate sensor uses that the heat flow rate can be determined by Equation 3.7.

$$\dot{Q}_h = \dot{m} \Delta H \quad (3.7)$$

To achieve the desired heat- or power consumption output, the load control adjust the load input to the heat pump. Notice that the input measurement to the controller represents the total heating rate. As a simplification to the control problem, all heat pumps are controlled by the same load signal. Inside the load control box in Figure 3.6, the load control signal from the load controller enters two components: a hysteresis component, and a Variable Speed Drive component (VSD), which is used to define and represent ramping-, power-up and roll out times for compressor. These are based on estimations for load gradients presented for the system in Esbjerg and is set to 120 s for 20-100 % ramp-up, 60 s for 100-20 % ramp down and ≈ 180 s for power up and run-down (0-10 % or 10 - 0 %).

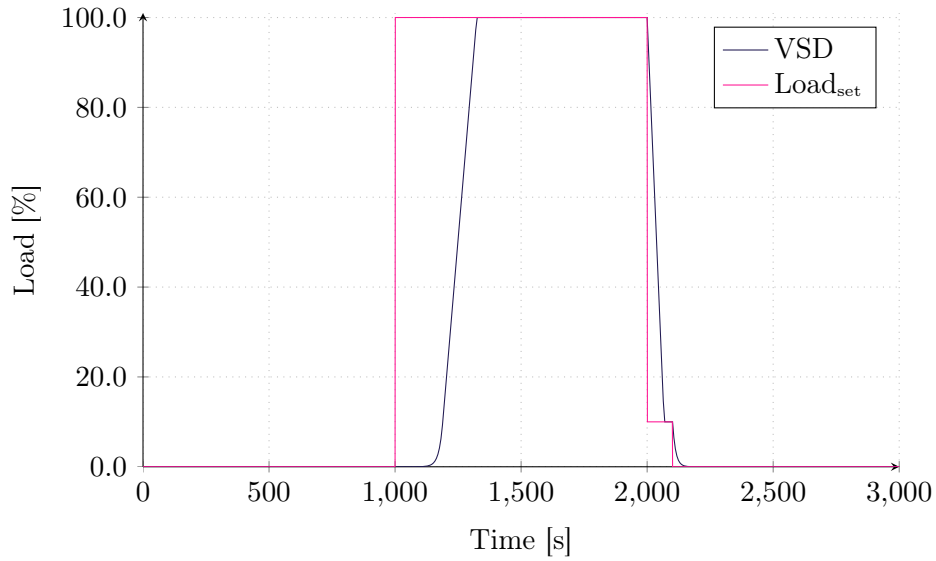


Figure 3.7: The VSD response representing the load gradients applied for the heat. The minimum load is set to 10 %, the time to reach minimum load is 180 s. The gradients are defined so that from 20-100 % the time is 120 s and from 100 - 20 % the time is set to 60 s.

The VSD response to load-setpoints is seen in Figure 3.7. Furthermore, the VSD is activated or deactivated by a boolean (true/false) signal. Whether the VSD is activated or not is determined by the hysteresis. By using the hysteresis, the modeller is allowed to set an upper load limit to achieve a *true* signal and a lower load limit to achieve a *false* signal. This is desirable in terms of load control strategies. The

values of the upper and lower limits depend on the strategy chosen by the modeller. The strategy chosen in this thesis is presented in Table 3.2.

Table 3.2: Hysteresis intervals for the control strategy chosen in this thesis.

Category	u_{low}	u_{high}
HP1-HP3	0	10
HP4-HP6	40	100
HP7-HP9	40	100

From Table 3.2 it appears as if the second and the third string will be activated simultaneously. However, the reason for this is that it is desired not to activate any additional string before reaching full load with those who are already in operation. To avoid the activation of the two strings simultaneously, a filter is used to ensure that string 2 is activated before string 3. An additional boolean variable for each heat pump is introduced to ensure that the VSD can only be activated if it is decided to include the heat pump in question in the simulation.

Nominal Design and Sizing

As presented in Section 3.1, the performance of the heat pump unit is based on manufacturer data from a single GEA screw compressor unit. Consequently, it is important to notice, that its performance is also defined from the nominal conditions which applies for the unit used for the map. Ideally, an extended map could be used to represent a wider range of design points, but for the extent of this thesis, the map is limited to represent a single unit with nominal conditions and specifications as presented in Table 3.3.

Table 3.3: Nominal conditions and design parameters for the heat pump used for the performance map.

Parameter	Nominal condition	Parameter	Nominal condition
Model	XFR-XF2655H-52	Cooling Capacity	8 MW
Frequency	400 V/50Hz	$T_{\text{eva,n}}$	-5 °C
Speed type	Variable	Super heat	0 °C
Refrigerant	R-717 (Ammonia)	$T_{\text{dh,out,n}}$	79 °C
Min speed	1500 RPM	Subcooling	10 K
Max speed	3600 RPM	Unit	Single stage

The relation between the scaling, δ , and the nominal capacity under the nominal operating conditions in Table 3.3 can be described by the simple linear relationship

shown in Equation 3.8.

$$\delta = 0.0756 \dot{Q}_{h,n} - 0.7e^{-15} \quad (3.8)$$

With $\dot{Q}_{h,n}$ being the desired nominal capacity of an individual heat pump in MW. The factor, δ , is used inside the heat mover model in Dymola to scale the heat pump. Notice, that the performance map is based on a nominal cooling capacity. Assuming that a linear scaling can be applied, this was converted to a corresponding nominal heating capacity to form Equation 3.8.

3.2.4 Functional Mock-up Units and pyFMI

With a heat pump performance map integrated in a heat pump model, which is implemented into a Dymola simulation model that include controls and concept-change opportunities the setup must be prepared for the optimisation. For this reason, the term Functional Mock-up Units (FMU) and pyFMI is introduced. FMU basically exists in two types: Model-Exchange (ME) and Co-Simulation (CS), which both are standard FMI (Functional Mock-up Interface) specifications. In short, FMI denotes an open standard for exchanging dynamic simulation models between different types of simulation tools, which is why it becomes relevant for the model exchange between Dymola and Python. Python will be used for the optimisation. Dymola has a build-in *export to FMU*-function, and the Python package PyFMI is introduced for loading an execution of the Dymola model in Python. [Andersson et al., 2016]

The assembled Simulation Setup

The sections Section 3.1 and Section 3.2 describe some of the essential steps taken to develop the setup used for optimisation. To summarise, a load dependent, performance map based heat pump model has been developed and implemented in a simulation model. The simulation model consist of nine heat pumps in total, in a 3-by-3 arrangement. The simulation model allow for all possible combinations of the nine heat pumps, and a variable $\dot{Q}_{h,n}$ is used scale the heat pumps to the desired nominal heating capacity. The mass flow rate is adjusted by a temperature control, and the load is controlled by the desired heating rate or the power consumption.

4 | Simulation Tests

This chapter presents some test conducted to validate and ensure that the simulation model presented in Chapter 3, performs reasonably. Since the performance map itself was tested and validated in the previous study [Thomassen, 2020], this is assumed valid and well tested. However, one of the main challenges in the modelling and preparation for optimisation, is to designed a simulation model which performs satisfyingly in all possible configurations and capacity combinations. For this reason, this chapter seeks to validate, that both the heat pumps, and the control functions as expected under various conditions and combinations.

4.1 Nominal Conditions

The assumed nominal conditions for the concept designed for the system in Esbjerg are as listed below:

- $T_{\text{dh,out}} = 60 \text{ }^{\circ}\text{C}$
- $T_{\text{sea}} = 4 \text{ }^{\circ}\text{C}$
- $\dot{Q}_{\text{h,n}} = 50 \text{ MW}_q$

The difference between the nominal conditions expected for the system in Esbjerg, and the the nominal conditions valid for the performance map has the consequence, that an example of a concept with $4 \times 12.5 \text{ MW}_q$ heat pump units does not necessarily produce 50 MW_q , when subject to the nominal conditions expected in Esbjerg. For this reason, the nominal capacities, $\dot{Q}_{\text{h,n},i}$ must be adjusted for the simulation, to ensure a nominal heating capacity of 50 MW_q . This was solved by implementing the nominal conditions (for Esbjerg) to the simulation model and iteratively change the values of $\dot{Q}_{\text{h,n},i}$ until reaching 50 MW_q . The concept chosen for this was for practical reasons a concept of four heat pump connected as two parallel strings each with two heat pumps. Referring to Figure 3.2, this corresponds to including HP1, HP2, HP4 and HP5. This concept will from now on be referred to as the *reference concept*. The important outcome of this investigation is that the reference configuration must consist of four heat pumps with a capacity of 13.6 MW_q to deliver 50 MW_q at the nominal conditions decided for the Esbjerg case. Figure 4.1 show the output from the scaled concept with $4 \times 13.6 \text{ MW}_q$ heat pumps units, and the heat output for a non-scaled concept with $4 \times 12.5 \text{ MW}_q$ units.

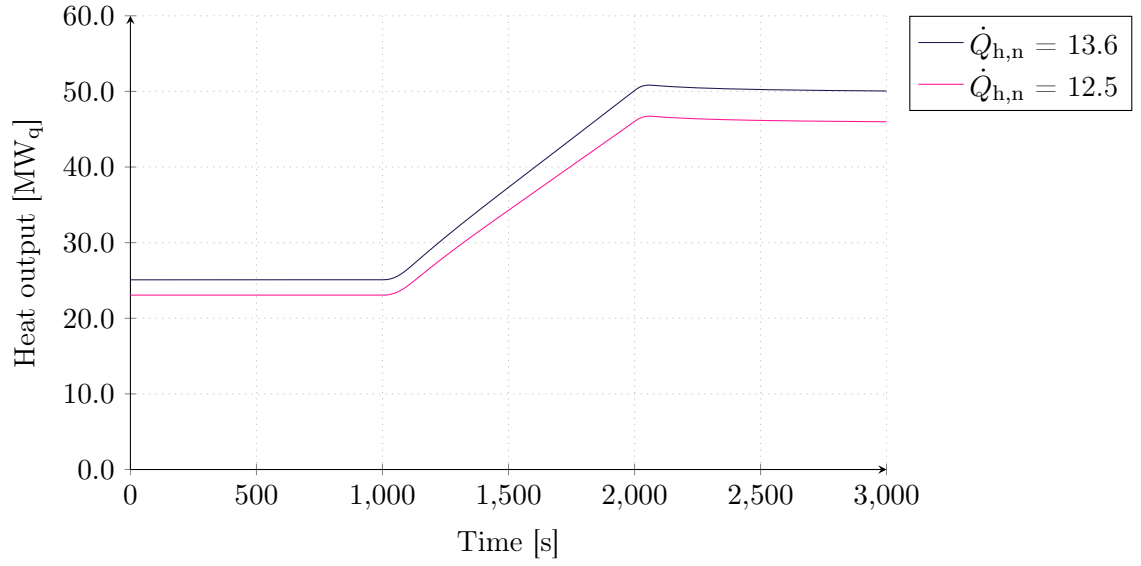


Figure 4.1: Capacity of reference heat pump configuration with different nominal capacities, when subject to nominal operating conditions and a ramp from 50 % load to 100 % load

As seen in Figure 4.1, the response for the reference concept with $4 \times 12.5 \text{ MW}_q$ units does not meet the requirement of 50 MW_q at nominal conditions. Accordingly this implies that total capacity of the scaled units in the reference concept is $\approx 54.5 \text{ MW}_q$ under the assumed nominal conditions.

4.2 System Test

One of the challenges in the design of the system, is to design the system, to operate and respond reasonable regardless of the concept design. Before exporting the model in Dymola to a FMU, three different configurations was tested and checked, to ensure a satisfying response. Table 4.1 lists the three heat pump concepts, which was used as test concepts in preparation for the optimisation.

Table 4.1: Test conditions for simulation model test. All simulation model test concepts have a total capacity of approximately 54.5 MW_q. $\dot{Q}_{h,n,1}$ refers to the nominal capacity of HP1 etc.

	Reference	Test 1	Test 2
$\dot{Q}_{h,n,1}$	13.6	18.3	9.1
$\dot{Q}_{h,n,2}$	13.6	18.3	9.1
$\dot{Q}_{h,n,3}$	0.0	18.3	0.0
$\dot{Q}_{h,n,4}$	13.6	0.0	9.1
$\dot{Q}_{h,n,5}$	13.6	0.0	9.1
$\dot{Q}_{h,n,6}$	0.0	0.0	0.0
$\dot{Q}_{h,n,7}$	0.0	0.0	9.1
$\dot{Q}_{h,n,8}$	0.0	0.0	9.1
$\dot{Q}_{h,n,9}$	0.0	0.0	0.0

The test concepts listed in Table 4.1 was subject to a system test, where the heat output set point was increased from 10 MW_q to 50 MW_q. The results of the test are presented in Figure 4.2.

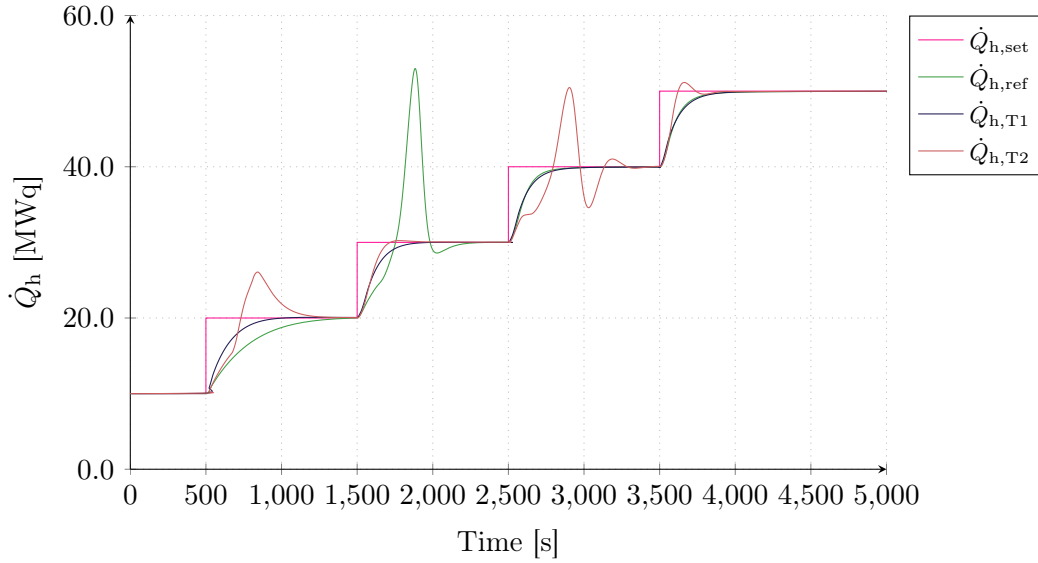


Figure 4.2: Heat output setpoint response for the three test concepts in the simulation model test.

For the reference case seen by the green curve, a significant peak is seen when the setpoint increases to 30 MW_q. The peak is caused by the deployment of the second string of heat pumps (HP4 and HP5). A similar observation can be made from Test 2, where two significant peaks are seen. Since all three parallel strings of heat pumps are included in the concept for Test 2, this also demonstrates how the load control

strategy operates. When the heat requirement increases from 10 to 20 MW_q, the second parallel string activates, and similar when the setpoint increases to 40 MW_q the last of the three parallel strings activates. Test 1 is a concept with only one string consisting of three heat pumps of high capacity connected in series. All three heat pumps are activated simultaneously, and no spikes are consequently seen.

One additional observation made from this test is the challenge related to the control of the system. As seen in Figure 4.2 the response, especially when additional heat pumps are activated, was found to experience both over- and undershoot. This is usually unwanted in control systems, but to avoid these phenomenons, a much more complex control system should be designed, which is beyond the extent of this thesis. To ensure, that the spikes in the response does not effect the optimisation results, awareness should be raised to ensure, that the system has reached steady state before evaluating.

5 | Optimisation

The heat pump and the simulation model described in Chapter 3 are intended to be used for optimisation and for sensitivity analysis. The following sections will describe how the optimisation problem is formulated in terms of optimisation variables, development of cost functions and briefly choice and principle of the optimisation algorithm.

5.1 The Optimisation Problem

The optimisation process and the following sensitivity analysis are divided in steps and pre-feasibility studies, but the two main objectives can be stated as:

1. Steady state optimisation of COP, heating capacity and CAPEX.
2. Concept investigations of response to ancillary services and control strategies.

Objective 1 consists of an optimisation using a micro genetic algorithm. This includes the development of a cost function that accounts for the performance, the heating capacity and the capital expenditures of the heat pump concept. The investigation of the dynamic response and the possibility of providing ancillary services, will be performed based on results from the steady state optimisation. A nonlinear optimiser, a micro Genetic Algorithm has been chosen to allow for further inclusion of dynamic response and ancillary services in the optimisation, if this can be quantified in a cost function.

5.1.1 Problem Definition and Reference Concept

The purpose of the optimisation is to find an optimum heat pump concept given some operational conditions based on the expected setup in Esbjerg. An example of how an expected heat production profile for the system could be for the future system in Esbjerg, is shown in Figure 5.1.

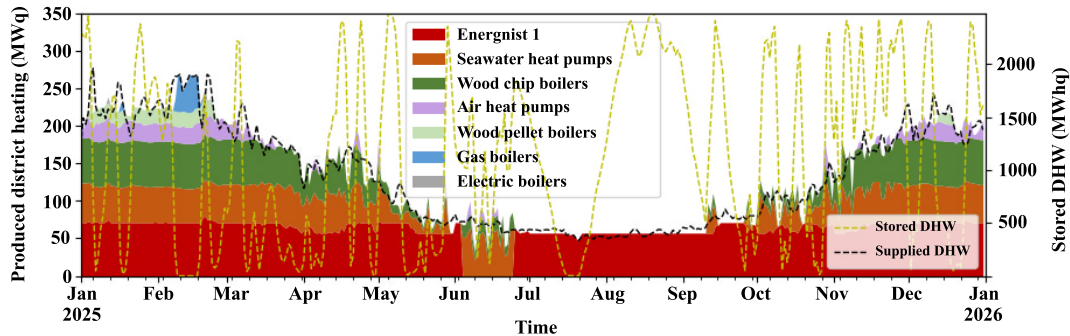


Figure 5.1: An example of heat production from the different plants.

This example of an operation profile, is based on a concept of four heat pumps each with a nominal capacity of approximately 12.5 MW_q . The concept is designed with two parallel strings each with two heat pumps in series as seen in Figure 5.2.

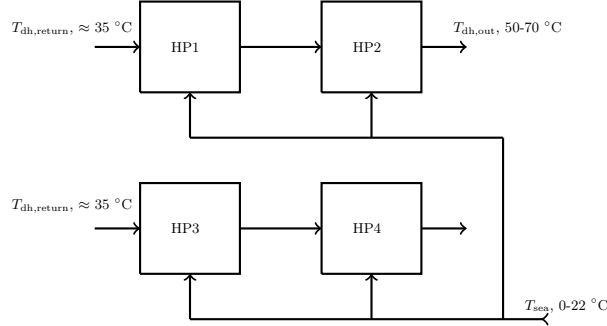


Figure 5.2: Heat pump system design used for the optimised operation profile. The heat pump concept consists of four heat pump units connected in series in pairs of two on the district heating line. For the seawater line, all units are connected in parallel.

In reality, the operation profile will most likely be optimised according to the capacity and performance of heat pumps, but including the entire portfolio of plants to optimise both concept and operating profile is beyond the topic of this thesis. The assumption will be, that the operation profile provides a realistic representation of the operation of the heat pumps. For now, it should just be noted, that this will cause the optimisation results to be biased towards the reference concept, since the operation profile is optimised according to this concept.

As seen from Figure 5.1, the heating demand from the sea water heat pumps, varies over the year, with a significant dominance of the winter-period, which naturally is expected. Additionally, the annual operation varies in terms of operating temperatures. Bearing in mind, that the optimisation should be used for both an initial concept optimisation and a sensitivity analysis, emphasis have been put on computation time, and the ability to easily make changes to the conditions which form the basis of the optimisation. For this reason, it was decided to divide the operation profile seen in Figure 5.1 into steady state categories. Another considerable argument for this, is that the categorised performance evaluation are presumably less biased towards the reference concept. The performance of each concept suggested by the optimisation, should be evaluated in terms of costs related to COP, heating capacity and investment. The categories as well as the evaluation of the costs will be defined relative to the reference case. The following section describes the reference case and the conditions of the categories.

Reference Concept and Categories for Operation

The categories are defined from the expected operation of the 2-by-2 reference concept, delivering a total of approximately 50 MW_q , each heat pump with a nominal

capacity of approximately 13.6 MW_q at the nominal conditions $T_{\text{dh,out}} = 60$ °C and $T_{\text{sea}} = 4$ °C. In general the categories must be representative of the operating conditions experienced by the heat pump during a year of operation. For this purpose, the evaluation of COP must cover the load-range seen by the heat pumps. Seven categories was found to be reasonable for this purpose. The categories are defined according to the temperature of the sea water, the temperature of the district heating water and the desired heat output ¹. The general categorisation for the COP evaluation is seen in Table 5.1.

Table 5.1: The definition of the seven categories developed for the COP evaluation. Heat load corresponds to the relative amount of heat delivered in each category (in MWh_q) on a yearly basis.

Category	T_{sea} [°C]	$T_{\text{dh,out}}$ [°C]	Heat load [%]	Reference load [%]
C1	>10	50-55	2	59.8
C2		60-70	23	86.4
C3	6-10	50-55	14	59.4
C4		60-70	11	69.2
C5	2-6	60-70	39	89.9
C6		50-55	3	90.6
C7	<2	50-55	9	95.2

The categories in Table 5.1 are hence defined both according to the temperatures, and the heat load. The heat load represents the relative amount of heat delivered in each category. Especially during the winter period, where sea water temperatures are relatively low, the heat pumps are expected to deliver a substantial amount of heat. Additionally, the load range based on the performance of the reference load starts at around 60 % to almost full load, which is especially interesting due to the load dependent heat pump model. Notice, that the load decrease observed at category 3 is caused by the activation of heat pump 3 and 4 (see Figure 5.2), which initially, due to a relatively low heating demand, are not in operation.

To evaluate the heating capacity, some additional categories must be defined. In practice, a heat pump manufacturer might not be able to deliver exactly the amount of heating capacity planned. However, a reduction in capacity will lead to extra costs since this will cause extra capacity to be delivered from other units (in this case: the wood chip boiler, the gas boiler and probably an air source heat pump). The additional four categories applicable for the heating capacity evaluation are listed with the categories for COP in Table 5.2.

For to both the seven categories for COP evaluation and the four categories for

¹Since some of the values used in the development of the categories are confidential, only a limited amount of the actual numbers will be presented as of the tender documents.[DIN Forsyning and Rambøll, 2020]

evaluation of the heating capacity, the boundary conditions and reference performance originates from the reference concept. The categories in Table 5.2 will be used as inputs to the simulation for the steady state optimisation. To ensure, that the system reaches steady state, each category is simulated for one hour.

Table 5.2: The boundary conditions and set points for the categories used for the COP evaluation for category 1-7 and for the maximum heating capacity for category 8-11.

Category	T_{sea} [°C]	$T_{\text{dh,out}}$ [°C]	$T_{\text{dh,return}}$ [°C]	$\dot{Q}_{\text{h,set}}$ [MW _q]
C1	13.7	55.0	36.7	21.2
C2	14.0	62.8	36.9	31.9
C3	7.3	54.6	35.1	34.2
C4	8.2	60	35.1	41.4
C5	5.3	60	35	49.2
C6	3.9	54.9	35	46.8
C7	1.1	53.0	35	44.5
C8	1.1	53.0	35	44.3
C9	4.0	55.3	35	49.3
C10	7.8	57.1	35.1	55.8
C11	14.0	62.3	36.9	66.7

The temperatures seen in Table 5.2 represent the mean temperatures. Note that the set points for the heat output in most cases is less than 50 MW_q, which is caused by part-load operation and general deviations from the nominal conditions. For the optimisation, the vector containing the boundary conditions is denoted \mathbf{V} , as seen in Equation 5.1.

$$\mathbf{V} = \{T_{\text{sea}}, T_{\text{dh,out}}, T_{\text{dh,return}}, \dot{Q}_{\text{h,set}}\} \quad (5.1)$$

Since the boundary conditions and the categories in general are based on the performance of the reference concept, the cost function should be defined relative to the reference concept as well.

Optimisation variables

As described in Chapter 3, the heat pump system modelled in Dymola was designed to allow for different concepts to operate, without having to change the model itself. This was done using the variable $\dot{Q}_{\text{h,n,i}}$, representing the nominal heating capacity of each individual heat pump.

The optimisation seeks to find the optimum solution to the capacities of each individual heat pump, corresponding to:

$$\mathbf{u} = \{\dot{Q}_{\text{h,n,1}}, \dot{Q}_{\text{h,n,2}}, \dot{Q}_{\text{h,n,3}}, \dot{Q}_{\text{h,n,4}}, \dot{Q}_{\text{h,n,5}}, \dot{Q}_{\text{h,n,6}}, \dot{Q}_{\text{h,n,7}}, \dot{Q}_{\text{h,n,8}}, \dot{Q}_{\text{h,n,9}}\}$$

Where $0 < \dot{Q}_{h,n,i} < 18.5 \text{ MW}_q$. If $\dot{Q}_{h,n,i} < 2$, the particular heat pump is not included in the concept. To avoid infeasible small units, the optimisation truncates all suggested heat pumps of a capacity, $\dot{Q}_{h,n,i} < 2$ to zero. The maximum capacity is set to 18.5 MW_q as it is approximately the minimum required capacity, if the solution should consist of only three heat pumps in series. Additionally, 18.5 MW_q is in the order of the largest units available for a single heat pump [GEA, 2020].

5.1.2 Performance Costs: COP maximisation

The performance of the heat pump concept can be evaluated directly from the total COP of the concept. In other words, the relation between the delivered heating rate, \dot{Q}_h and the power consumed by the heat pump concept, P . A concept with a COP that is generally lower than the corresponding COP of the reference concept, will consume more electricity than the reference and consequently, the costs increase. On the other hand, a concept that generally produces a higher COP than the reference concept consumes less electricity, and consequently, the costs for electricity reduces. The COP of the reference concept for category 1-7 can be found in Table 5.3. In the development of the COP cost function two main aspects must be considered:

1. Increase/decrease in costs related to electricity consumption due to reductions/improvements in COP.
2. The effect of performance in categories with the most operating hours (e.g. C2 and C5) must be more significant than those with less operating hours.

For the reference, the expected heat production is known and allocated among the categories as listed in Table 5.1. The same applies for electricity consumption. To estimate the costs of improvements or reductions in the COP, the COP of the reference case was reduced by 10 %, which naturally, gives rise to extra costs. The extra costs includes: ΔP (elspot + electricity taxes). The extra costs for a 10 % COP reduction are evaluated for category 1-7, to form the coefficients and the weighting between the categories, α_i . Assuming a linear change of costs, the final representation of the COP share of the cost function becomes as stated in Equation 5.2.

$$COST_{COP} = \alpha_1 \left(1 - \frac{COP_1}{COP_{ref,1}} \right) + \dots + \alpha_7 \left(1 - \frac{COP_7}{COP_{ref,7}} \right) \quad (5.2)$$

The coefficient, α_i , represents the extra costs associated with changes in COP compared to the reference COP for each category seen in Table 5.3. The values of α_i are seen in Table 5.4

Table 5.3: The definition of the seven operation categories used for the optimisation of the heat pump concept.

Category	COP _{ref,i} [-]
C1	5.0
C2	4.6
C3	4.4
C4	4.2
C5	3.9
C6	4.1
C7	3.9

Table 5.4: Actual values of the parameters representing the cost related to COP variations from the reference COP.

α_i	Cost [DKK]
α_1	638 385.0
α_2	9 077 708.9
α_3	5 681 650.3
α_4	4 600 325.3
α_5	17 502 111.2
α_6	1 153 986.6
α_7	4 132 657.0

However, if the heat pump concepts were purely evaluated based on COP, there is no guarantee, that the concept is capable of delivering the decided amount of heat.

5.1.3 Heating capacity

Similar to the COP, the cost function for the heating capacity, will be designed to penalise concepts, which cannot deliver the desired heating capacity. The heat output setpoint in category 8-11 represents the maximum heat output delivered by the reference concept when subject to the temperature inputs listed in Table 5.2. The cost function for the heating capacity takes the same form as was seen from COP, and can be found in Equation 5.3.

$$COST_{\text{heat}} = \beta_1 \left(1 - \frac{\dot{Q}_{h,8}}{\dot{Q}_{h,\text{ref},8}} \right) + \dots + \beta_4 \left(1 - \frac{\dot{Q}_{h,11}}{\dot{Q}_{h,\text{ref},11}} \right) \quad (5.3)$$

The coefficient, β_i is in the same way as α_i for COP found by reducing the capacity with 10 %. By reducing the capacity compared to the expected and optimised operation (Figure 5.1), the costs increase due to extra operation of other units. These units could be the wood chip boiler and the gas boiler. An example of the costs for delivering 1 MW_q for either of the units, is presented in Table 5.5.

Table 5.5: An example of the differences in cost for production of 1 MW_q between a wood chip boiler (with flue gas condensation), a gas boiler and a heat pump (assuming elspot = 400 kr/MWe and a COP of 4).

Unit	Cost [DKK]
Heat pump	170
Gas Boiler	481
Wood Chip Boiler	204

As seen, the cost increases significantly when the gas boiler is activated. Based on the extra costs for operation with other units, the β -values in Equation 5.3 sum to the values presented in Table 5.6.

Table 5.6: Actual values of the coefficients representing the cost related to capacity reductions relative to the reference maximum capacity at categories C8-C11.

β_i	Cost [DKK]
β_1	5 164 456
β_2	9 658 168
β_3	406 225
β_4	82 839

To summarise, if the concept in question fails to produce the requested heat output, the costs increases due to extra operation on other units when the capacity is reduced. On the other hand, increased heat production will not lead to any additional savings. For a new design of the entire portfolio of plants, an increase in heat pump capacity might lead to additional savings, but for the extent of this thesis, it has been decided, that the 50 MW_q determined by the operational optimisation remains the decided capacity, and consequently any increase in capacity will be truncated to 0 DKK extra cost. However, an oversized concept will probably be penalised and discarded in terms of investment cost, which will be further described in the following section.

5.1.4 Capital Expenditures

The optimisation variables $\dot{Q}_{h,n,1} - \dot{Q}_{h,n,9}$ represents two significant concept design variables: the size of each heat pump units and whether the particular unit is included in the concept. If the optimisation where to find a concept solely with regards to COP, the result would be a maximum amount of serial-coupled heat pumps [Rothuizen et al., 2015]. Additionally, an expectation could be that a large number of small heat pumps allow for better performance for possible ancillary services, since it prevents large units from operating at part load conditions, which is known to reduce

the COP significantly. However, the investment costs from buying a number of small heat pump units might be much greater than the investment costs from buying a few larger units. To find the optimum trade off between maximum performance and investment costs of the heat pumps, the concept of "economy of scale" is introduced. According to Danish Energy Agency and Energinet [2016], the effect of economy of scale for heat pumps is, however, very limited.

An estimation from Danish Energy Agency and Energinet [2016] is that a capacity increase of 100 % results in an increase in price of between 70 % and 90 %. Furthermore, the technology catalogue presents an example of costs for a 4 MW_q heat pump. The estimate of the economy of scale (EOS) effects and the data sheet found in the technology catalogue, form the basis of the investment-part of the cost function. The following assumptions were made:

- Economy of scale = 0.8
- Reference price for a 4 MW_q heat pump = 19.8 million DKK.

Notice, that these investment costs includes both the investment price for the heat pump unit itself and the prices of installation and other equipment (piping etc.). However, it is assumed, that the cost of installation and other equipment scales with the size of the heat pump unit itself. Under these assumptions, the total investment cost for a heat pump concept can be found from Equation 5.4.

$$COST_{\text{invest}} = \sum_{i=1}^9 6e6 \dot{Q}_{h,n,i}^{0.848} \quad (5.4)$$

Based on the reference price for the 4 MW_q, Equation 5.4 was made by applying the 80 % economy of scale on a 8 MW_q unit etc., to fit the relation. The larger a unit is, the more expensive the individual unit becomes, and additionally, the more units included (ie. the number of units with $\dot{Q}_{h,n,i} \geq 2$) the more expensive it becomes. Similar to $COST_{\text{COP}}$ and $COST_{\text{heat}}$ the investment costs should be expressed in terms annual costs relative to the reference concept. For this reason, two more steps must be taken. First of all, the reference investment price must be calculated using Equation 5.4, as presented in Equation 5.5.

$$COST_{\text{invest}} = \sum_{i=1}^4 6e6 \cdot 13.7^{0.848} \quad (5.5)$$

This give a total reference investment cost of 219 508 952 DKK. This investment cost is associated with a depreciation expense, which can be calculated from Equation 5.6.

$$DE = G \frac{r}{1 - (1 + r)^{-n}} \quad (5.6)$$

With G being the total investment cost, r the interest rate and n the loan period. The interest rate is assumed to be fixed at 1.8 % and the loan period is assumed to be 20

years. From these assumptions, Equation 5.6 results in a depreciation expense of 0.06. The final cost function for investment costs takes the form as seen in Equation 5.7.

$$COST_{CAPEX} = (0.06 COST_{invest} - 0.06 COST_{invest,ref}) \quad (5.7)$$

The penalty related to investment cost becomes the difference in depreciation expenses relative to the reference depreciation expenses. The investment cost represents the final part of the cost function used for the heat pump concept optimisation. The final cost function applied for the optimisation hence combines Equation 5.2, Equation 5.3 and Equation 5.7 to form Equation 5.8.

$$COST_{HP} = COST_{COP} + COST_{heat} + COST_{CAPEX} \quad (5.8)$$

Concept Optimisation Problem

To summarise, the concept optimisation problem can be described by Equation 5.9.

$$\begin{aligned} & \underset{\mathbf{u}}{\text{minimise}} && COST_{HP} \\ & \text{subject to} && \dot{\mathbf{x}}(t) = f(\mathbf{V}, \mathbf{u}, \mathbf{x}(t)), \\ & && \mathbf{G} \mathbf{u} \geq \mathbf{g}, \\ & && \mathbf{x}(0) \geq \mathbf{x}_0 \end{aligned} \quad (5.9)$$

With $COST_{HP}$ representing the annual costs of the heat pump, $\mathbf{x} \in \mathbb{R}^q$ is the system state vector, \mathbf{u} being the input vector containing the optimisation variables (solutions), and $\mathbf{V} \in \mathbb{R}^m$ representing a fixed input vector with external boundary conditions. f represents the nonlinear dynamic model of the heat pump system developed in Dymola. The inequality constraints related to the requirements for heat output are defined in the matrix \mathbf{G} and the vector \mathbf{g} . These are applied to the COP evaluation to ensure that only concepts producing sufficient heat output is considered, and states that $\dot{Q}_{h,i} \geq 0.98\dot{Q}_{h,i,set}$.

5.2 Optimisation Algorithm - μ GA

To solve the optimisation problem presented in Section 5.1, the mirco genetic algorithm (μ GA) proposed in Krishnakumar [1990] was used. The μ GA was chosen to solve Equation 5.8 since it is a relatively fast global optimisation method. A more thorough investigation of possible optimisation algorithms is additionally an interesting field of study, but for the extent of this thesis, it was decided that the μ GA was adequate to solve the problem.

The method used in the μ GA is illustrated in the flowchart in Figure 5.3. In the proposal from [Krishnakumar, 1990] a fixed population size of $N = 5$ is suggested. In general it is said that that small population Genetic Algorithms performs poorly due to insufficient information processing and early convergence to non-optimal results. A

method to succeed with small populations was further described and outlined. This includes the following four steps:

1. Random generation of small population.
2. Genetic operations are performed until nominal convergence.
3. A new population is generated by transferring the best individual in the converged population to the new population. The remaining individuals is generated randomly.
4. Repeat the process from step number 2.

These four steps are basically the approach that forms the basis of the implementation of the μ GA seen in Figure 5.3. Choosing a small population size of five, has the additionally useful feature that a standard computer usually has four cores, which is consistent with the need of four evaluations for each generation (the best individual from the previous generation is kept for the new generation), when parallel processing is applied. For computers with more than four cores, the population size can profitably be set to the number of cores + 1.

Initialisation

A typical population of $N_s = 5$ is used. Each possible solution, which is also called an individual, is denoted u_s with $s \in \{1, 2, \dots, N_s\}$. Each individual consists of the optimisation variables described in Section 5.1. The optimisation variables, which represent the capacity parameters are also called genes, and is denoted $\tilde{u}_{s,\chi} \in \mathbb{R}$ with $\chi \in \{1, 2, \dots, N_\chi\}$. The genes in the initial individuals are picked randomly using a Gaussian (normal) distribution, denoted $\mathcal{N}(\mu_\chi, \sigma_\chi^2)$, with center, μ_χ defined by the best solution, which initially is the reference scenario and a standard deviation $\sigma_\chi = 0.5(\tilde{u}_\chi - \underline{\tilde{u}}_\chi)$, which is defined by the minimum and maximum values for the optimisation variables (ie. the genes). If the random numbers for the genes are picked outside the search range, the value is truncated to the nearest bound. Using a normal distribution instead of the more common uniform distribution has the advantage, that it increases the chances of picking numbers close to the current best solution, but it also, due to the truncation, increases the changes of picking values at the minimum or maximum boundaries. In situations where the optimum is located at either the upper or lower boundary, this feature has good properties in terms of convergence speed [Vinther et al., 2017].

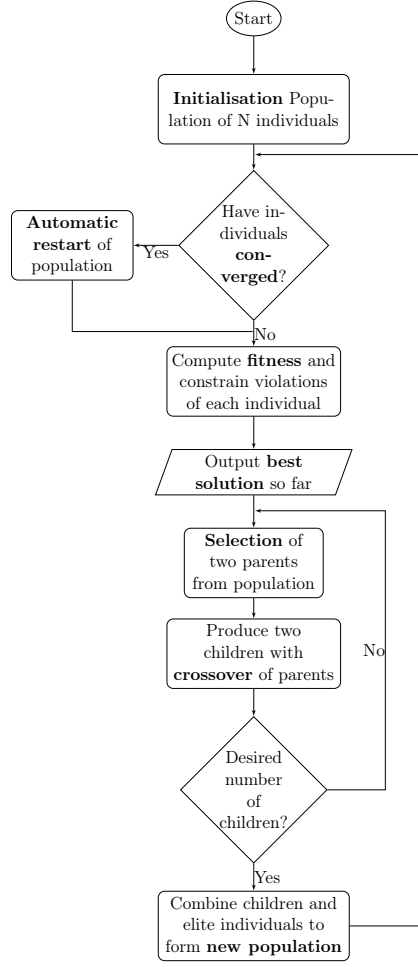


Figure 5.3: Flow chart of the μ GA used for the optimisation of the heat pump concept.

Convergence

Based on [Vinther et al., 2017] and [Senecal et al., 2000], a convergence criteria of 0.05 (i.e. 5 %) was chosen. The convergence criteria determines if an automatic restart is necessary or not. This happens, when all pairs in all individuals are within 5 % of their full range. This is calculated as the maximum euclidean distance between the specific gene in the individual relative to its full search range, as seen in Equation 5.10.

$$d_{\chi} = \max_{k,l} \left(\frac{|\tilde{u}_{k,\chi} - \tilde{u}_{l,\chi}|}{\tilde{u}_{\chi} - \underline{u}_{\chi}} \right) \quad (5.10)$$

With $l, k \in \{1, 2, \dots, N_s\}$ defining the individuals. The convergence criteria of 0.05 means, that if all maximum distances, d_{χ} , for $\chi \in \{1, 2, \dots, N_{\chi}\}$, becomes less than 0.05, an automatic restart is triggered. Note that the automatic restart keeps the elite individual, while choosing the remaining individuals as described in the initialisation.

Fitness Evaluation

Each generation of population is evolved through selection, crossover and elitism. In order to do so, it is important to be able to evaluate how good each solution (individual) is. In this case, a good solution would mean low annual costs, whereas a bad solution refers to a solution with high annual expenses. The fitness is consequently calculated from the cost function presented in Equation 5.8. The inputs to Equation 5.8 are based on simulation results achieved by simulating the model using the variables in the individual. That is, applying \mathbf{u} to the model and extracting the information necessary for Equation 5.8.

As stated in Section 5.1 regarding the development of the cost function, the simulation is running through 11 categories. Category 1-7 is used to evaluate the COP at different operating and load conditions. However, to ensure that the optimisation does not propose concepts, that cannot deliver the requested heat output during the COP evaluation, the constraints regarding the heat output was implemented. In many regular Genetic Algorithms, the constraints is handled by adding a penalty function to the fitness of the solution which violates the constraints. However, this approach depends a lot on the specific problem, where the size of the penalty must be considered according to the problem. A more general approach is to consider the total number of constrain violations instead, meaning that each constrain violation corresponds to an integer number, which in this case is one for all constraints, and the sum of constrain violations is then used to sort the individuals. By sorting the individuals with regard to the total number of constrain violations first and then the fitness, the best solution will always be the solution, that does not violate any constraints. This is due to the elitism, as long as the reference solution does not violate any constraints.

Selection

The next step in the μ GA, following Figure 5.3, is *selection*. Selection is the process, where promising parents for mating is found. For this, a male and a female is chosen through *deterministic tournament selection without replacement*. The point of the selection process is to ensure, that the individuals for the next generation are based on good individuals. The tournament strategy is one selection method for choosing individuals for mating. In the deterministic tournament selection, the best solution always wins, implying a high selection pressure, which is desirable in μ GA's. The reason for this is that the law of averages does not hold due to the small population, while converging towards a local optimum is avoided by the automatic restart. The deterministic tournament approach exists both with and without replacement. Without replacement means, that if N individuals are selected from a population of N individuals, each individual competes in k tournaments, with k being the tournament size, which due to the small population size is set to two. In practice it means that the individuals have the same probability for participating in the same number of tournaments, and avoids having an individual in tournaments with itself. However,

this does not prevent the same individual from being selected more than once (which will imply that the male and the female will be equal). This is however avoided by not allowing the male and the female to be the same individual, since two identical copies of that individual in the next generation is undesirable. [Goldberg and Deb, 1989]

Notice, that the fitness evaluation sorts the individuals prioritising low (zero) constrain violations over fitness. This also applies for the tournament selection.

Crossover

The promising solutions (parents) found through the tournament selection, are merged through crossover, to find better solutions (children). As stated in [Vinther et al., 2017], the cross over method used should provide the right balance between exploration and exploitation of the search space. To provide this, a Gaussian fitness based box crossover is used.

Each gene, $(\dot{Q}_{h,n,i})$, in the child, which is denoted \tilde{u}_c is picked from a normal distribution. The normal distribution is defined by the parents, which is denoted $\tilde{u}_{m,\chi}$ and $\tilde{u}_{f,\chi}$ for the male and the female respectively. The tails of the normal distribution is truncated to the boundaries set for the optimisation variables in \mathbf{u} , as seen in Equation 5.11 and Equation 5.12.

$$\tilde{u}_{c,\chi} = \begin{cases} \min(\tilde{u}_{m,\chi}, \tilde{u}_{f,\chi}) & \text{if } \eta_\chi < \min(\tilde{u}_{m,\chi}, \tilde{u}_{f,\chi}) \\ \max(\tilde{u}_{m,\chi}, \tilde{u}_{f,\chi}) & \text{if } \eta_\chi > \max(\tilde{u}_{m,\chi}, \tilde{u}_{f,\chi}) \\ \eta_\chi & \text{otherwise,} \end{cases} \quad (5.11)$$

$$\eta_\chi \in \mathcal{N}(\mu_\chi, \sigma_\chi^2) \quad (5.12)$$

The centre of the normal distribution is denoted μ_χ and will be located between the parents according to their normalised fitness values, which is denoted $y_{m,n}$ and $y_{f,n}$ for the male and the female respectively. Equation 5.13 and Equation 5.14 describes the evaluation of the centre of the normal distribution and the definition of the standard deviation, which is set to 50 % of the distance between the parents.

$$\mu_\chi = \begin{cases} \tilde{u}_{f,\chi} + \frac{y_{m,n}(\tilde{u}_{m,\chi} - \tilde{u}_{f,\chi})}{y_m + y_f} & \text{if } \tilde{u}_{m,\chi} \geq \tilde{u}_{f,\chi} \\ \tilde{u}_{m,\chi} + \frac{y_{f,n}(\tilde{u}_{m,\chi} - \tilde{u}_{f,\chi})}{y_m + y_f} & \text{if } \tilde{u}_{m,\chi} \leq \tilde{u}_{f,\chi} \end{cases} \quad (5.13)$$

$$\sigma_\chi = 0.5(|\tilde{u}_{m,\chi} - \tilde{u}_{f,\chi}|) \quad (5.14)$$

The normalisation of the fitness, was performed using Equation 5.15, with \mathbf{Y} denoting the population fitnesses as $\mathbf{Y} = \{y_1, y_2, \dots, y_{N_s}\}$.

$$y_{s,n} = \frac{y_s - \min(\mathbf{Y})}{\sum_{s=1}^{N_s} (y_s - \min(\mathbf{Y}))} \quad (5.15)$$

The Gaussian crossover box is just one method, which can be used for crossover. The advantage in this approach, is that it uses a normal distribution instead of a uniform distribution, and that the centre of the normal distribution is located at a fitness weighted arithmetic mean between the parents. A combination of Equation 5.11 to Equation 5.15, implies that the method gives high exploitation and less exploration of the search space. This is however compensated by the automatic restart. [Vinther et al., 2017]

5.3 Dynamic Response and Ancillary Services: System Setup

Aside from the concept optimisation of the heat pump system, an objective is to investigate possibilities for using heat pumps for ancillary services. For the extent of this thesis, this will be conducted by some simple tests on the reference concept and eventually the optimised concept. The purpose is to get an idea of the possible advantages and disadvantages of the two concepts. This section presents the setup of the system and some general ideas on how to evaluate the performance of different concepts when considering ancillary services. The dynamic test is conducted in Dymola using a setup as presented in Figure 5.4.

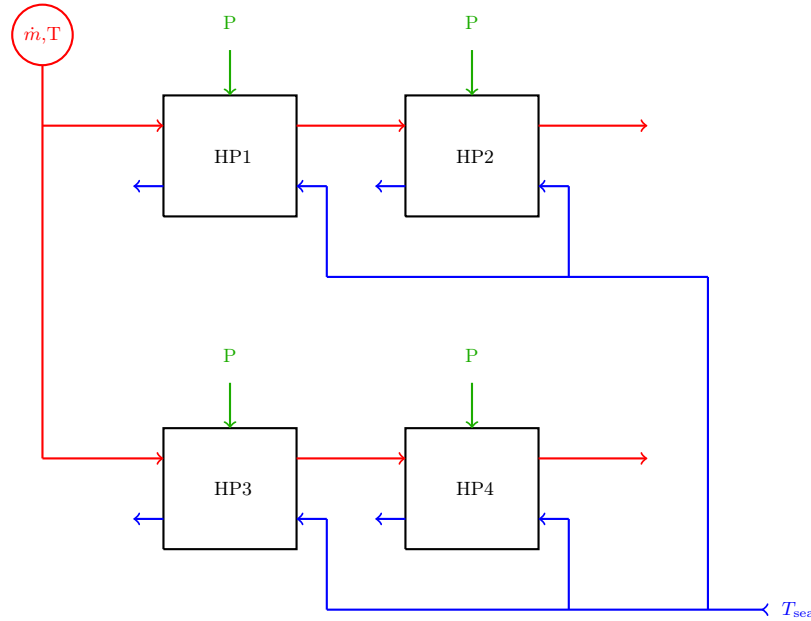


Figure 5.4: Simplified sketch of the test setup of the optimised heat pump concept for ancillary service tests.

Recalling the sketch of an example of the system in Esbjerg in Figure 1.4, the heat pumps are expected to operate along with an electric boiler and a wood chip boiler.

The wood chip boiler ensures, that the actual outlet temperature of the district heating water for the consumers remains at a satisfying level. The mass flow, which in the design for the optimisation was controlled to ensure a specified temperature, is in the system in Figure 5.4 considered as a fixed value. In practice, the mass flow rate will additionally be dependent on the consumers. A consequence of this is that the number of control-units can be reduced to one concerning the electricity consumption. As mentioned in Chapter 3, the control strategy is designed to allow for switching between a heat output setpoint and a power consumption setpoint. Inspired by the findings in the study from [Rambøll, 2019], power consumption control reduces the response time significantly which is desirable for the Ancillary service tests.

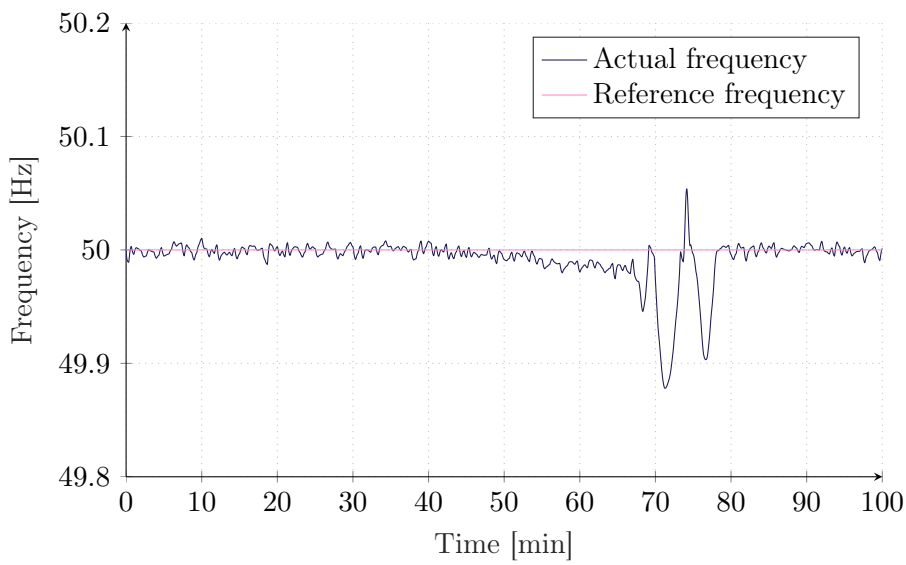


Figure 5.5: Frequency deviations representing an example on FCR.

An example of the frequency variations is seen in Figure 5.5. All frequency variations within the dead-band of ± 20 mHz, are neglected in terms of ancillary services. The aFRR is integrated as a single 6 MW_e activation with a total duration of 20 minutes. A power setpoint sequence containing both an aFRR event and FCR events is seen in Figure 5.6.

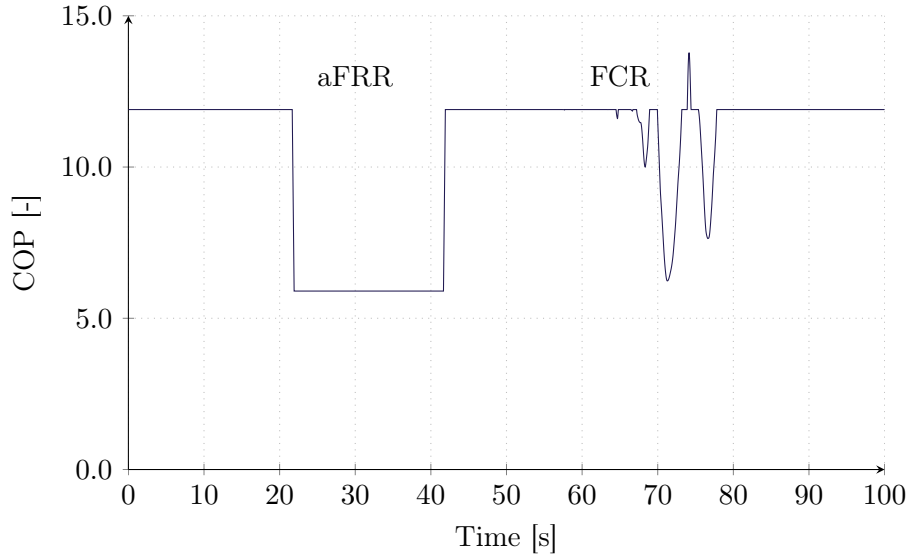


Figure 5.6: Power consumption setpoint sequence including aFRR and FCR events.

To participate on the reserve market, the heat pumps must naturally be capable of delivering the requested capacity within the required amount of time. The load gradients was implemented in the VSD-component presented in Chapter 3. To assist the heat pumps, the electric boiler is introduced in the Dymola setup as well. The Dymola implementation of the the ancillary services and the simplified electric boiler can be found in Enclosure A. By default, the electric boiler is switched off, and can thereby only assist the heat pumps when operate in part load and are too slow to follow the setpoint when increasing the load again.

Additionally a test will be made where the heat pumps are ramped from the maximum setpoint power consumption to 0. Afterwards the setpoint are stepped back to maximum. This test should identify the maximum capacity available for each concept before reducing below the minimum load of 10 %. Additionally, the step can give an indication of the time it takes either of the concepts to reach the set point after a full shut down. The dynamic response and the test results to the setpoint sequence presented in Figure 5.6 will be considered in terms of ability to follow the setpoints, and thereby the need of the electric boiler, and the influence on the temperature of the district heating water.

6 | Optimisation Results

This chapter presents and evaluates the results obtained from the optimisation presented in Chapter 5. The concept found from the optimisation will be presented together with a few test made to ensure, that the optimum heat pump concept have been reached.

Convergence

To ensure, that the optimisation have reached a global optimum, a convergence test was conducted. The test has two parts: a 500 generation run with reasonable initial guesses followed by a 500 generation run with random initial guesses. Reasonable initial guesses include the reference concept, a concept with three 18.3 MW_q heat pumps in series and a concept with three parallel strings each with two 9.1 MW_q heat pumps in series. If the 100 generation optimisation has converged towards a global optimum, the results from the 500 generation tests should correspond to the result achieved after 100 generations with reasonable initial guesses. The results achieved are presented in Table 6.1.

α_i is seen in

Table 6.1: Result from concept optimisation of heat pump concept after 500 generations with initial guess, 500 generations with no initial guess and 100 generations with initial guess.

	500 with init.	500 without init.	100 with init.
$\dot{Q}_{h,n,1}$ [MW _q]	18.3	18.3	18.3
$\dot{Q}_{h,n,2}$ [MW _q]	18.3	18.5	18.1
$\dot{Q}_{h,n,3}$ [MW _q]	18.1	17.9	18.3
$\dot{Q}_{h,n,4}$ [MW _q]	0.0	0.0	0.0
$\dot{Q}_{h,n,5}$ [MW _q]	0.0	0.0	0.0
$\dot{Q}_{h,n,6}$ [MW _q]	0.0	0.0	0.0
$\dot{Q}_{h,n,7}$ [MW _q]	0.0	0.0	0.0
Cost _{HP} [DKK]	- 1 905 866	- 1 918 607	- 1 886 414

Despite small deviations in the order of the heat pumps, the result of the three tests clearly indicate, that three large capacity heat pumps is the best solutions to the optimisation problem. The difference in costs for the three simulations is $\approx 32\,000$ DKK which compared to the order of the total cost reductions is insignificant. The development of the costs for the best fit in the convergence test with 500 generations with and without initial guess is seen in Figure 6.1.

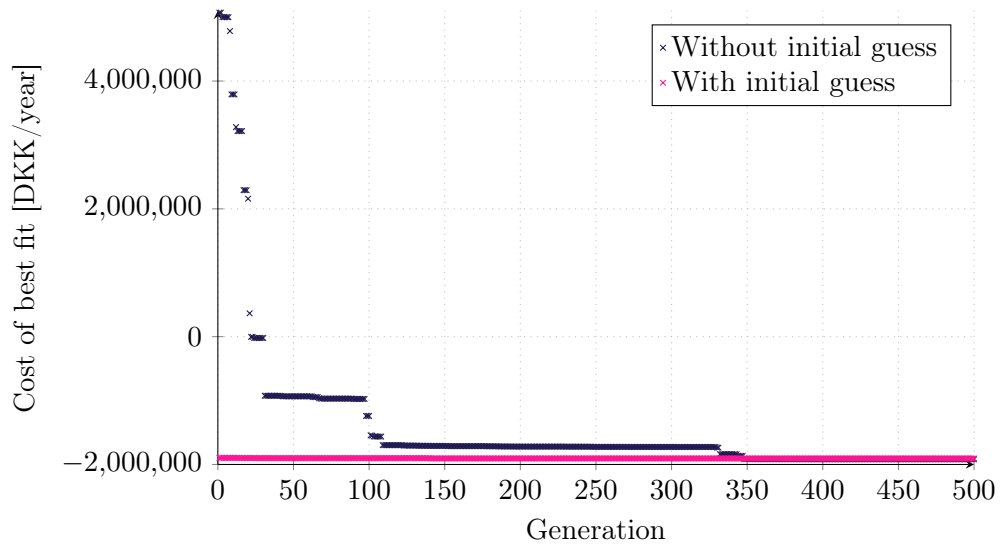


Figure 6.1: Cost of the best fit during the 500 generation test runs with and without initial guess.

Figure 6.1 show how the optimisation during the 500 generations converges towards the optimum solution, and how a good initial guess undoubtedly reduces the number of generations necessary for convergence. Since good results are found to be achieved with 100 generations if reasonable initial guesses are applied, this was decided to be sufficient. Another reason for this is the calculation time. The test with 500 generations without initial guess was simulated for ≈ 11 hours, using a Intel(R) Core(TM) i7-4910MQ CPU @2.9 GHz, where 100 generations with initial guess is finish within two hours.

A sketch of the optimised concept is seen in Figure 6.2.

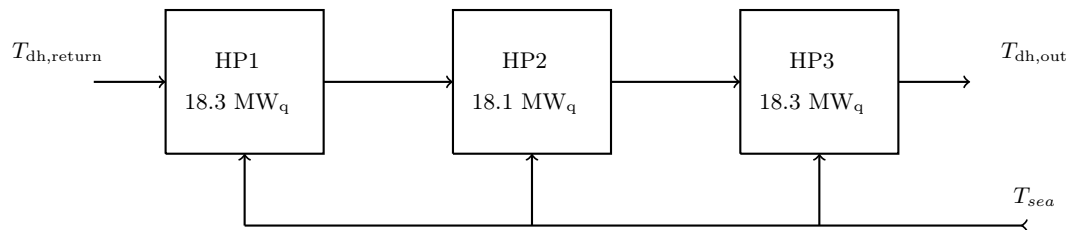


Figure 6.2: Optimised heat pump concept found from the optimisation consisting of three heat pumps in series with a capacity of 18.3 MW_q, 18.1 MW_q and 18.1 MW_q respectively.

6.1 Cost Allocation

From the optimisation results, the output of the cost function for each individual or each simulation can give an indication of which of the three elements in the cost function that effects the optimisation the most.

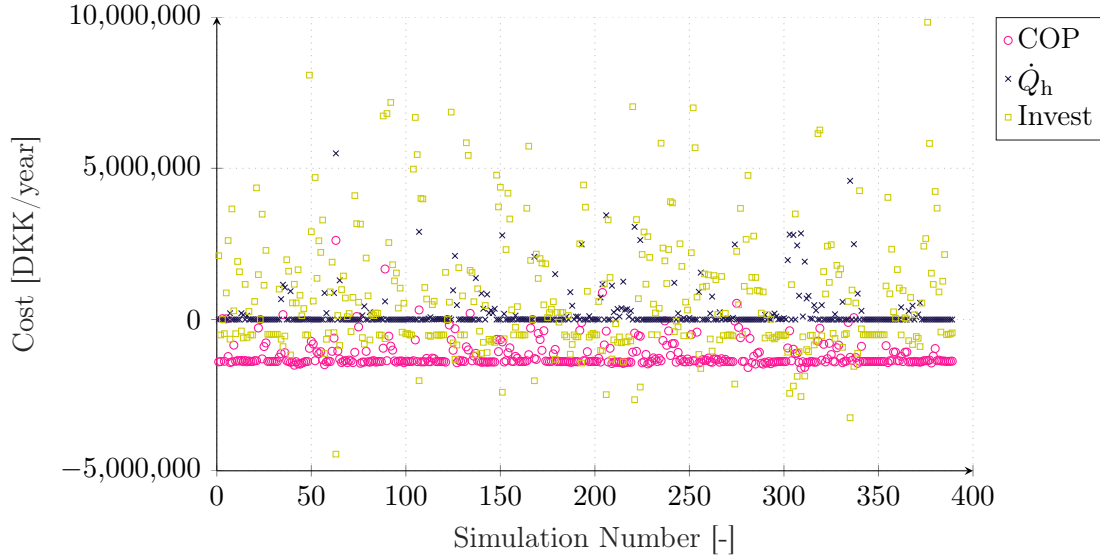


Figure 6.3: The contribution of the three elements in the cost function for the 100 generation run with initial guess.

Figure 6.3 clearly indicates, that the investment cost produces the highest fluctuations both in the positive and in the negative direction. Most of the major cost increases, seems to be produced by high investment costs. These concepts does most likely produce more than the nominal $\approx 54.5 \text{ MW}_q$, which naturally causes the investment cost to increase. The effect of improved COP seems to dominate the end cost and choice of concept. With the exception of a few, very investment-saving concepts, the COP generally seems to produce significant savings compared to the two other cost-contributions.

6.1.1 COP

The results obtained from the optimisation indicate, that especially the improvement in COP causes the 3-in-series concept to outmatch the reference concept. Figure 6.4 also show, that with exception of category 1, the COP for optimised concept has been improved compared to the reference.

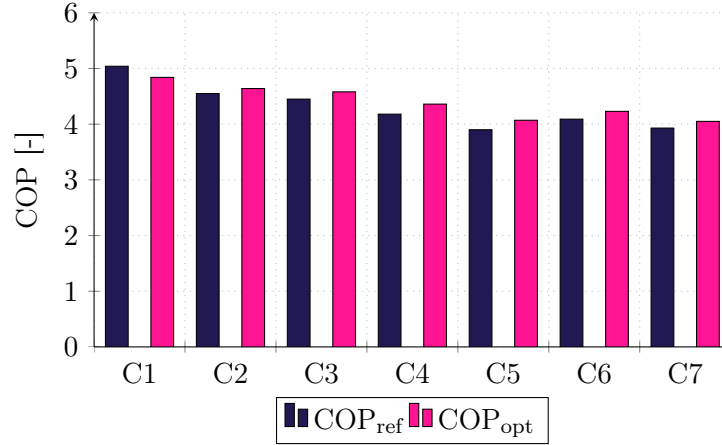


Figure 6.4: Comparison of the COP during simulation of category 1-7 used for the COP evaluation

Recalling the coefficients for the COP-cost function in Table 5.4, the penalty or cost reduction for reduced or improved COP in category 1 is much lower than for e.g. category 2 and 5. As an example, the COP is improved from 3.90 to 4.07 in category 5, the corresponding cost reduction sums to 762 913 DKK/year. The improvements in COP lead to a reduction in costs for electricity. The total costs for COP in the optimised concept amounts to: $\text{COST}_{\text{COP, opt}} = -1\,385\,935$ DKK/year.

6.1.2 Heat Output

The heat output evaluated in categories 8-11, penalises concepts with capacities lower than the required 50 MW_q which for this setup corresponds to $\approx 54.5 \text{ MW}_q$. Additionally, concepts which do not deliver the requested heat during the evaluation of COP are also rejected by the constraints.

The heat output from the reference and from the optimised concept is seen in Figure 6.5. Where two things should be noticed: Firstly, the system does reach steady state within the hour simulated for each category. Secondly, the response for the optimised concept at the last, high capacity requiring category, is as seen from Figure 6.5 just below the set point. A further observation of the results, show that the penalty for this capacity reduction becomes insignificant. A comparison of the maximum heat output and the related cost is found in Table 6.2.

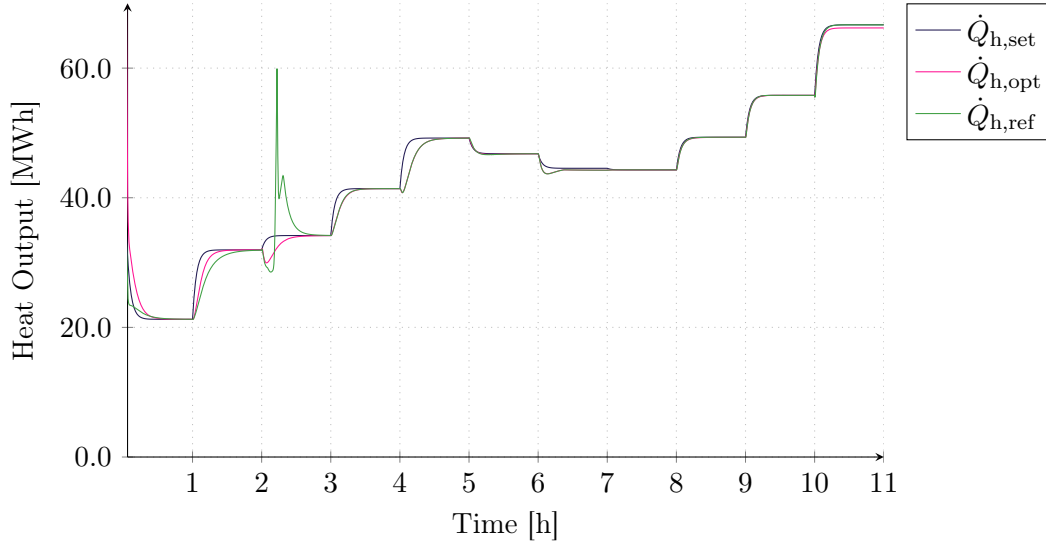


Figure 6.5: Comparison of the heat output during simulation of category 1-7 used for the COP evaluation and for category 8-11 for the evaluation of the maximum heating capacity.

The capacity deficiency for the last category does consequently not have any significant influence on the final cost. Recalling that the penalty, β_4 which is applied for category 11, is the category with the lowest penalty. This explains why the penalty for the capacity reduction in category 11 is insignificant.

Table 6.2: Comparison of the heat output measured in category 8-11 for the optimised heat pump concept.

	Reference Concept	Optimised Concept
$\dot{Q}_{h,max,8}$ [MW _q]	44.3	44.3
$\dot{Q}_{h,max,9}$ [MW _q]	49.3	49.3
$\dot{Q}_{h,max,10}$ [MW _q]	55.8	55.8
$\dot{Q}_{h,max,11}$ [MW _q]	66.7	66.2
Cost _{heat} [DKK/year]	≈ 0	1417.1

6.1.3 Investment Cost

As was seen from Figure 6.3, the investment cost is evidently the cost/penalty that varies the most for the solutions suggested by the optimisation algorithm. The investment cost for the reference is naturally 0, while the optimised concept produces a depreciation expense of -501 896.4 DKK pr. year. Generally, the investment cost appears to be challenged of the heat capacity requirement. Some concepts, which are preferable in terms of investment cost are rejected due to insufficient heating capacity. Other concepts with sufficient capacity will be rejected because they are

oversized and does thereby produce high investment costs.

6.2 Cost Comparison

To exemplify the effects of some of the choices made in the development of the cost function, a few examples of rejected individuals/solutions from the optimisation have been picked for comparison. Table 6.3 lists the total capacities and the allocation of the costs for each.

Table 6.3: Comparison of a cheaper concept with a constrain violation, another feasible but more expensive solution, an undersized and an oversized concept.

		Cheapest	Feasible	Undersized	Oversized
Capacity	[MW _q]	53.8	54.6	37.9	69.6
Cost _{COP}	[DKK/year]	-1 941 799	-1 442 964	2 240 381	-1 211 528
Cost _{heat}	[DKK/year]	236 408	10 109	4 569 925	9
Cost _{CAPEX}	[DKK/year]	-422 823	48 018	-3 397 244	4 489 989
Total Cost	[DKK/year]	-2 128 215	-1 384 837	3 412 063	3 278 469

The concept denoted *Cheapest*, does actually provide a reduction in annual costs compared to the optimised concept, but it does additionally violate one of the constraints for the heat output. Despite not being penalised significantly by the capacity-part of the cost function, it is however an undesirable concept. The concept denoted *Feasible*, has a total capacity similar to the concept chosen by the optimisation algorithm, but allocated on five heat pumps instead of three. This is naturally also reflected in the investment costs since the economy of scale increases the price for the small units relative to the larger ones. On the other hand, the *feasible* concept does actually give rise to a further reduction in cost for COP compared to the concept chosen by the optimisation. Consequently, the investment costs become the decisive effect. The remaining two concepts, *undersized* and *oversized* do as the denotation indicate refer concepts which have too little and too much capacity compared to the requested capacity. The *undersized* concept are penalised significantly for its capacity deficiency, whereas it naturally reduces the investment cost. For the oversized system, there is no penalty for capacity, since the concept easily meets the requirement. However, with a total capacity of 69.6 MW_q, the investment costs dominates and the concept is consequently rejected.

Summarising the findings from the concept optimisation and the comparison of some of the details obtained from the optimisation, the concept consisting of three serial connected heat pumps with a capacity of ≈ 18.2 as was illustrated in Figure 6.2, was found to be the best solution to the optimisation problem. A further investigation

of the details of the optimisation showed that concepts with good COP but slightly insufficient capacities was rejected and that other feasible results in terms of COP and heat output was found, but penalised from the investment costs. These observations is consistent with expectations but also raises questions in terms of robustness of the optimised concept, as the current optimisation is highly dominated by the balance between maximum COP and minimum investment costs. The total cost reduction achieved from the optimisation adds to 1 886 414 DKK/year.

6.3 Ancillary Services and Dynamic Response

Similar to the dynamic setup presented for the reference concept in Chapter 3, a simulation model for evaluation of the dynamic response of the optimised concept is developed. A simplified sketch is seen in Figure 6.6.

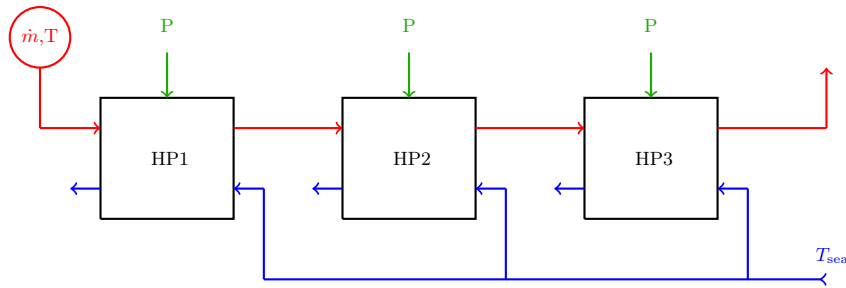


Figure 6.6: Dymola representation of the optimised concept used for dynamic simulations.

The system in Figure 6.6 has the same control as the system presented for the reference case, and each concept are subject to the same aFRR and FCR events. The Dymola setup can be seen in Figure A.3 in Enclosure A.

6.3.1 Power consumption

As was found and suggested in the report from [Rambøll, 2019], the fastest response for ancillary services is achieved by controlling the heat pumps by their power consumption. As mentioned in Chapter 5, two tests of the dynamic response of the system are conducted; One to test the capabilities of each concept when subject to an electricity consumption profile and one to test the maximum available capacity, if the heat pumps are allowed to reduce their load to a minimum of 10 %. The power consumption-profile for the first test includes a single 6 MW_e aFRR event of 20 minutes followed by some shorter FCR events. Figure 6.7 shows the power consumption from the optimised concept and the reference concept, when subject to an example of aFRR and FCR events. The base setpoint of ≈ 12 MW_e, corresponds to 97.6 % load for the reference and 100 % load for the optimised concept. The reason for the difference in load is that the optimised concept operates at higher COP than the reference. The mass flow are set as a constant of 550 kg/s, which for the reference

concept is divided evenly into the two parallel strings. The dynamic applied to all heat pumps in both concepts are equal. For this reason, it is expected, that there are no significant differences in the response between the two concepts.

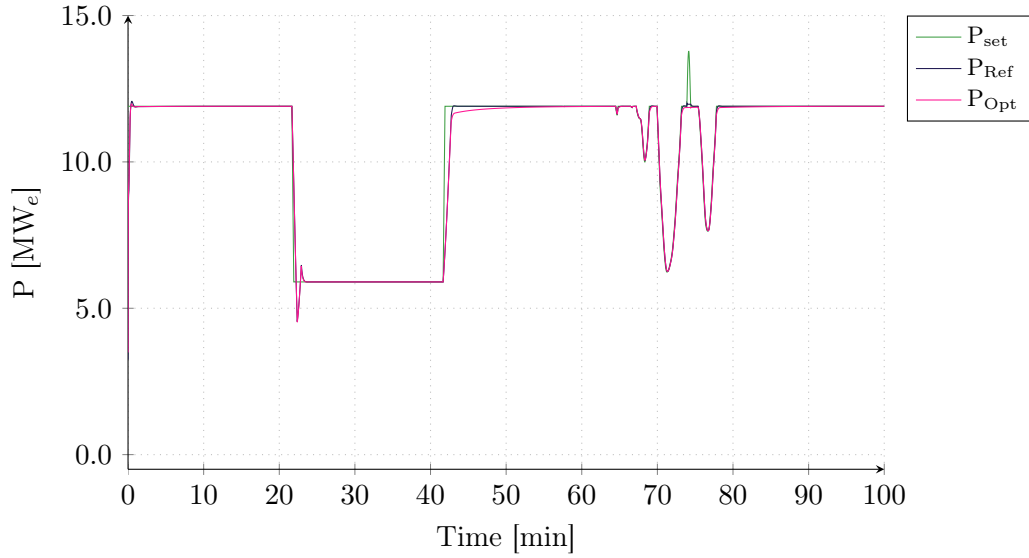


Figure 6.7: The power consumed by both the reference- and the optimised heat pump concept and the power setpoint from the controller including a 6 MW_e aFRR event and examples of FCR events.

The result of the test in Figure 6.7 shows, that there is no significant difference between the response of the reference concept and the response of the optimised concept.

The electric boiler supports the heat pumps when they are incapable of consuming the required amount of electricity. Figure 6.8 illustrates the operation of the electric boiler during the examples of ancillary services.

As expected, the electric boiler is deployed when the heat pumps are returning to the ≈ 12 MW_e base load. The fluctuations just after 20 minutes could probably be eliminated by an improvement of the controller. However, the peak just after 40 minutes represents the delay for the heat pumps when increasing the load. The electric boiler for the optimised concept must consume a little more than the one for the reference concept. The difference is however relatively insignificant.

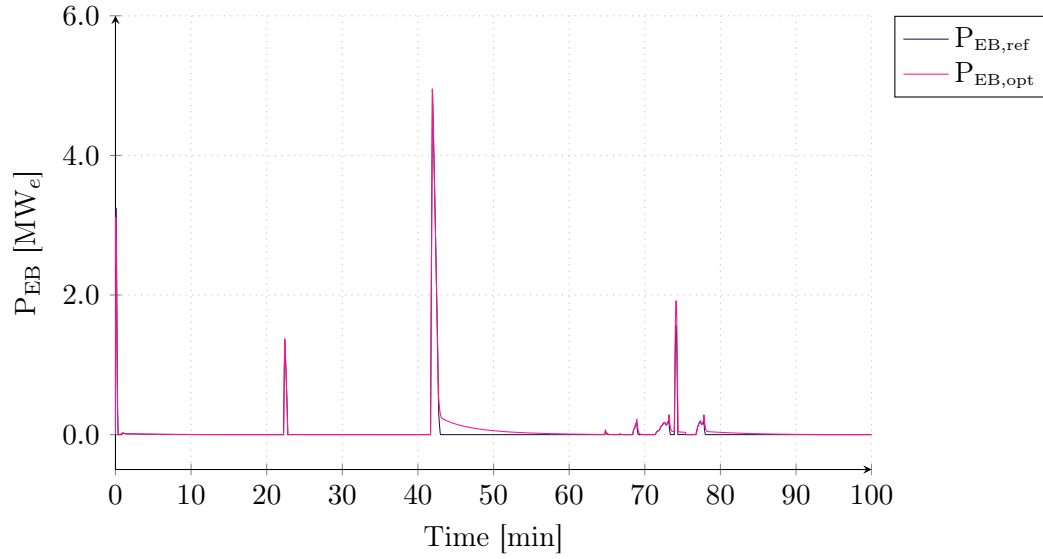


Figure 6.8: Power consumption from the electric boiler supporting the heat pumps, during the examples of aFRR and FCR events.

6.3.2 Temperature Response

The corresponding response of the district heating water temperature was measured as well and is seen in Figure 6.9.

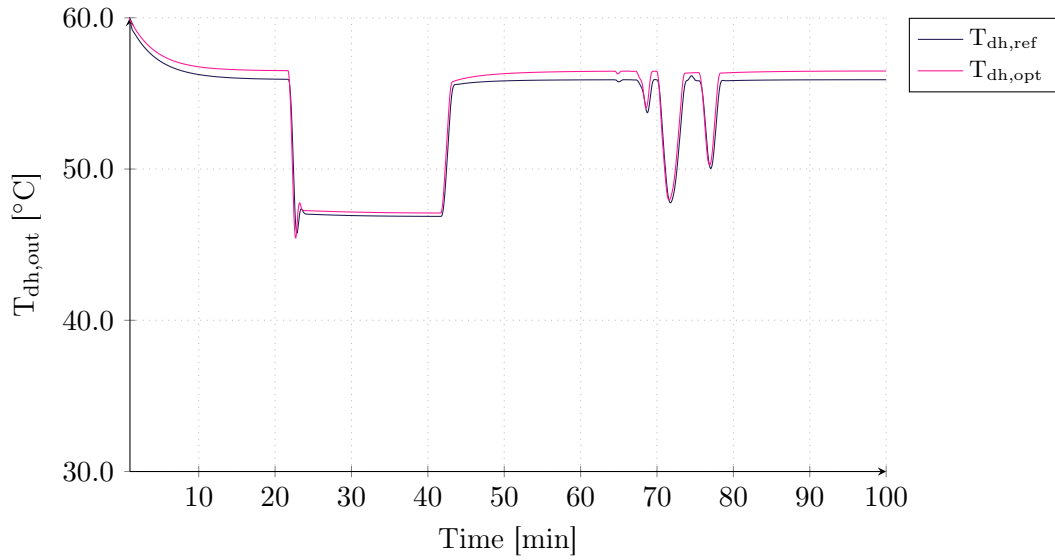


Figure 6.9: Temperature response for the reference concept and for the optimised concept when subject to examples of ancillary services.

As seen, both temperatures follows the progress of the operation profile in Figure 6.7.

The small temperature difference between the two concepts is again due to the improved COP in the optimised case. Aside from the temperature difference between the cases, there is no noticeable or unexpected tendencies observed for the temperature of the district heating water either. Both concepts appear to perform reasonably.

6.3.3 Maximum Capacity Test

A second test was made with regard to dynamic response and ancillary services. The test was conducted to investigate the maximum capacity for each concept assuming a minimum load of 10 %. Considering the reference concept, the load control and the applied load strategy implies that the second parallel string of heat pumps should switch off when the load reduces below 40 %. The remaining parallel string should, similar to all units in the optimised concept, switch off when reaching the minimum 10 % load. At this point, the minimum capacity is measured. Figure 6.10 show the result. The small fluctuation seen for the reference concept is caused by the second parallel string switching off. The optimised concept reaches its minimum load at 10 % at $\approx 1.5 \text{ MW}_e$ whereas the reference concept reduces to $\approx 0.8 \text{ MW}_e$.

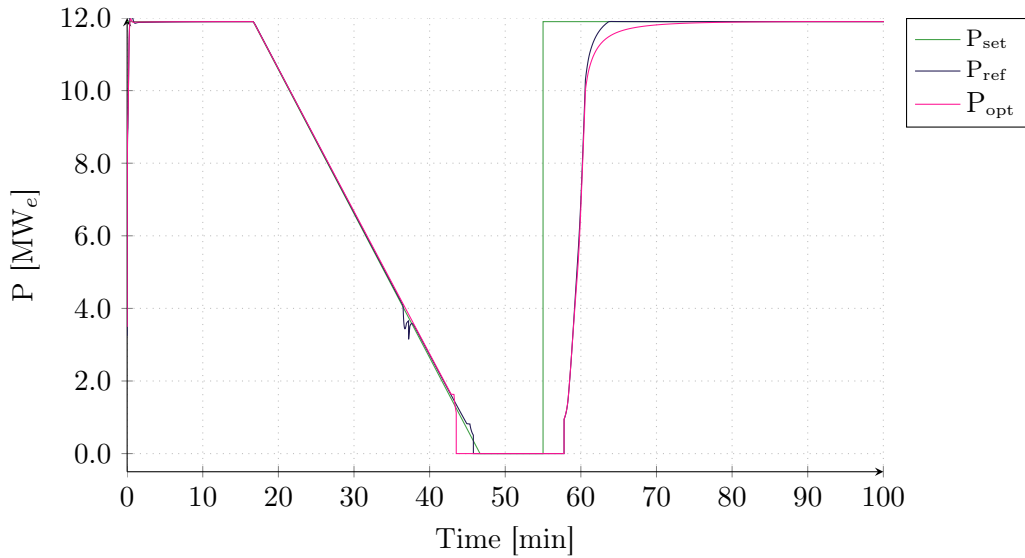


Figure 6.10: Maximum capacity test for the optimised and reference concept.

Generally, the tests indicate that there are no significant difference in performance and potential to provide ancillary services.

7 | Sensitivity Analysis

The sensitivity analysis is conducted to investigate the influence of variations in boundary conditions and reference assumptions made for the cost function to the optimisation results presented in Chapter 6. The purpose of the sensitivity study is to examine how significant variations or changes in terms of electricity price and investment costs must be to influence the choice of heat pump concept. In other words; to study the robustness of the optimised heat pump concept.

7.1 COP - Sensitivity to Electricity Costs

The sensitivity study investigates the effect of two parameters: electricity cost and investment cost. The electricity cost affects the COP, since higher electricity prices (elspot) most likely pushes the optimisation towards concepts with high COP. On the other hand, if the electricity costs reduces significantly, high COP will most likely be less influential.

The sensitivity to variations or uncertainties in the cost for electricity, was investigated by initially reducing or increasing the expected elspot price in each category with $\pm 40\%$. This gives rise to new cost function coefficients, which are presented in Table 7.1.

Table 7.1: Recalculated α -coefficients used for the sensitivity study of variations in electricity costs.

	Elspot - 40 %	Elspot + 40 %	Reference
α_1	481 330.2	795 439.9	638 385.0
α_2	7 020 854.7	11 134 563.3	9 077 709.0
α_3	4 320 498.9	7 042 801.8	5 681 650.3
α_4	3 603 196.7	5 597 453.2	4 600 325.0
α_5	13 350 258.2	21 653 964.1	17 502 111.1
α_6	940 724.3	1 367 248.8	1 153 986.6
α_7	3 131 853.6	5 133 461.0	4 132 657.3

Applying these recalculated α -values for new optimisations, produced the two optimised concepts seen in Figure 7.1.

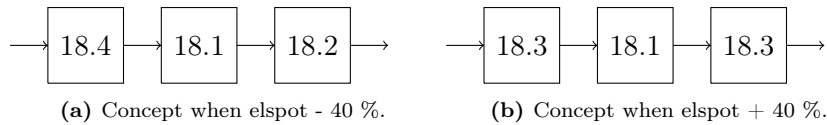


Figure 7.1: A sketch of the final concepts found from the optimisation when the elspot price is either reduced or increased by 40 %.

Based on the optimised concepts seen in Figure 7.1, the concept found in the original optimisation seems to be very robust to changes in electricity prices.

7.1.1 Elspot - 40 %

A further investigation of the results obtained from the optimisation conducted with a 40 % reduced cost for elspot indicates that there is a small reduction in the savings achieved from the optimum concept. Observing the distribution of the elements in the cost function seen in Figure 7.2, there is no significant difference from the original optimisation in Figure 6.3.

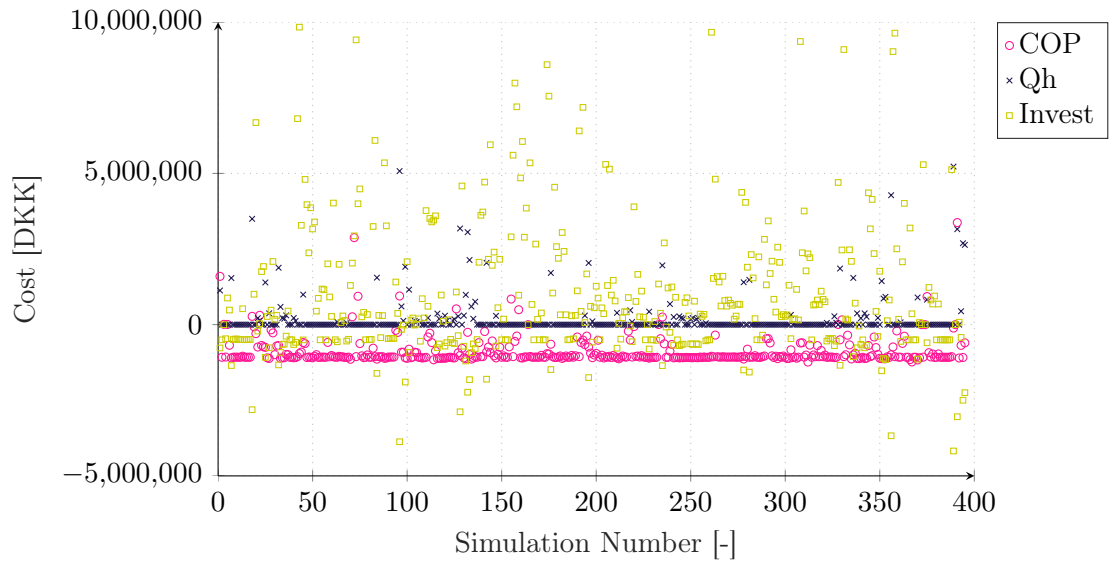


Figure 7.2: Output of the three costs that contributes to the overall cost function, when reducing the assumed elspot by 40 %.

The effect of the investment cost appears to be slightly higher. This is consistent with expectations, since lower cost for electricity naturally decreases the importance of high COP. A comparison of the optimised costs is found in Table 7.2.

Table 7.2: Cost reductions related to COP and total cost reduction for the optimised concept and an optimised concept assumed a 40 % reduction in costs for elspot.

	Original optimisation	Optimisation @Elspot - 40 %
COST_{COP} [DKK/year]	- 1 385 935	- 1 078 343
$\text{COST}_{\text{Total}}$ [DKK/year]	-1 886 414	- 1 578 865

The share of the total cost as a result of the COP reductions however reduces from 73 % for the original optimisation to 68 %.

7.1.2 Elspot + 40 %

Bearing in mind the results found by reducing elspot by 40 %, and the results from the original optimisation, the results from increasing the elspot price by 40 % is not surprising. Figure 7.3 show the cost allocations for the individuals.

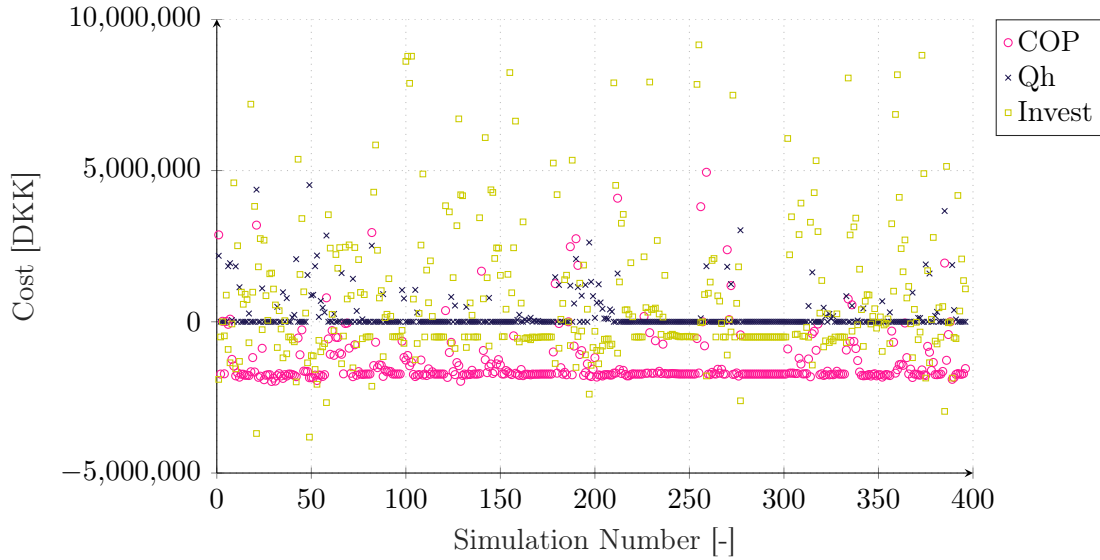


Figure 7.3: Output of the three costs that contributes to the overall cost function, when increasing the assumed elspot by 40 %.

An increase in cost for electricity is expected to increase the sensitivity to COP. Comparing Figure 7.3 with the result presented in Chapter 6 in Figure 6.3, the variations in COP seems to be more fluctuating, but since the results was already dominated by the profit achieved from a COP improvement, the final result was almost unaffected. A comparison of the optimised costs is found in Table 7.3.

Table 7.3: Cost reductions related to COP and total cost reduction for the optimised concept and an optimised concept assumed a 40 % increase in elspot.

	Original optimisation	Optimisation @Elspot + 40 %
COST_{COP} [DKK/year]	- 1 385 935	- 1 728 332
$\text{COST}_{\text{Total}}$ [DKK/year]	- 1 886 414	- 2 228 542

When increasing the cost for electricity, the share of the total cost reductions as a result of reduced COP increases to 77 %.

7.2 Investment Cost

The investment cost for each individual heat pump was defined from guidelines in [Danish Energy Agency and Energinet, 2016]. However, these numbers are associated with a number of uncertainties, which is supported by the experiences described in [Rambøll et al., 2019], where it is shown how the investment costs from existing units varies a lot even for equal sized systems. The specific investments cost for heat pump units of less than 1 MW_q was found to vary from around 3 million DKK/MW_q to around 22 million DKK/MW_q.

By increasing the cost pr. MW_q the penalty from choosing several smaller heat pumps compared to the penalty of choosing a few larger units increases as well. The economy of scale used for the optimisation was assumed to be 0.8, meaning that a capacity increase of 100 % corresponds to an increase in investment costs of 80 %.

From the technology catalogue [Danish Energy Agency and Energinet, 2016], the uncertainties related to the investment costs of the heat pump is additionally assessed both in terms of performance and costs. An upper and a lower estimate for the 2020 price and performance levels is presented. Table 7.4 shows the estimated costs for a lower and upper (denoted high) expected cost margin.

Table 7.4: Estimations of costs for large scale heat pumps suggested by [Danish Energy Agency and Energinet, 2016].

Unit capacity [MW _q]	Investment [DKK/MW _q]
4 (ref)	4 950 000
3 (low)	3 750 000
6 (high)	7 500 000

Based on the estimations from the technology catalogue regarding economy of scale and base price, the four test conditions presented in Table 7.5 were applied for the sensitivity study.

Table 7.5: Conditions and recalculated reference cost and investment cost equation for the sensitivity study of the investment costs.

	EOS ₁₀₀	EOS ₅₀	Invest _{ref,low}	Invest _{ref,high}
Cost _{CAPEX,ref}	272 000 000.0	198 554 156.0	150 209 142.2	365 848 253.1
Cost Equation	$5e6\dot{Q}_{h,n}$	$7e6\dot{Q}_{h,n}^{0.7505}$	$4e6\dot{Q}_{h,n}^{0.848}$	$1e7\dot{Q}_{h,n}^{0.848}$

7.2.1 Economy of Scale

The optimised results achieved by changing the effect of economy of scale to 50 % and by removing the effects completely are seen in Figure 7.6a and Figure 7.4b.

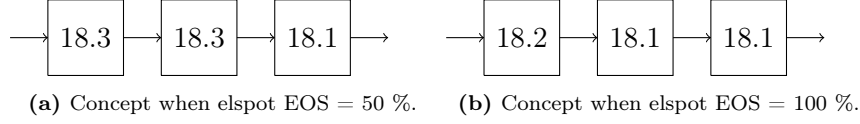


Figure 7.4: A sketch of the final concept found from the optimisation when EOS is set to 50 % and the concept found by removing the effects of EOS.

Similar to the results found by applying changes to the electricity costs, the optimised concept remains almost identical.

By increasing the effects from economy of scale, the optimisation is pushed towards a concept with few large units. However, since the original optimised concept does already use a minimum number of units to achieve the desired capacity (when assuming $\dot{Q}_{h,n,\max} = 18.5 \text{ MW}_q$), it is expected, that the result remain unchanged. A comparison of the costs for investment when EOS = 50 % is seen in Table 7.6

Table 7.6: Cost reductions related to investment costs and the total cost reduction for the optimised concept and an optimised concept assumed a EOS of 50 %.

	Original optimisation	Optimisation @EOS = 50 %
$\text{COST}_{\text{CAPEX}} [\text{DKK}/\text{year}]$	- 501 896	- 777 417
$\text{COST}_{\text{Total}} [\text{DKK}/\text{year}]$	- 1 886 414	- 2 179 368

The interesting aspect is that for the original concept, the investment cost was responsible for 26 % of the total cost reduction where as for an optimum concept with EOS = 50 %, the share increases to 36 %. This however causes no changes in the results, since the original optimisation already chose a concept favouring a few but large units.

If the effect of economy of scale is neglected it implies, that there is no difference in investment costs if the optimisation chooses nine small units or chooses three units with three times the capacity of each of the small ones. By removing the effect of EOS, the favouring of large units is smoothened and the optimisation should be more likely to choose smaller units as well. The results achieved with EOS = 100 % is listed in Table 7.7.

Table 7.7: Cost reductions related to investment costs and total cost reduction for the optimised concept and an optimised concept assumed a EOS of 100 %.

	Original optimisation	Optimisation @EOS = 100 %
$\text{COST}_{\text{CAPEX}}$ [DKK/year]	- 501 896	16 480
$\text{COST}_{\text{Total}}$ [DKK/year]	- 1 886 414	- 1 329 852

When there is no effect of economy of scale, reducing the costs for investment becomes tricky, since it would require a reduction in capacity. A consequence of this is additionally, that the optimisation reduces the capacity to a minimum before being penalised significantly on the heating capacity. The penalty for the heating capacity is in fact ≈ 25 times higher than the original optimisation with 73 530 DKK/year compared to 2 889 DKK/year for the original optimisation.

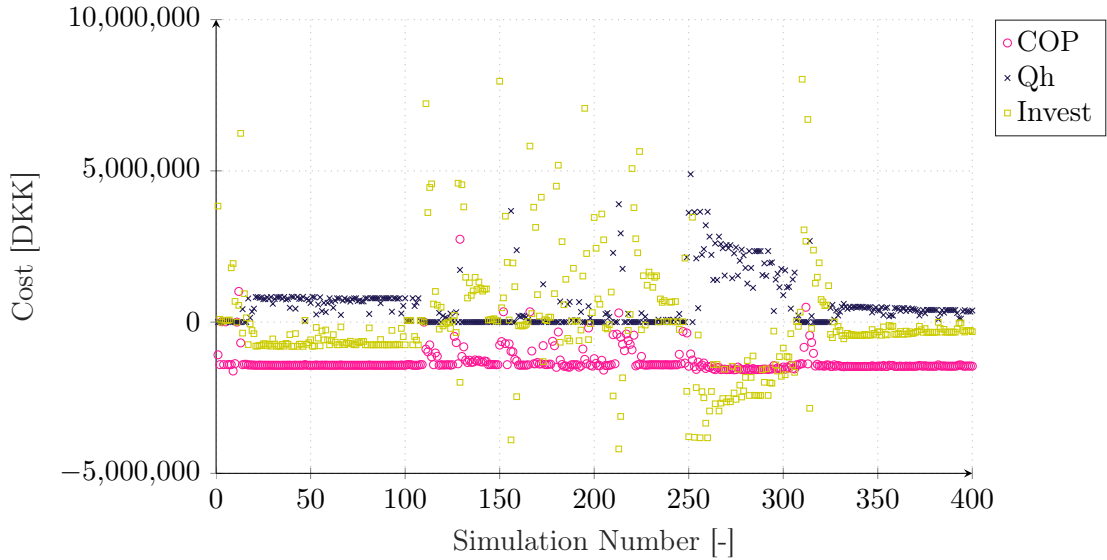


Figure 7.5: Output of the three parameters that contributes to the overall cost function, when removing the effects of economy of scale.

Figure 7.5 correspondingly shows, that there is a significant correlation between the investment cost and the penalty for heating capacity. Most of the solutions suggested in the first 100 generations reduce the investment cost but cause increased cost due to the reduced capacity. From generation 100 to 250, the general tendency is that the solutions does not produce any extra cost for heating capacity, but a lot of expensive solutions in terms of investment cost are suggested. From 250 to 350, the optimisation attempts to reduce the capacity and thereby the investment cost, but this is penalised by the cost for capacity. Overall, the trade off between minimum investment cost and the capacity requirement was however not found to produce significant changes to

the optimised concept.

7.2.2 Investment benchmark

The last changes made for the cost function are regarding the cost used as benchmark for the investment cost evaluations. Similar to the effect of economy of scale, the effects of changing the reference for the cost calculations is investigated. The benchmark-change is made according to the suggestions in [Danish Energy Agency and Energinet, 2016]. However, the results, presented in Figure 7.6 once again demonstrated the robustness of the concept found in the original optimisation.

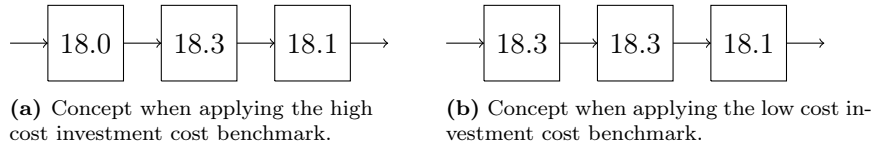


Figure 7.6: A sketch of the final concepts found from the optimisation when changing the benchmark for the investment cost evaluation

Both concepts have a total capacity of around 54.5. By choosing the *high* benchmark based on a 6 MW_q unit with a cost of 7 500 000 DKK/MW_q, the investment cost becomes more significant in the final cost than by choosing the *low* benchmark with a cost of 3 750 000 DKK/MW_q. This also explains the small difference between the capacities of the *high* benchmark and the *low* benchmark optimised concept. Table 7.8 lists the optimised investment cost for the two concepts.

Table 7.8: Cost reductions related to investment costs and total cost reduction for the optimised concept and an optimised concept assumed a EOS of 100 %.

[DKK/year]	Original optimisation	High benchmark	Low benchmark
COST_{CAPEX}	- 501 896	- 922 706	- 566 689
COST_{Total}	- 1 886 414	- 2 257 019	- 1 968 952

For the concept with the *high* benchmark, the share of investment cost reduction to the total cost reduction is around 40 %. Generally, the *high* benchmark increases the significance of the investment, meaning that the optimised concept is not only dominated by high COP. However, the reference cost for investment implies that the optimisation, similar to the test with EOS = 100 %, reduces the capacity to a minimum in order to minimise the investment costs. This additionally implies, that a lot of solutions are rejected since they violate the constraints set for the heat output during the COP evaluation.

The *low* benchmark produces results almost identical to the original optimisation. This is consistent with expectations, since lower investment costs imply that the penalty for capacity reductions is more significant than the savings from reduced investment costs, which is also seen from the original optimisation.

All in all the optimised concept is found to be very robust to changes in both reference cost for the COP and for investment. The original optimisation problem itself favours concepts that with the lowest possible investment cost meet the requirements for the heating capacity while seeking for the highest possible COP. All tests where either the influence of COP is increased or the cost for small units is increased, the optimisation is pushed towards increased effects of parameters that are already dominating the original optimisation. By reducing the effect of COP or by removing or reducing the profitability of large units, the costs are affected but not to an extent that changes the heat pump concept. This even though the sensitivity tests were conducted with some extreme changes to the original costs.

A combination of reduced elspot and reduction of EOS-effects possibly changes the outcome, but this would be an even more extreme condition which is unlikely. Instead, a plausible case could be that the manufactures can not deliver heat pumps with enough capacity.

7.3 Maximum Capacity Reduction

Assuming that the maximum capacity of a single heat pump unit is 15.5 MW_q instead of 18.5 MW_q , the heat capacity requirements can not be achieved from just three heat pumps. The optimised concept given these capacity limitations is shown in Figure 7.7

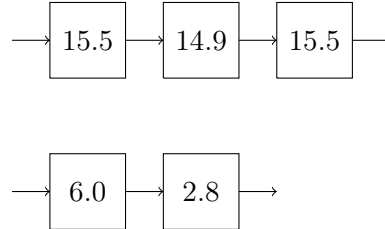


Figure 7.7: A sketch of the final concept found by limiting the maximum capacity of a single heat pump unit to 15.5 MW_q

The concept seen in Figure 7.7 consists of five heat pumps; three large heat pumps in series which is in parallel with a series of two smaller heat pumps. An investigation of the 500 generation simulation conducted with the reduced maximum capacity gives a further idea of the balance between COP maximisation and investment cost minimisation. In addition to the optimum concept found by the optimisation, four other concepts with reasonable performance were picked for comparison. These alternative

concepts (AC) are listed in Table 7.9 and the corresponding cost and cost allocation is listed in Table 7.10.

Table 7.9: The alternative concepts picked for further investigation based on optimisation result achieved by reducing the maximum allowable capacity to 15.5 MW_q.

	AC_{best}	AC₁	AC₂	AC₃	AC₄
$\dot{Q}_{n,1}$ [MW _q]	15.5	15.5	15.5	15.5	15.5
$\dot{Q}_{n,2}$ [MW _q]	14.9	10.7	15.1	14.9	15.2
$\dot{Q}_{n,3}$ [MW _q]	15.4	15.5	15.5	13.2	13.1
$\dot{Q}_{n,4}$ [MW _q]	6.0	6.1	8.5	3.0	5.6
$\dot{Q}_{n,5}$ [MW _q]	2.8	2.7	0.0	2.7	5.1
$\dot{Q}_{n,6}$ [MW _q]	0.0	4.4	0.0	0.0	0.0
$\dot{Q}_{n,7}$ [MW _q]	0.0	0.0	0.0	2.2	0.0
$\dot{Q}_{n,8}$ [MW _q]	0.0	0.0	0.0	3.4	0.0
$\dot{Q}_{n,9}$ [MW _q]	0.0	0.0	0.0	0.0	0.0

Table 7.10: Costs allocations for different alternative concepts found by reducing the maximum allowable capacity to 15.5 MW_q.

Cost [DKK/year]	AC_{best}	AC₁	AC₂	AC₃	AC₄
Cost_{COP}	- 1 476 928	- 1 570 123	-1 015 727	- 1 565 224	-1 493 992
Cost_{heat}	4 275	7.0	9.0	7.0	46 749
Cost_{CAPEX}	236 945	674 749	- 9495	763 557	295 835
Cost_{Total}	- 1 234 807	- 895 367	- 1 025 213	-801 659	- 1 151 406

The results presented in Table 7.10 answer some of the questions, that could be raised regarding the results achieved from the optimisation with 15.5 MW_q limitation on capacity. The concept denoted AC₁ is a concept with three relatively large heat pumps in series, which is in parallel with three smaller heat pumps also in series. As expected, this implies that the COP improves and thereby the COP-saving for AC₁ is increased by $\approx 100\,000$ DKK/year compared to the best alternative concept. However, by introducing an additional heat pump, the investment cost increases with $\approx 350\,000$ DKK/year, which consequently causes AC₁ to be rejected. With this result, another interesting concept is the concept denoted AC₂, which has three heat pumps with nearly the maximum allowable capacity in series with a single 8.5 MW_q heat pump in parallel. However, by removing the serial coupling in the second parallel string, the savings obtained from improved COP is almost 450 000 DKK/year less than from the best alternative concept. On the other hand, AC₂ actually produces savings in terms of investment costs. However, the the saving achieved from the in-

vestment cost reduction insufficient to counterbalance the reduced saving from COP. A concept, which similar to AC_1 is included with a view to increased COP, is AC_3 . AC_3 has similar to the other concepts three relatively high capacity heat pumps in series which is in parallel with two strings, each with two small heat pumps in series. This concept increases the savings for COP with $\approx 90\,000$ DKK/year, but similar to AC_1 the investment costs increase significantly, and the concept is for this reason rejected. The last concept in question is AC_4 , which is similar to the best alternative concept. The only difference is that the heat pumps in the second string is nearly equal-sized. The end result is very close to the best alternative fit. AC_4 improves the saving in COP by $\approx 17\,000$ DKK, but on the other hand, the investment cost and the penalty for heating capacity increase. The reason for the increase in the penalty for heating capacity is most likely since the total capacity of AC_4 is a little lower, than the total capacity for the best alternative.

All in all the test of different alternative concepts gives an indication of how the optimisation seeks to find the optimum balance between reductions achieved by COP and the penalty from increasing investment costs.

7.4 Comparison

To summarise the findings from the sensitivity study, the costs and cost allocation for each of the tests conducted from the sensitivity study is found in Figure 7.8.

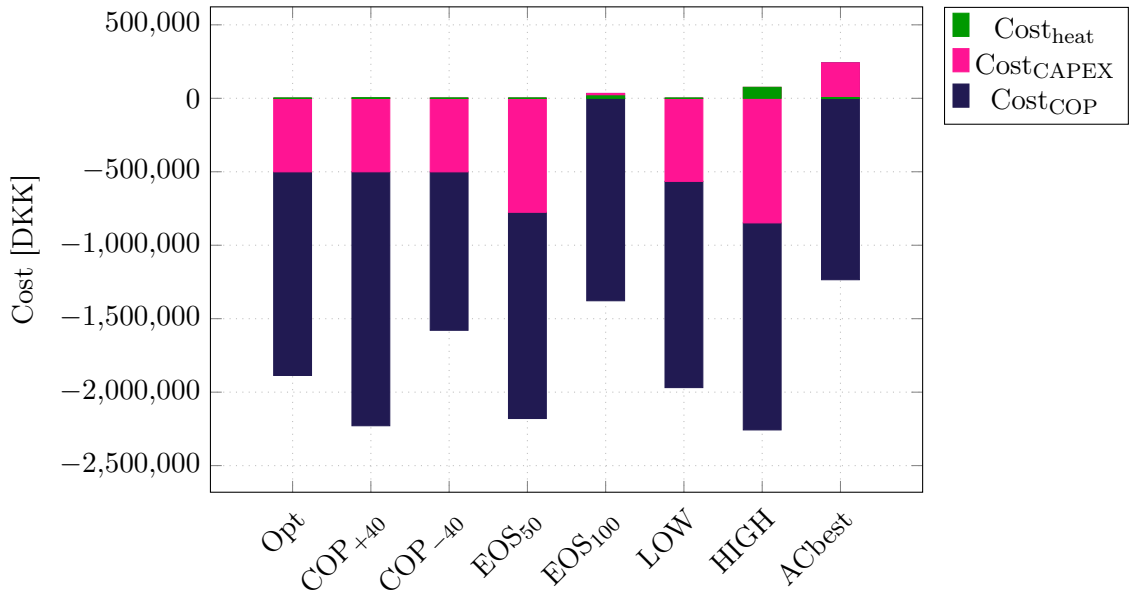


Figure 7.8: Comparison of the cost allocation for the tests conducted in the the sensitivity analysis.

Common to all the tests are that the effect of the penalty for reduced heat capacity

is insignificant compared to the savings achieved from the investment cost and COP improvement. Contrary to the costs for investment and costs for COP, there is no possibilities for savings by increased heat capacity. For this reason, the best possible solution in terms of costs for heat capacity is a solution that produces zero extra costs. As seen in Figure 7.8 the contribution from the heat capacity cost only appears to have a small influence for the test conducted with the high reference cost.

Another noticeable effect is seen from the test where the effects of economy of scale is removed. This implies that the possible savings obtained from larger units disappear. For the last test with reduced maximum capacities, reduced investment costs similarly become a challenge, since the number of units can not be reduced compared to the reference. The concept found by the optimisation consist of five heat pumps, which naturally cause the investment cost to increase, but the concept however improves the COP to achieve the final savings.

Overall, the sensitive analysis shows that the concept found by the optimisation is very robust to changes. The allocation of the cost reductions are affected but the optimised concept is in all cases three units in series of $\approx 18.3 \text{ MW}_q$ each. Only by changing the maximum allowable capacity of the individual units a new optimised concept was found.

8 | Discussion

This chapter presents, evaluates and discusses the potential and limitations of the model in Dymola and the chosen optimisation algorithm together with the results and the cost functions with an eye to the practicalities of the projecting and the implementation of large scale heat pump systems. In continuation hereof, some considerations on the possibilities and potentials for heat pumps to deliver ancillary services are discussed.

The Modelling Approach

Essential for the general approach to the problem - especially due to the performance-map approach - is that all results and all possible conclusions are a consequence of choices and assumptions made during the process. This is not necessarily a negative feature, since it provides the opportunity for a various number of studies, but it requires some awareness when drawing conclusions. The performance map approach does among other things imply, that the modelled heat pump performance rely solely on the performance data provided from a single unit, a single set of nominal conditions and a single unit type and underlying capacity, moreover it is assumed to be scalable for adjustments in Dymola. This has the two noticeable consequences, that the validity of the results are contingent on operational conditions, and more importantly that some essential information on dynamic behaviour is lost. The relevant dynamic effects, especially relevant on the power consumption, is instead implemented based on assumptions on the load-gradient limitations. The immediate consequence of this, is that the results are an outright reflection of the assumptions and not the actual physical limitations. The advantage is however, that the effects of changes in dynamics is easily available for further investigation. Another example of a consequence of the modelling approach is related to the construction of the map, which has some inappropriate build-in errors to be aware of.

One of the advantages of the performance map used in this thesis is that it includes the performance degradation associated with part load operation. The disadvantage of this feature is that the performance map does not ensure that COP and \dot{Q}_h equals 0 when the load equals 0. The reason for this is that the map aside from load is described by the evaporation temperature and the outlet temperature of the district heating water. To avoid that the heat pump model allows for heat production at zero-load at all temperature combinations, it would require that the map was able to force the output to 0, whenever the load is 0. With the current design and otherwise sufficient performance of the map, this is not a straightforward adjustment to the map itself. Instead, an adjustment was implemented in Dymola, which ensures that the heat pump does not produce heat, when the load equals zero. Returning to the discussion about the dynamic effects or the map-build-in absence of these, the major advantage of the choice of Modelica/Dymola as a tool, is that additional adjustments

and dynamic effects is easily implementable. The model applied in this study is in fact a case in point, since both the thermal dynamics and the effects of compressor dynamics have been integrated without modelling any actual heat exchangers or compressors.

Optimisation and Optimisation Results

Bearing in mind that the choices made during the modelling process are reflected in the results, one of the main objectives in this study was to investigate how an optimum heat pump concept should be designed giving some operating conditions. In this process, some further questions could be raised both regarding the optimisation approach, but most interesting regarding the potential and possible challenges related to the results obtained.

The first question to be raised could be whether the results are significantly affected by the integrated biasing that favour the reference concept. The operating profile is based on the reference concept and so is the heating load and the number of operational hours. The categorisation smooths out some of these effects, but a further optimisation of the operating profile would probably increase the profit from the optimised heat pump concept. Since the optimised concept with three large heat pumps in series appears to improve COP, the optimised operating profile used as the underlying basis of the concept optimisation, would most likely increase the profit achieved from the optimising the heat pump concept. The optimisation of the operating profile considers (among other things) the heat pump performance, electricity costs and the fuel costs for other units in the system. Specifically, a consequence of this is that the cost reduction of $\approx 1\,900\,000$ DKK/year possibly could be reduced even further.

Additionally, when considering the possible cost reductions, an interesting assumption regarding the heat capacity penalty β is worth discussing. One of the important assumptions is that the costs scale linearly. Especially for the the heating capacity penalty, this might be associated with a number of uncertainties. Recall that the β values used for the capacity evaluation are divided into four categories of significantly different magnitude, meaning that a capacity reduction in category 2 is almost 120 times as expensive as a capacity reduction in category 4. This has two reasons: firstly, the categories represent different operating conditions. Category 4 represents the conditions for the summer period, where the heating demand is low and where the amount of full-load hours are significantly reduced compared to category 2, which account for a significant amount of the total heat delivered ($> 40\%$). For this reason, it naturally becomes more expensive to operate with reduced capacity during periods with high heating demand than in periods with low heating demand. Secondly, the calculation of the β -values is based on a 10 % capacity reduction. For the periods with low heating demand, the heat pumps operate in part load most of the time. A consequence of this is that a 10 % capacity reduction most likely just implies that the heat pumps increase the load, and thereby no extra costs occur due to extra

operation of other units. However, a 20 or 30 % capacity reduction most likely gives rise to extra operation of those units, which in reality increases the cost significantly more, than what is represented in the β -value. In other words, the assumed linear scaling of the cost of capacity reductions does not prove correct. The consequence of this is however relatively insignificant. First of all, the reason for this is that if the concept fulfil the heating capacity requirement for the categories which is already expensive, the concept is most likely also capable of meeting the requirements for the categories with low penalty. In addition, the total cost for all concepts tested are generally much more influences by the savings achieved from COP improvements and investment cost reductions, than they are from the heating capacity. To make a simple test of the effects of this assumption, the capacity penalties were recalculated, with $\beta_3 = 4\,062\,250$ DKK/year and $\beta_4 = 1\,656\,780$ DKK/year which corresponds to a penalty increase with a factor of 10 and 20 respectively. The results are displayed in Figure 8.1.

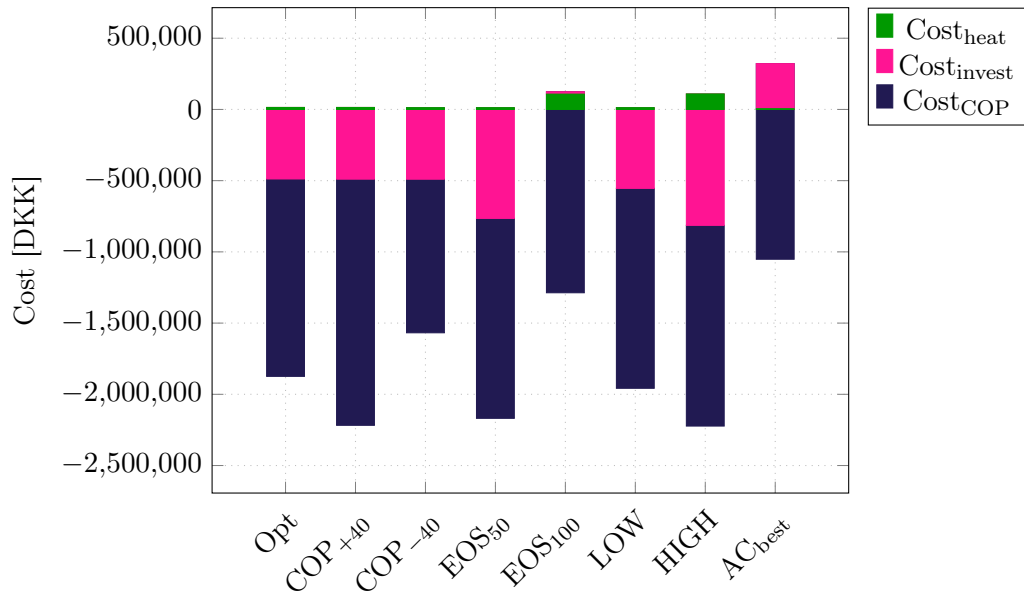


Figure 8.1: Comparison of the cost allocation for the tests conducted in the the sensitivity analysis, with β_3 and β_4 increased by a factor of 10 and 20 respectively.

The test results in Figure 8.1, indicates that despite being associated with uncertainties which might have influence on other matters, the optimisation results will most likely not be affected significantly if the penalty in category 10 and 11 increases. Generally, it should be noticed, that the weighting is based on the reference concept, and all results is thereby an indication of the penalty of saving relative to the reference.

Sensitivity Analysis and Practical Considerations

Despite of the biasing for the reference concept both the optimisation and the sensitivity study almost without exception indicate that the optimum between COP and investment cost while meeting the heat capacity requirements is found by arranging three $\approx 18.2 \text{ MW}_q$ heat pumps in series. Generally, this choice of concept is not surprising, as the optimisation seeks to maximise the COP, which it achieves by the maximum allowable serial connections of three. At the same time, the optimisation attempts to reduce the costs for investment, which due to the EOS-effects favours large units. Basically, it means that for the optimisation to propose any other concepts, the effects of EOS should be reduced significantly or removed completely while the costs for electricity should be reduced to a degree where the effect of COP additionally becomes insignificant. Alternatively, if the expected operating profile for some reason includes a significant amount of part load operation, the optimisation would most likely be more disposed to seek for concepts with more than one parallel string. That said, a number of other parameters/conditions that might change the tendencies observed for the current optimisation and sensitivity analyse, could be interesting to consider for further extension of the optimisation problem. This could be:

- **Maintenance:** which represents some costs which should be minimised. Additionally, these costs depend on the heat pump concept. If the concept consists of three large but identical heat pumps, the cost for maintenance and spare parts will naturally be lowered, compared to a concept with nine heat pumps of various capacity. On the other hand, the introduction of these effects, would probably favour the concept already suggested by the optimisation.
- **Redundant Capability:** in continuation of considerations regarding maintenance, ensuring redundancy is additionally essential when planning large scale heat pump projects. In practice, this would typically include requirements for guaranteed temperature of the district heating water and/or some minimum requirements for the delivered heating output when a unit fails. Bearing this in mind, it is conceivable that a guarantee on the outlet temperature is easily achievable for a concept with several parallel strings as the reference, since the desired outlet temperature is already produced by both parallel strings. For a serial based concept as the one suggested by the optimisation, ensuring redundancy becomes more tricky and will most likely give rise to increased investment and construction costs due to the need for extra piping for bypass etc..

Furthermore, in terms of ensuring redundancy for a purely serial connected concept, it is not insignificant which type of compressors the concept consists of. The performance map is based on a high pressure screw compressor (GEA), which most likely would be able to deliver e.g. 70°C regardless of failure of a unit. However in reality, if the optimised concept was implemented, it would be a combination of low pressure and high pressure compressors, which, depending on the unit that fails, could entail

that the requested district heating water temperature cannot be guaranteed. For e.g. turbo-compressors, ensuring redundancy would be even more challenging for the optimised concept, since these are designed for some given temperatures, specifically. On the other hand, it is not always a priority to maintain a specific district heating water temperature. For the system in Esbjerg, the heat pumps will (most likely) be controlled by the electricity consumption especially for the purpose of providing ancillary services. The temperature of the district heating water is instead mixed to reach the desired temperature later in the system, meaning that severe requirements for the outlet temperature become of less relevance.

In relation to this, one of the considerations presented in the sensitivity analysis involved the maximum capacity of the individual units. The question is, if it is actually feasible to have units of $\approx 18.2 \text{ MW}_q$ (or, ≈ 16.7 if leaving out of account the scaling performed to adapt to the performance map). The subsequent question is then why the optimisation does not suggest a concept with two parallel strings each with three serial connected heat pumps instead of two strings, one with three large heat pumps in series and one with two small heat pumps for supplement during peak load. The immediate answer is that the investment costs become the dominating factor. Due to the effects of economy of scale, the increase in COP does not compensate for the increased investment cost. However, by removing these effects, the optimisation does actually suggest a concept with six heat pumps, two parallel strings, each with three heat pumps. The cost allocation of this concept is seen in Table 8.1.

Table 8.1: Comparison of the cost allocation for an optimised concept with maximum capacity limitations of 15.5 per heat pump unit and no effects of economy of scale

Cost [DKK/year]	New optimisation
Cost_{COP}	- 1 721 945
Cost_{heat}	52 540
Cost_{Invest}	38 286
Total Cost	- 1 631 119

The results in Table 8.1 indicate, that even if the original optimised concept turns out to be infeasible because of the high capacity requirements, a similar concept, with smaller units and an additional parallel string, annual cost reductions could be achieved. Furthermore, in this context it should be considered whether the construction of the model limits the optimisation inappropriately by allowing for a maximum of 3-serial coupled heat pumps. This limitation is set based on a general rule of thumb, which states that no more than three heat pumps in series is feasible, as it simply becomes too difficult in terms of control. It is conceivable that this might be related to the temperature of the district heating water. If this is the case, it would probably be interesting to include an extra (or more) serial coupled heat pump, since

the project in Esbjerg as mentioned does not consider the outlet temperature as an important parameter. This does however depend a lot on the specific system, and more effort should probably be put to investigate the exact consequences of *many* serial coupled heat pumps.

Control Strategy and Ancillary Services

With regard to control, control strategies and dynamic response, some further interesting considerations could be done. The results from the dynamic tests indicated, that under the conditions presented in this study, there are no significant differences in the potential for providing grid balancing services. An argument for choosing a concept similar to the reference could be that it, contrary to the original optimised concept, allows for switching off units during ancillary services. This would be particularly beneficial if the heat pump concept provides many hours of high-capacity ancillary services. The reference concept would most likely be able to switch off one parallel string while being able to operate at relatively high COP in the meantime. On the contrary, the original optimisation would have to reduce its load significantly. Recalling the performance degradation when the load reduces below 40 %, this will most likely increase the operating cost. However, looking at the historical data for ancillary services [Dalgas Rasmuseen and Energinet.dk, 2020], the above mentioned might not prove correct. Statistically, the capacity for FCR and aFRR is $\approx 1\%$ and 25% of the bid. So for a case as the one in Esbjerg, 10 MW_e might be the maximum capacity of a bid. This means, that the average FCR activation is 0.1 MW_e and the average aFRR activation is 2.5 MW_e . The response for each concept is seen in Figure 8.2.

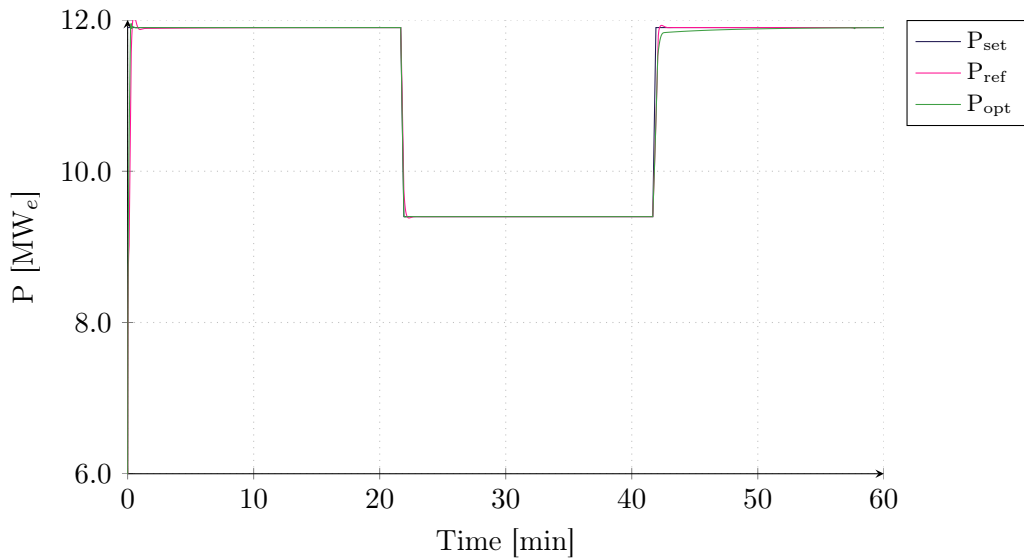


Figure 8.2: Power response for the reference concept and the concept suggested from the optimisation to a 2.5 MW_e aFRR event.

The load during the 2.5 MW_e aFRR event in Figure 8.2 is $\approx 82\%$ for the reference and 84 % for the optimised concept. This indicates, that there for the typical aFRR and FCR events would be no significant difference in performance. With the existing setup, the control strategy should however be reconsidered, to challenge this observation. As for all results presented, they are all a consequence of the conditions defined for the problem. If significant changes to the hysteresis levels applied for the heat pumps changes, this would most likely affect the results. Similarly, if an individual load control for each heat pump was implemented, the tendencies could easily change.

The essential and interesting thing about the optimisation in combination with the setup in Dymola is exactly, that it allows for both ancillary services and load strategies to be included. The common challenge for these is to quantify and evaluate them fairly against the general performance of the system as presented in this study. Although the results from both the optimisation and the following sensitivity study indicate a very robust heat pump concept, there are plenty of other considerations and parameters to include, which the setup at the same time is prepared for.

9 | Conclusion

This study introduces and demonstrates the application of a heat pump concept optimisation setup. Based on an ongoing project in Esbjerg, a 50 MW_q sea water heat pump concept is to be developed. For this reason a performance map based heat pump model is implemented in the multi-domain modelling language, Modelica. A heat pump system model allowing for simulation of a various number of heat pump concepts is exported to Python using a Functional Mock-up Unit. In Python, the nonlinear optimiser, μ -Genetic Algorithm is implemented. Relative to a reference heat pump concept, the optimisation seeks to find the best heat pump concept with regard to COP, heating capacity and investment costs. A further sensitivity study is carried out to investigate whether and to what extent the optimised heat pump concept is robust to changes in costs for electricity and changes in the basis of the investment costs.

The heat pump simulation model in Dymola (Modelica) is designed to allow for the optimisation to combine a total of nine individual heat pumps. The concept can as a maximum include three heat pumps in series and three heat pumps in parallel. By the use of a single variable for each heat pump, $\dot{Q}_{h,n}$, representing the nominal capacity of the heat pump, the number of heat pumps, the connections between the heat pumps and the size of each individual heat pump can be set.

The simulation model in Dymola is exported to Python and implemented in a μ Genetic Algorithm, which aside from searching for an optimum heat pump concept with regard to COP, heating capacity and investment cost, also allows further integration of dynamic response and ancillary services. The optimisation is evaluated in 11 steady state categories during the optimisation. The categories are defined based on an example of the expected operational hours and heat output of the system in Esbjerg. The categories represent the operating conditions in terms of both seawater temperatures, district heating water return- and forward temperatures and setpoints for the heat output. The categories are based on the performance of a reference heat pump concept with four heat pumps arranged in a 2-by-2 configuration. The cost evaluation represents the penalty or possible profit achieved by the reductions or improvements of performance during the 11 categories relative to the reference concept. The cost functions are hence a reflection of the performance of a heat pump concept relative to the reference concept weighted according to expected operational hours and heat output.

The optimisation found that a heat pump concept of three large serial coupled heat pumps with a capacity of ≈ 18.2 MW_q is the best choice both in terms of COP and investment costs when complying with the heating requirements. Compared to the reference concept, the optimised heat pump concept is found to reduce the annual costs by $\approx 1\,900\,000$ DKK.

The sensitivity study further indicated, that the optimised concept is fairly robust with regard to changes in both electricity costs and changes to the underlying basis of the investment costs. The cost for elspot was reduced and increased with ± 40 % without having any significant influence on the final optimisation result. Similarly, the effect of economy of scale was first increased to 50 %, and then removed completely. The optimised concept was however unchanged, despite observing some significant changes in the cost allocation for the concepts. If the maximum allowable capacity is reduced, an additional optimisation indicates, that the optimum concept remains as three large heat pumps (of $\approx 15 \text{ MW}_q$ each) but supported by two small units in series during peak load periods.

A following investigation of the optimised concept in comparison with the reference concept regarding the potentials to provide ancillary services indicated, that there is no significant difference in performance when subject to examples of both aFRR and FCR events. A further discussion of the potentials and possible changes that could affect the performance of the concepts is presented, and some conceivable interactions and considerations for future use of the modelling and optimisation setup is presented. This includes maintenance, redundancy and dynamic properties.

Bibliography

- Andersson et al., 2016.** Christian Andersson, Johan Åkesson and Claus Führer. *PyFMI: A Python Package for Simulation of Coupled Dynamic Models with the Functional Mock-up Interface*. Technical Report in Mathematical Sciences, 2:2016, 2016.
- Bach et al., July 2016.** Bjarne Bach, Jesper Werling, Torben Ommen, Marie Münster, Juan M. Morales and Brian Elmegaard. *Integration of large-scale heat pumps in the district heating systems of Greater Copenhagen*. Energy, 107, 321–334, 2016. ISSN 0360-5442. doi: 10.1016/j.energy.2016.04.029. URL <http://www.sciencedirect.com/science/article/pii/S0360544216304352>.
- Baik et al., 2013.** Young-Jin Baik, Minsung Kim, Ki-Chang Chang, Young-Soo Lee and Ho-Sang Ra. *Potential to enhance performance of seawater-source heat pump by series operation* / Elsevier Enhanced Reader, 2013. URL <https://doi.org/10.1016/j.renene.2013.09.021>. Library Catalog: reader.elsevier.com.
- Boye Petersen, August 2018.** Alexander Boye Petersen. *Elvarmeafgift - betydning for lempelse af lempelse af elvarmeafgiften for eldrevne varmepumper i fjernvarmen*, 2018.
- Dalgas Rasmuseen and Energinet.dk, 2020.** Thomas Dalgas Rasmuseen and Energinet.dk. *Krav til godkendelse af systemydelse / Energinet*, 2020. URL <https://energinet.dk/El/Systemydelse/indkob-og-udbud/Krav-til-systemydelse>.
- Danish Energy Agency and Energinet, August 2016.** Danish Energy Agency and Energinet. *Technology Data - Generation of Electricity and District heating*, Danish Energy Agency & Energinet, August 2016. URL https://ens.dk/sites/ens.dk/files/Analyser/technology_data_catalogue_for_el_and_dh.pdf.
- DIN Forsyning and Rambøll, 2020.** DIN Forsyning and Rambøll. *DIN FORSYNING A/S PROJEKTFORSLAG HAVVANDSOG LUFT VARMEPUMPEANLÆG SAMT FLISKEDELANLÆG*, Esbjerg Kommune, 2020. URL <https://dinforsyning.dk/da-dk/fremtidens-fjernvarme/projektdokumenter>.
- Dott et al., 2013.** Ralf Dott, Thomas Afjei, Andreas Genkinger, Antoine Dalibard, Dani Carbonell, Ricard Consul, Andreas Heinz, Michel Haller, Andreas Witzig, Jorge Facão and Peter Pärish. *A technical report of subtask C Report C2 Part C – Final Draft*. 2013, 97, 2013.

- Elmegaard et al., 2015a.** Brian Elmegaard, Wiebke B Markussen, Torben Ommen and Jonas Kjær Jensen. *Energy systems integration for the transition to non-fossil energy systems*. Technical University of Denmark, Roskilde, 2015. ISBN 978-87-550-3970-4. OCLC: 956288130.
- Elmegaard et al., 2015b.** Brian Elmegaard, Wiebke B Markussen, Torben Ommen and Jonas Kjær Jensen. *Trends in energy supply integration*, DTU, 2015b. URL https://backend.orbit.dtu.dk/ws/portalfiles/portal/119583296/DTU_International_Energy_Report_2015_rev.pdf.
- Energinet, 2019.** Energinet. *Årlig statistik over rådighedsbetaling for reserver i øst- og vestdanmark, samt statistik over omfanget af specialregulering inkl. nøgletal for 2019*, 2019. URL <https://energinet.dk/El/Systemydelser/indkob-og-udbud/Pris-paa-reserver>.
- Energinet.dk, 2018.** Energinet.dk. *Introduktion Til Systemydelesr*, Energinet.dk, Fredericia, 2018. URL <https://energinet.dk/-/media/41F2C6A30A834208B0225DB3132560C7.PDF>.
- Energinet.dk et al., 2019.** Energinet.dk, HEP and LKB. *Udbudbetingelser ofr systemydelser til levering i Danmark*, Energinet.dk, Fredericia, 2019.
- Farouk Fardoun et al., May 2011.** Farouk Fardoun, Oussama Ibrahim and Assaad Zoughaib. *Dynamic modeling of an air source heat pump water heater*. 2011.
- Friotherm AG, 2017.** Friotherm AG. *Värtan Ropsten - the largest sea water heat pump facilty worldwide, with 6 Unitop 50FY and 180 MW total capacity*, 2017. URL https://www.friotherm.com/wp-content/uploads/2017/11/vaertan_e008_uk.pdf.
- GEA, 2020.** GEA. *Industrial heat pumps with screw compressors*, 2020. URL <https://www.gea.com/en/products/gea-fx-p.jsp>.
- GEA Group, 2019.** GEA Group. *GEA RTSelect software*, 2019. URL <http://www.gea.com/en/articles/rtselect/index.jsp>.
- Goldberg and Deb, 1989.** David E. Goldberg and Kelyanmoy Deb. *A comparative Analysis of Selection Schemes Used in Genetic Algorithms*. 1989. ISSN 1081-6593.
- Grønnegaard Nielsen et al., 2016.** Maria Grønnegaard Nielsen, Juan M. Morales, Marco Zugno, Thomas Engberg Pedersen and Henrik Madsen. *Economic valuation of heat pumps and electric boilers in the Danish energy system*. 2016. ISSN 0306-2619. doi: <https://doi.org/10.1016/j.apenergy.2015.08.115>.

- Henrik et al., 2018.** Pieper Henrik, Torben Ommen, Fabian Buhler, Bjarke Lava Paaske, Brian Elmegaard and Wiebke B Markussen. *Allocation of investment costs for large scale heat pumps supplyind districct heating*. 2018. doi: 10.1016/j.egypro.2018.07.104. URL <https://doi.org/10.1016/j.egypro.2018.07.104>.
- Hoffmann and Forbes Pearson, 2011.** Kenneth Hoffmann and David Forbes Pearson. *Ammonia Heat Pumps for District Heating in Norway – a case study*. page 8, 2011. URL <http://ammonia21.com/files/district-heating-norway.pdf>.
- Jin and D. Spilter, 2002.** Hui Jin and Jeffrey D. Spilter. *A Parameter Estimation Based Model of Water-to-Water Heat Pumps for Use in Energy Calculation Programs*. 2002, 18, 2002. URL <https://pdfs.semanticscholar.org/b182/597163525b0a44dfe4c2753d3b7ef5fc0890.pdf>.
- Klima-, energi- og forsyningsministeriet, 2019.** Klima-, energi- og forsyningsministeriet. *Klimapolitisk redegørelse 2019*. 2019, 26, 2019. URL <https://kefm.dk/media/12968/klimapolitisk-redegoerelse-2019.pdf>.
- Kortegaard Støchkel et al., December 2017.** Hanne Kortegaard Støchkel, Bjarke Lava Paaske and Kim S. Clausen. *Drejebog til store varmepumpeprojekter i fjernvarmesystemet*, Grøn Energi, PlanEnergi, DFP, December 2017. URL https://ens.dk/sites/ens.dk/files/Varme/drejebog_for_store_varmepumper.pdf.
- Krishnakumar, 1990.** Kalmanje Krishnakumar. *Mircro-Genetic Algortihms For Stationary And Non-Stationary Function Optimisation*. page 9, 1990. doi: 10.1117/12.969927.
- Lund et al., 2016.** Rasmus Lund, Danica Djuric Ilic and Louise Trygg. *Socioeconomic potential for introducing large-scale heat pumps in district heating in Denmark | Elsevier Enhanced Reader*. 2016. doi: <http://dx.doi.org/10.1016/j.jclepro.2016.07.135>. URL <https://doi.org/10.1016/j.jclepro.2016.07.135>.
- M. Tiller, 2014.** Dr. Michael M. Tiller. *Modelica by Example*, 2014. URL <https://mbe.modelica.university/>. Library Catalog: mbe.modelica.university.
- Meesenburg et al., 2018.** Wiebke Meeseburg, Torben Ommen and Brian Elmegaard. *Dynamic exergoeconomic analysis of a heat pump system used for ancillary services in an integrated energy system*. page 12, 2018. ISSN 0360-5442. doi: 10.1016/j.energy.2018.03.093. URL <https://doi.org/10.1016/j.energy.2018.03.093>.

- Moll Rasmussen et al., 2019.** Iben Moll Rasmussen, Mette Larsen and Morten Egestrand. *Analyse forudsætninger til Energinet 2019 (AF2019)*, Energinet, 2019. URL https://ens.dk/sites/ens.dk/files/Analyser/analyseforudsætninger_til_energinet_2019.pdf.
- Møller et al., 2018.** Claus Møller, Kim Behnke and Anders Stouge. *Elektrificering af Danmarks fjernvarmesektor*, Siemens A/S, Intelligent Energi, Grøn Energi, 2018.
- Møller Thomsen et al., 2018.** Søren Møller Thomsen, Anders Dyrelund, John Flørning, Klaus Fafner and Thomas Rønn. *Dansk Fjernvarme - koncepter for smart integration af vedvarende energi i fjernvarmesektoren*, 2018.
- Popovski et al., 2019.** Eftim Popovski, Ali Aydemir, Tobias Fleiter, Daniel Bellstädt, Richard Büchele and Jan Steinbach. *The role and costs of large-scale heat pumps in decarbonising existing district heating networks - A case study for the city of Herten in Germany* | Elsevier Enhanced Reader, 2019. URL <https://doi.org/10.1016/j.energy.2019.05.122>. Library Catalog: reader.elsevier.com.
- PricewaterhouseCoopers, 2019.** PricewaterhouseCoopers. *Overskudsvarmeafgift – regelændring på vej*, 2019. URL <https://www.pwc.dk/da/artikler/2019/09/overskudsvarmeafgift-regelaendring-paa-vej.html>.
- Rambøll, 2019.** Rambøll. *Ancillary Services From New Technologies*, Rambøll, 2019.
- Rambøll et al., October 2019.** Rambøll, Dansk Fjernvarme and Grøn Energi. *STORE VARMEPUMPER I FJERNVARMEN DRIFTSERFARINGER*, October 2019.
- Richert et al., April 2004.** Felix Richert, Joachim Rückert, Axel Schloßer and Dirk Abel. *Comparison of Modelica and Matlab by Means of a Diesel Engine Model*. IFAC Proceedings Volumes, 37(22), 287–292, 2004. ISSN 1474-6670. doi: 10.1016/S1474-6670(17)30358-0. URL <http://www.sciencedirect.com/science/article/pii/S1474667017303580>.
- Rothuizen et al., 2015.** Erasmus Rothuizen, Brian Elmegaard, Wiebke B Markussen, Claus Madsen, Martin F Olesen and Marie Ø Sølvsten. *High efficient heat pump system using storage tanks to increase COP by means of the ISEC concept - Part 1: Model validation*. High efficient heat pump system using storage tanks to increase COP by means of the ISEC concept, 2015. URL https://backend.orbit.dtu.dk/ws/portalfiles/portal/119688915/ISECManuscript_submitted.pdf.
- Rudio and Controls, May 2010.** Christian Rudio and Johnson Controls. *Water to Water Heat Recovery Concepts and Applications*, 2010.

- Senecal et al., 2000.** Peter Senecal, David Montgomery and Rolf Reitz. *A methodology for engine design using multi-dimensional modelling and genetic algorithms with validation through experiments*. (1), 229–248, 2000. doi: 10.1243/1468087001545155.
- Siemens A/S et al., June 2018.** Siemens A/S, Intelligent energi and Grøn energi. *Elektrificering af Danmarks fjernvarmesektor*, 2018. URL <https://assets.new.siemens.com/siemens/assets/api/uuid:78a2f43866759ca965d7a8b08beed706a94a1c1/version:1566301498/elektrificering-af-fjernvarmesektoren-siemens-0618.pdf>.
- Smed and Rambøll, December 2019.** Jes Smed and Rambøll. *Energinet Elsystemansvar A/S*, Rambøll, December 2019.
- Terros et al., 2020.** O. Terros, J. Spreitzhofer, D. Bascoitti, R.R Schmidt, T. Esterl, M. Pober, M. Kerschbaumer and M. Ziegler. *Electricity market options for heat pumps in rural district heating networks in Austria*. 2020. doi: <https://doi.org/10.1016/j.energy.2019.116875>.
- Thomassen, January 2020.** Signe Thomassen. *Design and Optimisation of HeatPump Concepts for future DistrictHeating Investments*, Aalborg University/Added Values A/S, Added Values, January 2020.
- Tran et al., 2016.** Cong-Toan Tran, Philippe Riviere and Paul Waide. *Energy Efficiency Modelling of Residential Air Source Heat Pump Water Heater*, Mines ParisTech, PLS Research unieristy, 2016. URL <http://dx.doi.org/10.13044/j.sdewes.2016.04.0007>.
- Vinther et al., May 2017.** K. Vinther, Rene J. Nielsen, Palle Andersen and Jan D. Bendtsen. *Optimization of interconnected absorption cycle heat pumps with micro-genetic algorithms*. Journal of Process Control, 53, 26–36, 2017. ISSN 09591524. doi: 10.1016/j.jprocont.2017.02.011. URL <https://linkinghub.elsevier.com/retrieve/pii/S0959152417300379>.
- Wetter et al., July 2014.** Michael Wetter, Wangda Zuo, Thierry S. Noudui and Xiufeng Pang. *Modelica Buildings library*. Journal of Building Performance Simulation, 7(4), 253–270, 2014. ISSN 1940-1493, 1940-1507. doi: 10.1080/19401493.2013.765506. URL <http://www.tandfonline.com/doi/abs/10.1080/19401493.2013.765506>.

A | Performance Map Test

To ensure, that unexpected and unrealistic solutions does not occur, if the heat pump is forced slightly outside the range, the plots seen in Figure A.1 and Figure A.2 were made. The plots represent the surfaces of the equations developed for the performance map in Equation 3.2 and Equation 3.1 at a constant load of 100 % and temperatures from -10 to 30 °C for the evaporation temperature and 20 to 90 °C for the outlet temperature of the district heating water.

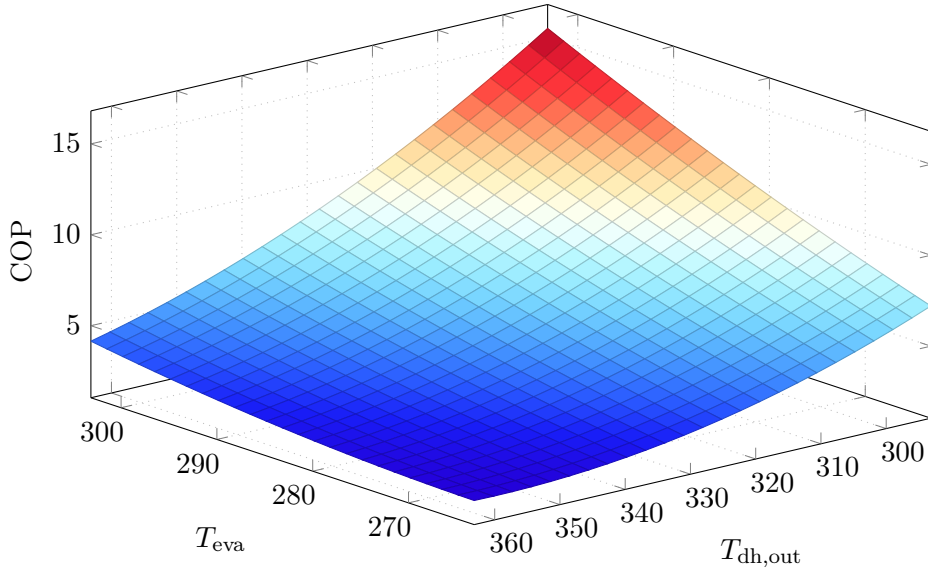


Figure A.1: Surface plot of the regression equation for COP, with a constant load of 100 %. The temperatures are varied from -10 °C to 30 °C for the evaporator temperature and from 20 °C to 90 °C for the district heating water outlet temperature.[Thomassen, 2020]

Observing Figure A.1 it is seen that the closer the evaporation temperature and the outlet temperature of the district heating water get, the higher the COP. This is consistent with expectations. Similar, at very low evaporation temperatures and very high district heating outlet temperatures, the COP reduce significantly. This is also consistent with expectations. However, at $T_{eva} = -10$ °C and $T_{dh,out} = 90$ °C, the temperatures are far outside the range of the map, meaning that the accuracy of 7 % cannot be ensured [Thomassen, 2020]. On the other hand, the performance outside the range does seem to follow the expectations of COP behaviour.

For Figure A.2 a constant load of 100 % implies that heat output is described by two first order terms. Naturally, no unexpected gradients occurs from this, but similar to the COP, the accuracy cannot be guaranteed outside the range of development for the performance map.

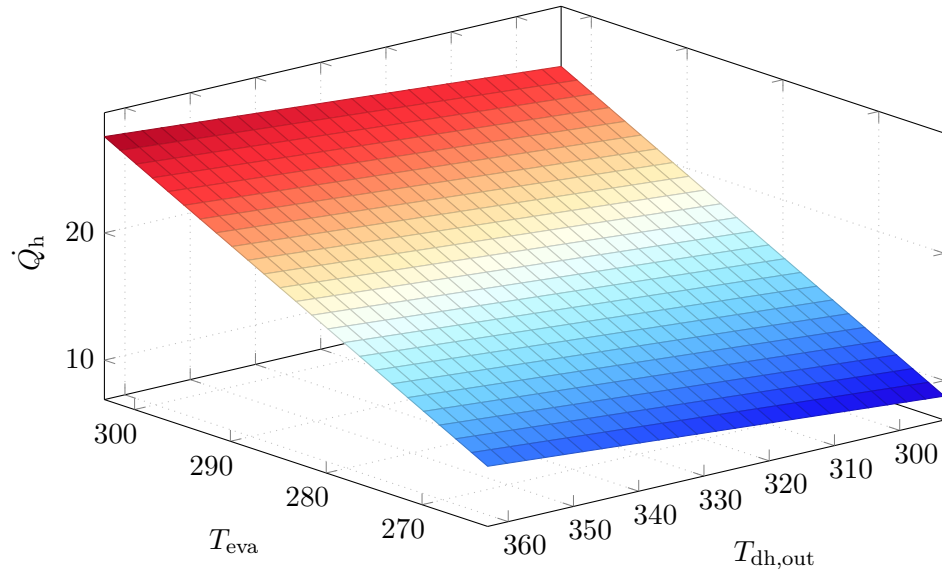


Figure A.2: Surface plot of the regression equation for \dot{Q}_h , with a constant load of 100 %. The temperatures are varied from -10 °C to 30 °C for the evaporator temperature and from 20 °C to 90 °C for the district heating water outlet temperature.[Thomassen, 2020]

B | Ancillary Services

This appendix is an introduction to the danish ancillary service market. Some more detailed descriptions of the different reserve types as well as requirements, qualification and more detailed data on prices and tendencies from previous years are found in this appendix.

B.1 Introduction to ancillary services

The danish electricity grid is divided into two areas: DK1 and DK2, with DK1 belonging to the western part of Denmark and DK2 to the eastern part. The demands for delivery of ancillary services are naturally also different in DK1 and DK2, and Energinet (EN), which is the Danish Transmission System Operator, buys the reserves for the two areas separately. Since the case study in this thesis is based on a current project in Esbjerg (western Denmark), most considerations will be regarding requirements for DK1. [Energinet.dk, 2018].

B.1.1 Reserve Types and Market Requirements

For participating in the reserve market, the unit/system must verify its capability to provide the specific ancillary service. This includes the specified response time and technical requirements for the specific service.

For DK1, the following three frequency ancillary services are described:

- Frequency Containment Reserves (FCR).
- Automatic Frequency Restoration Reserve (aFRR).
- Manual Frequency Restoration Reserve (mFRR).

For example system in Esbjerg, the main focus is regarding FCR and aFRR, and for this reason, mFRR will not be considered in this appendix. The following sections outlines the differences and requirements regarding the FCR and aFRR.

Frequency Containment Reserves (FCR)

The primary reserve is also called FCR, which is the Frequency Containment Reserve, is responsible for balancing the frequency around 50 Hz. For FCR, the requirements for the response and response time mean, that the reserve must be delivered with a frequency deviation up to ± 200 mHz compared to the reference frequency of 50 Hz. In other words, this mean that FCR must deliver reserves to balance variations from 49.8 Hz - 50.2 Hz. A ± 20 mHz dead-band is allowed. FCR does additionally require, that the capacity is delivered within a relatively short amount of time. FCR must as a minimum be delivered linearly, and the first 50 % of the reserve, must be delivered within 15 s. The last part must be fully delivered within 30 s. The

minimum requirement for the extent of the FCR is 15 minutes, and the reserve must additionally be reestablished after 15 minutes. FCR can be delivered by both single units and as a combination of units (applies for both production and consumption units).

In the synchronous area in which DK1 belong, EN together with all other members in the area, share the responsibility to ensure, that enough FCR will be available for large fault disturbances, corresponding to ± 3000 MW. DK1's (EN's) share is determined by the production and consumption in DK1, which as of 2020 is ± 21 MW. [Smed and Rambøll, 2019]

The frequency deviations is caused by imbalances between the power consumed and produced. It is automatically regulated and can be delivered of both producing and consuming units. The upward and downward regulation are requested separately. Energinet are responsible for buying the FCR reserve. FCR are traded at daily auctions. The daily auction applies for the following day, which is divided into six blocks each of four hours. Bids for the daily auctions must be submit latest at 3 PM the day ahead operation, and must on hourly basis indicate the capacity and price. The capacity and price applies for the entire 4-hour block. The minimum capacity of a bid is 0.3 MW_e . All bids are sorted by Energinet, starting with the bid with the lowest price pr. MW_e . All bids accepted by Energinet receives an availability payment corresponding to the prices of the most expensive bid. This applies for both upward and downward regulation. There are no payments for the delivered capacity. As a rule, all bids will either be accepted with their full capacity or not at all.

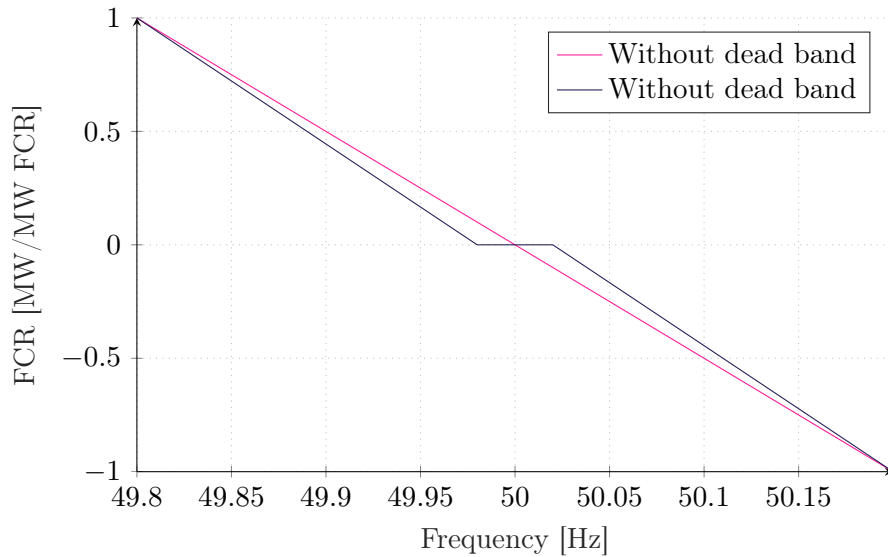


Figure B.1: Frequency deviations in the grid. ± 20 mHz is the size of the dead band which, before the operation of the production unit is affected.

Today, the majority of FCR is delivered by either thermal- or natural gas power plants or electrical boilers. FCR is as mentioned a fast responding reserve used to stabilise the frequency close to the reference frequency of 50 Hz. If a unit is tasked to provide FCR, should be able to measure the frequency and automatically activate the reserves. The reserve must be activated when the frequency deviations exceed ± 20 mHz and up to ± 200 mHz. The acceptable dead band of ± 20 mHz is shown in Figure B.1.

Within the first 15 seconds after the activation, the first half of the activated reserve must be provided, while the remaining half must be provided within 30 seconds. Faster response time are allowed provided that it is approximately linear and proportional to the frequency deviation. The reserve must be reestablished after 15 minutes following an activation.

FCR - economical considerations

From the 2019 statistics on availability payments, some key numbers are listed in Table B.1 [Energinet, 2019].

Table B.1: 2019 average, minimum and maximum price for upward and downward balancing services for the FCR.

	Upward	Downward
Average price [DKK/MW/h]	276	26
Min 2019 price [DKK/MW/h]	47	11
Max 2019 price [DKK/MW/h]	650	59

Automatic Frequency Restoration Reserve (aFRR)

The aFRR is used to replace FCR, since these have typically have limited availability (minimum requirement of 15 minutes). Units and plants in operation as well as fast starting units can be used to deliver the aFRR supply capacity. The delivered aFRR capacity can be from either a single unit or an aggregated portfolio of units.

From January 2020, new rules regarding aFRR applied. This mean, that aFRR is purchased from monthly auctions, to ensure the required amount. For 2020, this amount was ± 90 MW. Furthermore, the 2020 rules requires the supply of aFRR to be ≤ 15 minutes response time. In most cases, this also mean that units or plants approved for FCR can be approved for aFRR, provided that the reserve can be maintained continuously.

Bids on aFRR must applies for the entire month, and must have a minimum capacity of 1 MW_e and a maximum of 50 MW_e. Similar to FCR, all bids will either be accepted

in their full capacity or not at all. Energinet chose between the bids to ensure that the total necessary capacity is covered with the lowest possible cost. All accepted bids receive the payment, that was informed in the bid (pay-as-bid). Furthermore, activation of aFRR also implies a payment for the amount of delivered capacity. For upward regulation the payment is the elspot price + 100 DKK/MW_e and conversely for downward regulation the payment is elspot price - 100 DKK/MW_e. From 2015 up to and including 2019, most of the aFRR services was delivered from Skagerrak 4, due to an agreement. In this period, most of the aFRR services was delivered from this agreement. This mean, that payments most likely changes for the continuous market.

Different from FCR, the aFRR auctions are on a monthly basis, and the necessary capacity is as a rule ± 90 MW_e. The reserves are always symmetrical. However, Energinet can increase these levels, but is as a rule set by recommendation from ENTSO-E RG Continental Europe [Energinet.dk et al., 2019].

The general technical concept of FCR and aFRR is illustrated in Figure B.2.

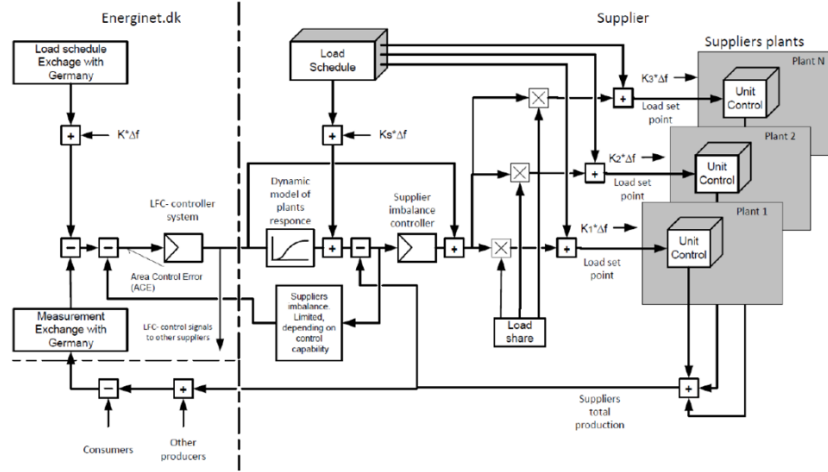


Figure B.2: General concept of FCR and aFRR in DK1. [Energinet, 2019]

The dashed line represents the boundary between Energinet and the balance responsible party (BRP). Energinet further cooperates with Germany, which is represented by the horizontal dashed line. On the BRP side, the *load schedule* represents the expected production for the units - which in terms of this thesis, will be the heat pumps. When the $K_i \cdot \Delta f$ applies, it mean that a bid on FCR was chosen. It can be seen as a simple proportional controller with k being the proportional gain k_p . This mean, that the controller *overwrites* the original electricity consumption setpoint of the heat pump. The aFRR signal comes from Energinet, represented as the string starting from the area control error (ACE). It adds directly to the planned production of the particular unit. The area control error represents the sum of the power control error ΔP and the frequency control error $K_i \cdot \Delta f$. ΔP represents the difference

between the actual power interchange value, P , and the control program called P_0 . Activating aFRR is in other words to minimise ACE, so that at the end of a delivery, the frequency has returned to the nominal 50 Hz and the ACE has returned to 0. [Energinet, 2019]

A | Dymola: System setup

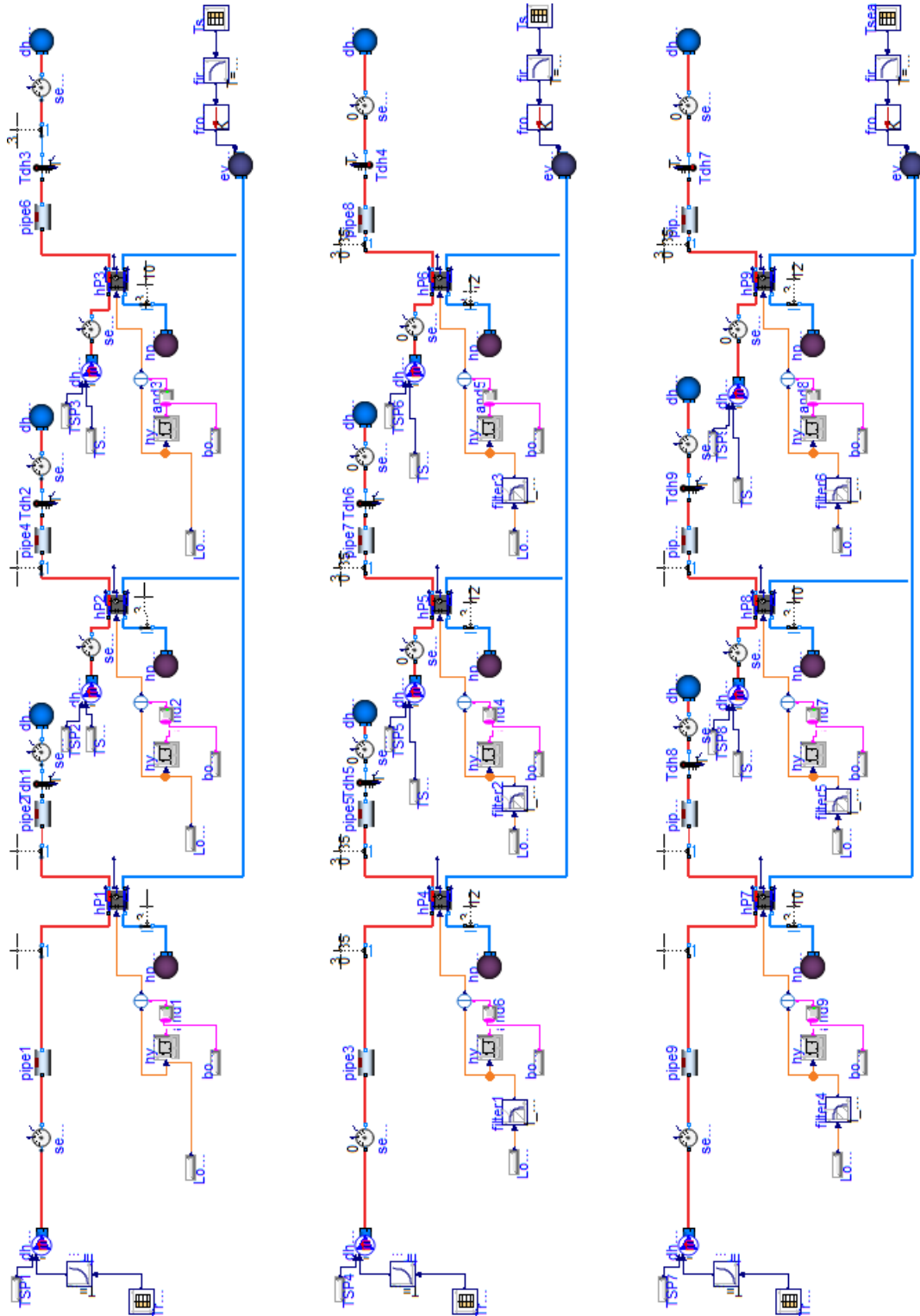


Figure A.1: Overview of the full system of heat pumps developed for the optimisation.

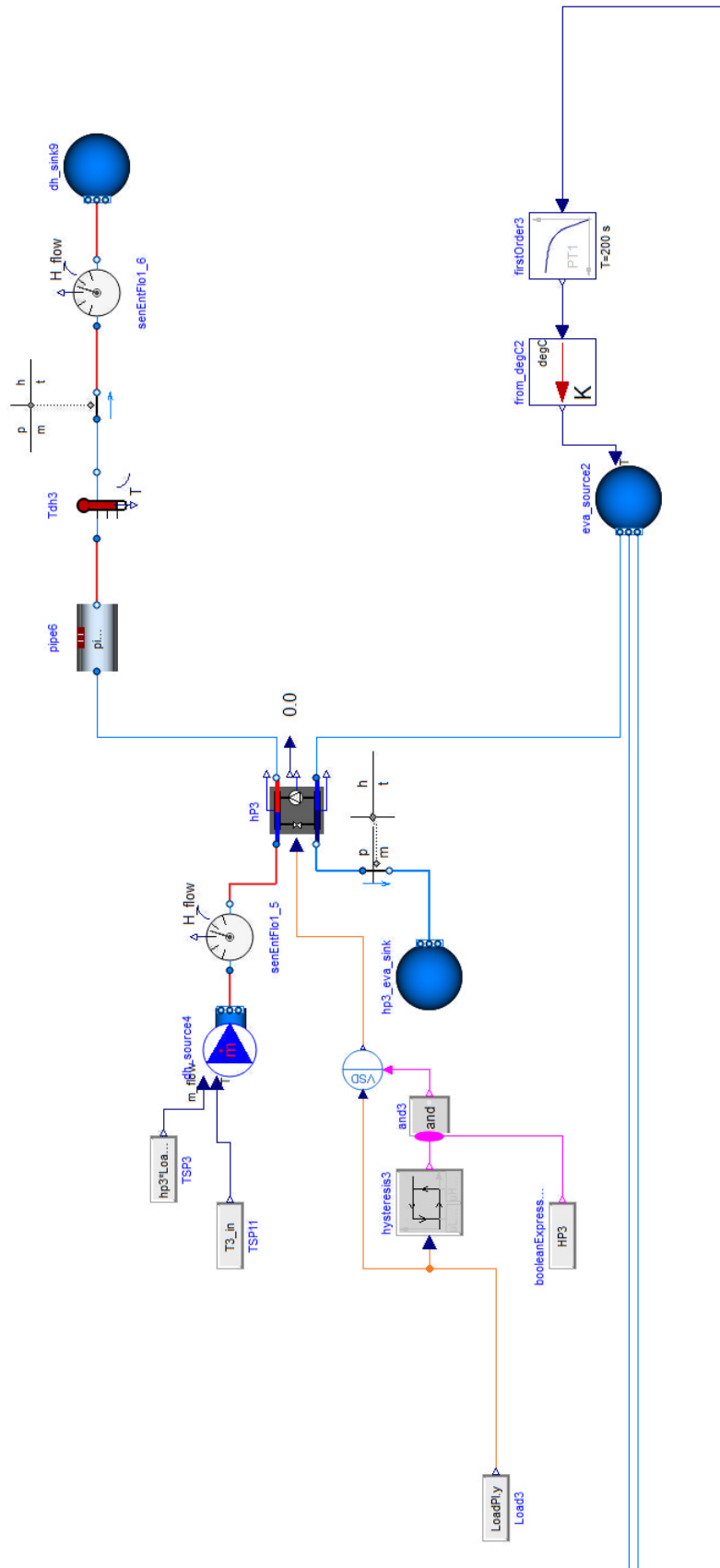


Figure A.2: Example of a single heat pump unit in a setup used for dynamic tests.

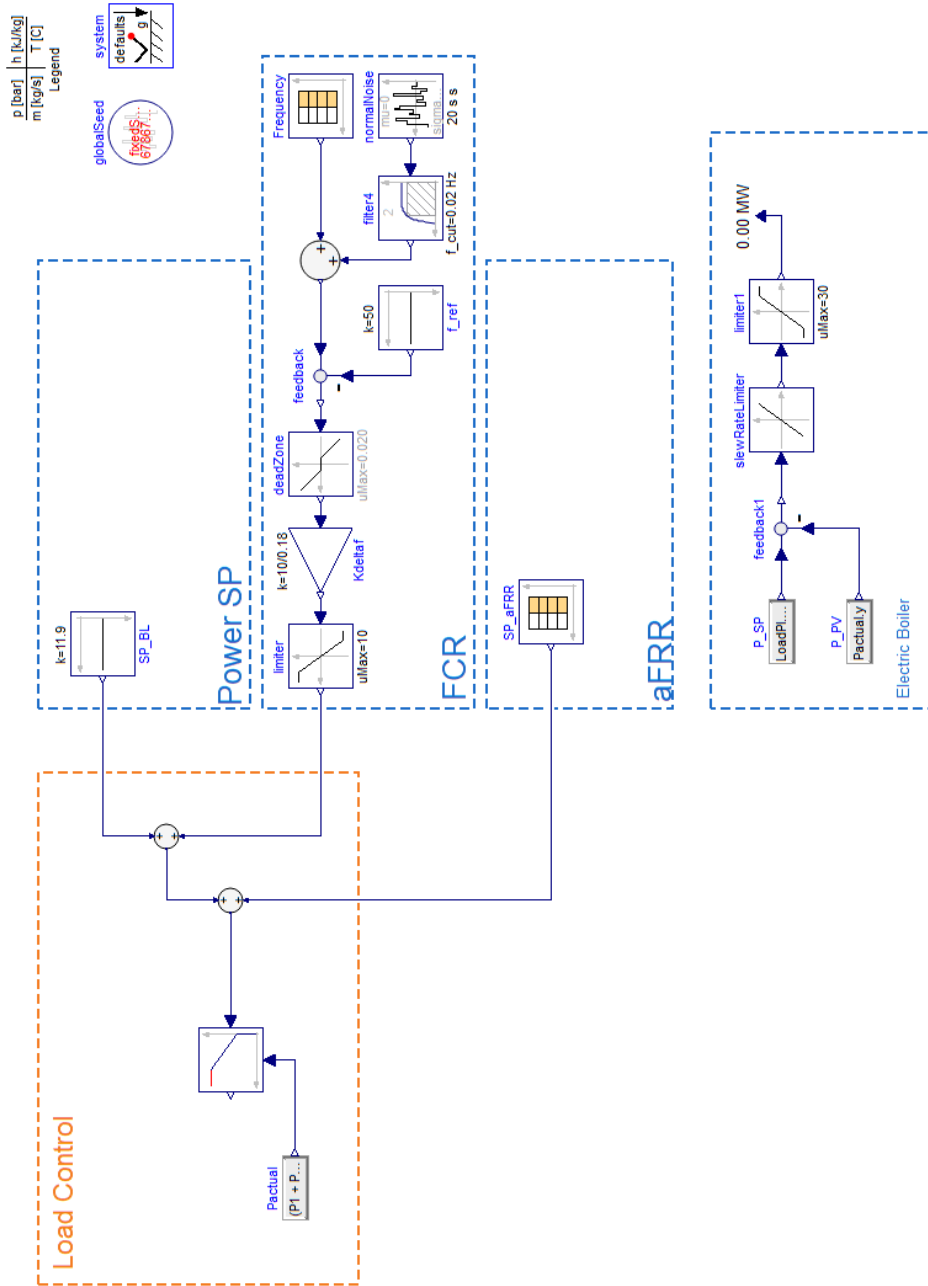


Figure A.3: Control setup and implementation of example ancillary services.

B | μ GA Python code

Enclosure with relevant Python code snippets from the micro Genetic Algorithm used for optimisation.

Simulation setup

Defines simulation time, sampling rate, defined the number of constraints, the number of results to save for post processing and the minimum and maximum values for the optimisation variables.

```
1  ## Simulation
2  sim_start = 0
3  sim_end = 39600
4
5  # time between samples
6  Ts = 1
7
8  #number of communication points in simulation (sample points)
9  sim_com = sim_end/Ts
10 sim_timeout = 180
11
12 #number of constraints in optimization problem
13 no_constraints = 7
14
15 #number of datapoints to save in results
16 res_misc_length = 32
17
18 # Minimum capacities
19 min_array = [0, 0, 0, 0, 0, 0, 0, 0, 0]
20
21 #Maximum Allowable capacities
22 max_array = [15.5, 15.5, 15.5, 15.5, 15.5, 15.5, 15.5, 15.5, 15.5]
23
24 COST_invest = [0 for x in range(9)]
```

Listing B.1: Simulation Setup

Parameters for μ GA

Sets the default number of generations, the population size, the number of individuals to save for next generation (elitism), the tournament size and possible mutation rate.

```
1  # GA parameters
2  test_number = 0
3  run_number = 0
4
5  #how many generations to simulate
6  gen_length = 100
7
8  #population size (number of chromosomes)
```

```

9 count = 5
10
11 #how many elitist individuals to select in pop (min 1 individual)
12 elitist_count = 1
13
14 #number of individuals picked in each tournament (only used when
15 # tournament selection is picked)
16 tournament_size = 2
17
18 #the likelihood of individuals to crossover (range: 0-1).
19 precombination = 1.0
20
21 #the likelihood of an individual to mutate - only one gene in individual
22 # is mutated (range: 0-1).
23 pmutate = 0.0
24
25 #number of optimization parameters
26 length = len(min_array)

```

Listing B.2: Parameters for micro Genetic Algorithm

Initial Guess

Creates the initial individuals.

```

1 # Insert initial guess
2 init_individual = [numpy.zeros(length)]
3 init_individual_ref = [numpy.zeros(length)]
4 init_individual_ser = [numpy.zeros(length)]
5 init_individual_serpar = [numpy.zeros(length)]

```

Listing B.3: Initial Guess

Main Loop - Initial population

The initial individuals are inserted to the initial population, and automatic restart and computation of population fitness are defined.

```

1 def MainLoop():
2
3     # Generate start population
4     pop = population(count-4, len(min_array), min_array, max_array,
5                       init_individual, 3)
6     #insert nominal case (so we dont do worse than that)
7     pop.append(init_individual)
8     pop.append(init_individual_ref)
9     pop.append(init_individual_ser)
10    pop.append(init_individual_serpar)
11    gen_count = 0
12
13    # Automatic restart if population has collapsed (Obtain new
14    # population but keep best individual - pop[0])
15    if pop_collapsed == True:

```

```

15         if print_stuff:
16             print('automatic restart')
17         best_pop = pop[0]
18         #normal randomly picked
19         pop = population(count, len(min_array), min_array, max_array,
20             best_pop, 3)
21         #keep best solution from before
22         pop[0] = best_pop
23
24     # Compute fitness of population
25     graded = compute_fitness_of_pop(pop, q)
26     gen_count += 1

```

Listing B.4: Main Loop - creating initial population

Crossover

Solutions/parents found through the tournament selection is merged (through crossover) for better solutions (children).

```

1     # Produce children for next generation through selection,
2     # crossover, and mutation
3     desired_length = count - elitist_count
4     children = []
5     while len(children) < desired_length:
6
7         # Selection
8         male, female, male_fit, female_fit =
9         selection_tournament_with_fit(graded, parents, tournament_size)
10
11        # Crossover
12        child_1, child_2 = crossover_box_gaus(male, female,
13            precombination, min_array, max_array, male_fit, female_fit)
14
15        # Mutation
16        child_1 = mutate_uniform(child_1, pmutate, min_array, max_array)
17        child_2 = mutate_uniform(child_2, pmutate, min_array, max_array)
18
19        # Add to pool of children
20        children.append(child_1)
21        children.append(child_2)
22
23        # Add children to elitist group to form next generation of
24        # population
25        next_generation.extend(children)
26        pop = next_generation

```

Listing B.5: Crossover - create children using a normal distribution

Function: Creating individuals

Creates new individuals using a normal distribution.

```

1 def individual(length, min_val, max_val, center, method):
2     ind = numpy.zeros(length)
3     for i in range(length):
4
5         #pick a random number with either uniform, triangular, or normal
6         # distribution
7         if method == 1:
8             ind[i] = numpy.random.uniform(min_val[i],max_val[i])
9         elif method == 2:
10            #extend triangular random search range by 10%
11            triag_extend = 0.1
12            ind[i] = numpy.random.triangular(min_val[i]-(max_val[i]-
13            min_val[i])*triag_extend, center[0][i], max_val[i]+
14            (max_val[i]-min_val[i])*triag_extend,1)
15        elif method == 3:
16            #standard deviation set to 50% of full range (see also Y. Yoon
17            # paper)
18            sigma_value = 0.5*(max_val[i]-min_val[i])
19            if sigma_value <= 0:
20                ind[i] = min_val[i]
21            else:
22                ind[i] = numpy.random.normal(center[0][i], sigma_value,1)
23        #make sure that individual is within the bounds
24        if ind[i] < min_val[i]:
25            ind[i] = min_val[i]
26        if ind[i] > max_val[i]:
27            ind[i] = max_val[i]
28
29    return [ ind ]

```

Listing B.6: Function that creates the new individuals

Function: Fitness

Calculates the fitness of individuals. Import of FMU and sets problem specific constraints. Additionally allows to change the values of variables in Dymola model. Additional solver options can be set.

```

1 def fitness(individual,q,model_no):
2
3     model = load_fmu(os.path.join(path_to_fmu,'
4     HeatPump_FMUSimulations_COP_v20_0' + str(model_no) + '.fmu'),
5     log_level=0)
6
7     #To reject heat pumps with a size less than 2 MW
8
9     if MWl_current <= 2:
10         MWl_current = 0
11     else:
12         pass
13

```

```

14     #Ensure that a heat pump is off, when MW=0.
15     if MW1_current == 0:
16         HP1_current = False
17     else:
18         HP1_current = True
19
20
21 # Change values of variables in the Dymola Model
22 model.set('MW1', MW1_current)
23 model.set('MW2', MW2_current)
24 model.set('MW3', MW3_current)
25 model.set('MW4', MW4_current)
26 model.set('MW5', MW5_current)
27 model.set('MW6', MW6_current)
28 model.set('MW7', MW7_current)
29 model.set('MW8', MW8_current)
30 model.set('MW9', MW9_current)
31 model.set('string1', HP1_current)
32 model.set('HP2', HP2_current)
33 model.set('HP3', HP3_current)
34 model.set('string2', HP4_current)
35 model.set('HP5', HP5_current)
36 model.set('HP6', HP6_current)
37 model.set('string3', HP7_current)
38 model.set('HP8', HP8_current)
39 model.set('HP9', HP9_current)
40
41
42 # Set simulation options
43 opts = model.simulate_options()
44 ##opts["CNode_options"]["atol"] = 1e-6 #Change the absolute tolerance
45 ##opts["CNode_options"]["discr"] = "Adams" #Change the discretization
46 #from BDF to Adams
47 opts["ncp"] = sim_com
48 opts["result_handling"]="memory"
49 opts["filter"] = ["P", "Qh", "time", "string1", "HP2", "HP3", "string2",
50 "HP5", "HP6", "string3", "HP8", "HP9", "MW1", "MW2", "MW3", "MW4",
51 "MW5", "MW6", "MW7", "MW8", "MW9"]
52
53 # Simulate
54 try:
55     res = model.simulate(final_time=sim_end, options=opts)
56 except:
57     print('ups - simulation failed')
58     model.reset()
59     while 1:
60         dummy = 1
61         #endless loop (wait for process to time out)

```

Listing B.7: Fitness function: imports FMU.

Cost Function: Heating capacity and Investment cost

The implementation of the cost functions for heating capacity and investment costs. Includes options for sensitivity for investment cost.

```

1      ## Qh cat1
2      if 5164456*(1-(Qh[28700]/Qh_set1)) < 0:
3          Qh1 = 0
4      else:
5          Qh1 = 5164456*(1-(Qh[28700]/Qh_set1))
6      ## Qh cat2
7      if 9658168*(1-(Qh[32300]/Qh_set2)) < 0:
8          Qh2 = 0
9      else:
10         Qh2 = 9658168*(1-(Qh[32300]/Qh_set2))
11     ## Qh cat3
12     if 406225*(1-(Qh[35900]/Qh_set3)) < 0:
13         Qh3 = 0
14     else:
15         Qh3 = 406225*(1-(Qh[35900]/Qh_set3))
16     ## Qh cat4
17     if 82839*(1-(Qh[39500]/Qh_set4)) < 0:
18         Qh4 = 0
19     else:
20         Qh4 = 82839*(1-(Qh[39500]/Qh_set4))
21
22
23     #Heat costfunction
24     COST_heat = [Qh1, Qh2, Qh3, Qh4]
25     print('Cost Qh', COST_heat)
26
27
28     size = [MW1[-1], MW2[-1], MW3[-1], MW4[-1], MW5[-1], MW6[-1], MW7[-1],
29             MW8[-1], MW9[-1]]
30     HP = [HP1[-1], HP2[-1], HP3[-1], HP4[-1], HP5[-1], HP6[-1], HP7[-1],
31           HP8[-1],
32           HP9[-1]]
33     print('size', size)
34     print('hp', HP)
35     for l in range(len(HP)):
36         # For sensitivity study changes
37         # COST_invest[l] = 10000000*(size[l])**0.848) #high
38         # COST_invest[l] = 4000000*(size[l])**0.848) #LOW
39         # COST_invest[l] = 6000000*(size[l])**0.848) #ref
40         # COST_invest[l] = 7000000*(size[l])**0.7505) #0.5 EOS
41         COST_invest[l] = 5000000*(size[l])**0.7505) #1 EOS
42     print('COST_invest', COST_invest)
43     print ('sum', sum(COST_invest))

```

Listing B.8: Implementation of cost functions for heating capacity and investment cost

Constraint: Heat output

Example of constrain for heat output

```

1  # Constraints
2  constraint_violations = 0;
3
4  if Qh[2598] < Qh_cop1*0.98:
5      constraint_violations += 1
6      #if print_stuff:
7          print('Qh1 constraint violated')
8
9  res_misc[0] = constraint_violations
10

```

Listing B.9: Heat output constraint

Fitness calculation

The fitness of each individual is calculated from z. An offset of 1 000 000 000 is set to avoid issues for negative values.

```

1  # Calculate fitness (we want to minimize z)
2  z = (1000000000+(a1*(1.00-((Qh[3598]/P[3598])/COP_ref1))+a2*(1.00-((Qh
   [7198]/P[7198])/COP_ref2))+a3*(1.00-((Qh[10798]/P[10798])/COP_ref3))+
   a4*(1.00-((Qh[14398]/P[14398])/COP_ref4))+a5*(1-((Qh[17998]/P[17998])/
   COP_ref5))+a6*(1-((Qh[21598]/P[21598])/COP_ref6))+a7*(1-((Qh[24198]/P
   [24198])/COP_ref7))+sum(COST_heat)+((sum(COST_invest)*0.06)-(cost_ref
   *0.06))))*(-1);
3  #if print_stuff:
4  print('Fitness',z)
5
6  res_misc[31] = z
7  model.reset()
8  q.put([model_no,z,res_misc])

```

Listing B.10: Calculation of fitness for individuals

Function: Cross over with normal distribution

Function that creates children from a normal distribution.

```

1  def crossover_box_gaus(male,female,precombination,min_constr,max_constr,
   fit_male,fit_female):
2
3      if precombination > numpy.random.random():
4          child_1 = [numpy.arange(size(male), dtype=numpy.float)]
5          child_2 = [numpy.arange(size(male), dtype=numpy.float)]
6          for i in range(size(male)):
7              if male[0][i] >= female[0][i]:
8                  max_val = male[0][i]
9                  min_val = female[0][i]
10                 if max_val == min_val:

```

```

11         center = min_val
12     else:
13         if fit_male == 0:
14             center = min_val
15         else:
16             center = min_val + (fit_male/(fit_female+fit_male)
17 )*(max_val-min_val)
18     else:
19         max_val = female[0][i]
20         min_val = male[0][i]
21         if max_val == min_val:
22             center = min_val
23         else:
24             if fit_female == 0:
25                 center = min_val
26             else:
27                 center = min_val + (fit_female/(fit_female+
28 fit_male))*(max_val-min_val)
29         sigma_value = 0.5*(max_val-min_val) #standard deviation set to
30 50% of full range (see also Y. Yoon paper)
31         if sigma_value <= 0:
32             child_1[0][i] = min_val
33             child_2[0][i] = min_val
34         else:
35             child_1[0][i] = numpy.random.normal(center,sigma_value,1)
36             if child_1[0][i] < min_val:
37                 child_1[0][i] = min_val
38             if child_1[0][i] > max_val:
39                 child_1[0][i] = max_val
40             if binary_indicator[i] == 1:
41                 if child_1[0][i] > 0.5:
42                     child_1[0][i] = 1
43             else:
44                 child_1[0][i] = 0
45             child_2[0][i] = numpy.random.normal(center,sigma_value,1)
46             if child_2[0][i] < min_val:
47                 child_2[0][i] = min_val
48             if child_2[0][i] > max_val:
49                 child_2[0][i] = max_val
50             if binary_indicator[i] == 1:
51                 if child_2[0][i] > 0.5:
52                     child_2[0][i] = 1
53             else:
54                 child_2[0][i] = 0
55     else:
56         child_1 = male
57         child_2 = female
58     return child_1, child_2

```

Listing B.11: Function for normal distribution for cross over